GIACOMO ARIANI

Neural representations of movement planning within the human prehension system

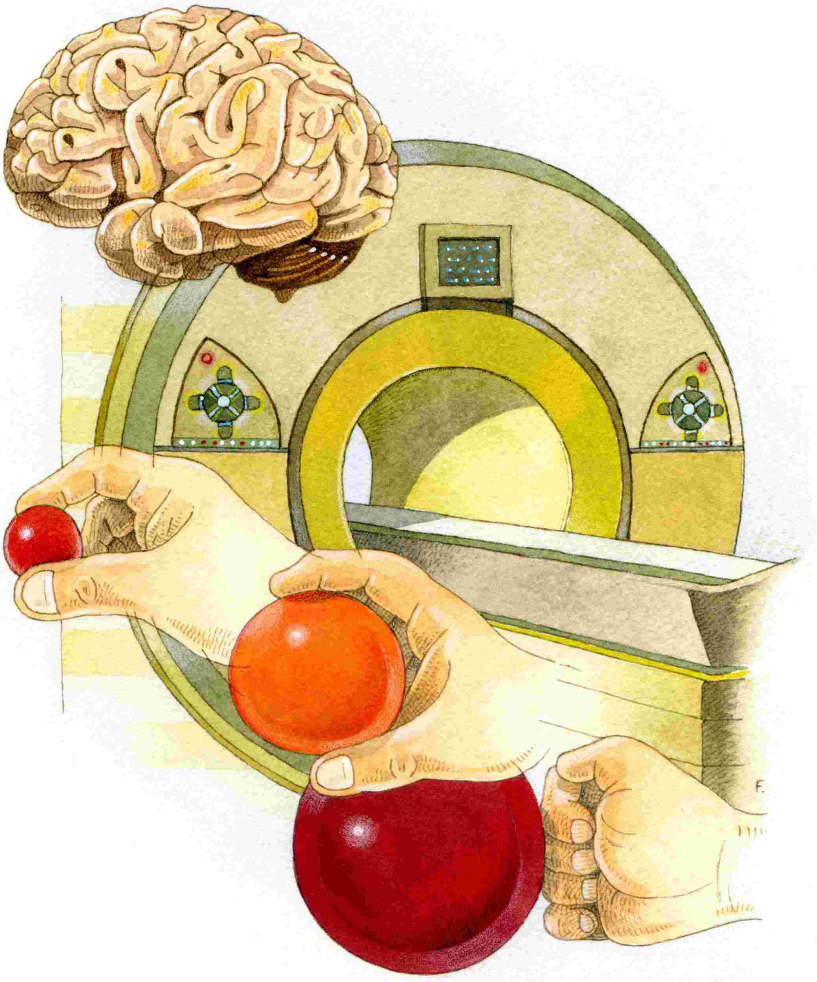

2016 - PhD Thesis

UNIVERSITY OF TRENTO

" […] This is what allows us to carry on the epic learning game that we call science. Science formalizes our special kind of collective memory, or species memory, in which each generation builds on what has been learned by those that came before, following in each other's footsteps, standing on each other's shoulders. Each generation values what it can learn from the one before, and prizes the discoveries it will pass on to the next, so that we see farther and farther, climbing an infinite mountain."

– Jonathan Weiner, The Beak of the Finch (1994)

The studies described in this thesis were carried out
at the Center for Mind/Brain Sciences of the
University of Trento, Italy.

Cover design and illustrations
Fulvio Ariani (www.fulvioariani.it)

Printed by
TIPOGRAFIA MILANI S.r.l.
Via Schiaparelli, 11 (ZAI) 37135 Verona – Italy

Proofreading
Megan Varano and Poppy Sharp

University of Trento
Center for Mind/Brain Sciences (CIMeC)

Doctoral School in Cognitive and Brain Sciences
Cycle XXVIII | 2012-2016

PhD Thesis

Neural representations of movement planning within the human prehension system

Doctoral Student: **Giacomo Ariani**
Center for Mind/Brain Sciences, University of Trento, Italy

Advisor: **Dr. Angelika Lingnau**
Center for Mind/Brain Sciences, University of Trento, Italy
Department of Psychology & Cognitive Science, University of Trento, Italy
Department of Psychology, Royal Holloway University of London, United Kingdom

Contents

Figures and Tables

Overview

Object manipulation is central to our daily interactions with the environment. Failing to select, prepare or perform correct prehension movements results in dramatic limitations for the affected individual. Whereas we begin to have a better understanding of the neural mechanisms underlying the execution of object-directed movements, less is known about how exactly our brain makes the plan for action. The first chapter of this thesis (Chapter 1) provides the reader with a general introduction on movement planning of prehension movements in monkeys and humans, from neurophysiology to neuroimaging and the development of advanced multivariate analysis methods. Chapter 1 ends with open questions that are at the core of the following experimental chapters.

Previous studies examining movement planning suggested that neuronal populations in parieto-frontal areas contain information about upcoming movements moments before they actually take place. However, such studies typically used experiments in which the participant was instructed about the movement to plan with visual or auditory cues, making it difficult to disentangle movement planning from the processing of cues and stimulus-response (S-R) mapping. Chapter 2 describes a functional magnetic resonance imaging (fMRI) study (Study I) in which we compared an instructed condition with a free-choice condition that allowed participants to select which prehension movement to perform: a condition in which the task was not tied to specific external cues (i.e., no direct S-R mapping). Using

multi-variate pattern analysis (MVPA), we found contralateral parietal and frontal regions containing abstract representations of planned movements that generalize across the way these movements were generated (internally vs externally).

The majority of previous studies were based on delayed-movement tasks, which introduce brain responses unrelated to movement preparation. Consequently, whether these findings would generalize to immediate movements remained unclear. Chapter 3 reports a second fMRI study (Study II), where we directly compared delayed and immediate reaching and grasping movements. Using time-resolved MVPA allowed us to reveal shared representations for delayed and non-delayed movement planning in human primary motor cortex and examine how movement representations unfolded throughout the different stages of planning and execution.

The last chapter of this thesis (Chapter 4) begins with a short summary of the main experimental findings. Next, it discusses the results of the two experiments in the wider context of the existing literature on movement planning and how these extend our current knowledge with respect to previous neuroimaging studies on neurologically-intact human volunteers. The last sections of Chapter 4 are dedicated to a brief account of the limitations, future directions and possible implications for applied research.

Chapter 1.

Introduction and Background

1.1 The origin of movement

"Why do we and other animals have brains? […] Now, you may reason that we have one to perceive the world or to think, and that's completely wrong. […] We have a brain for one reason and one reason only, and that's to produce adaptable and complex movements. There's no other reason to have a brain. Think about it, movement is the only way you have of affecting the world around you."

– Daniel Wolpert, TED talk "The real reason for brains" (2011)

According to Daniel Wolpert, Professor of Neuroscience at the University of Cambridge (UK), understanding movement (i.e., the mechanisms and apparatus that allow our body to move) is key to understanding brain function as a whole. In his view there would be no evolutionary advantage to evolve sensory, memory, and other cognitive functions if it were not to somehow affect future behavior. Indeed, movement is the only way we have of interacting with the world around us. Everything we do, including any form of communication (e.g., speech, gestures, writing, drawing), is made

possible through contraction of muscles mediated via the motor system in the brain.

Movement generation involves a series of interacting steps that transform the perception of the environment (the "what") into an appropriate motor response (the "how"). In order to produce movement we need a mechanism that translates the abstract, general concept of a motor goal into a specific, concrete course of action (Fig. 1.1, Wong et al., 2015). This is what scientists in the field of movement research call movement planning.

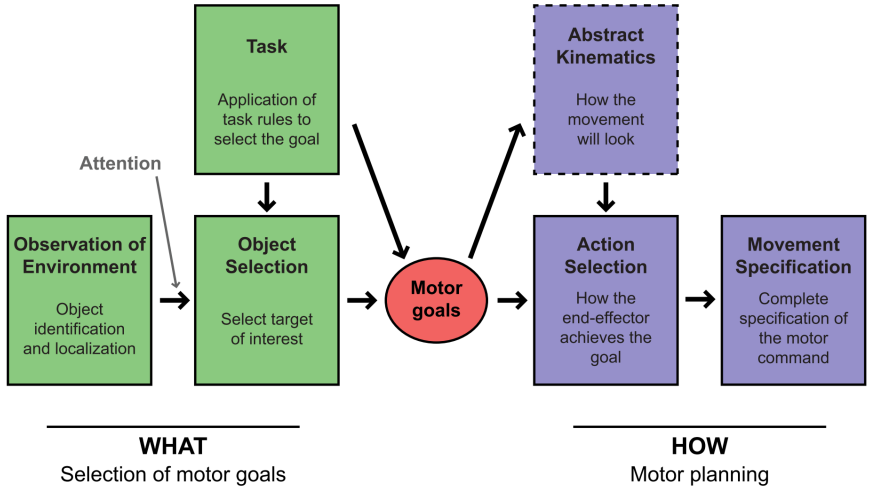

Figure 1.1 Movement planning comprises the sensorimotor processes that bridge the gap from perception to action. Adapted from Wong et al. (2015).

A classical example to showcase what this means in everyday life situations is offered by object manipulation. Let us suppose that we are thirsty and, with the overarching purpose to quench our thirst, we decide to grasp a glass of water that is placed on the kitchen table. Even for simple

reach-to-grasp movements a large amount of information must be processed by the brain in order to prepare our body for action. For instance, before any movement occurs, a series of processes must unfold enabling the brain to perceive the surrounding environment (e.g., the kitchen), select a target object of interest (e.g., the glass), decide when, where and how to approach it (e.g., reach and grasp), and issue a motor command to achieve the desired outcome (e.g., drinking). Movement planning encompasses all the neural computations and sensorimotor transformations between the definition of a movement intention and the execution of a motor program. Clearly, this constitutes a complex process that can be described at different levels of analysis (e.g., from high-level motor goals to low-level movement kinematics) and which entails close links and interactions with other cognitive functions like perception, decision-making, language and memory. Nonetheless, in healthy individuals, planning of most actions can be normally achieved in just a few hundred milliseconds, with several brain regions working together in concert to orchestrate behavior. How exactly our brain enables us with this remarkable ability at the origin of every human movement is something that we do not yet fully understand.

1.2 Prehension as a working model for movement research

All movements that human and non-human animals are capable of performing require some level of preparation. Although certain aspects of movement planning (e.g., brain regions recruited, activity profiles, temporal dynamics) vary and can be very specific for different actions, planning itself is not a unique prerogative of any one particular type of movement (e.g.,

jumping, throwing, looking), or movement effector (e.g., legs, arms, eyes). We do not only plan arm or hand movements. Rather, planning could be regarded as a (nearly automatic and often subconscious) component of the process by which our brain generates action. However, to investigate movement planning, researchers need to focus on a set of movements that can be studied in experimental settings and, at the same time, offer broader insight about brain functioning. Tool use and object manipulation fit the requirements in that they are very common and of great evolutionary importance, both for human and non-human primates, being at the very core of our daily interactions with the environment. Think about normal daily activities like giving, taking, opening, closing, cooking, writing, washing. They all have in common the need to deal with tools and objects. Moreover this class of actions can easily be used in a number of experimental ways to answer questions about sensory and motor processing in the brain. Experimenters can manipulate the type, the size or the weight of objects, their location in space, the task rules that determine the interaction (e.g., introducing delays, obstacles, occluders, specific instructions, etc.).

Prehension, the ability to reach and grasp objects, is a particular case of object manipulation, often the first step preceding the use of a tool. It is generally subdivided in two main components: reaching (or transport), i.e., the hand approaching an object; and grasping, i.e., preshaping the hand to interact with the object according to its intrinsic properties (e.g., shape and size). Given the aforementioned qualities, a large number of studies focused on the neural basis of reaching and grasping (for recent reviews, Crawford et al., 2011; Turella and Lingnau, 2014). Furthermore, beyond a good balance between ecological and experimental validity, another advantage to the study

of these movements lies in the possibility of conducting comparative studies with non-human primates (mostly macaque monkeys) that can well complement human research.

Indeed previous studies in both monkeys and humans have shown that both species have a dedicated circuitry to accomplish this kind of complex behavior, the "grasping network", or "prehension system" (Filimon, 2010; Grafton, 2010; Davare et al., 2011).

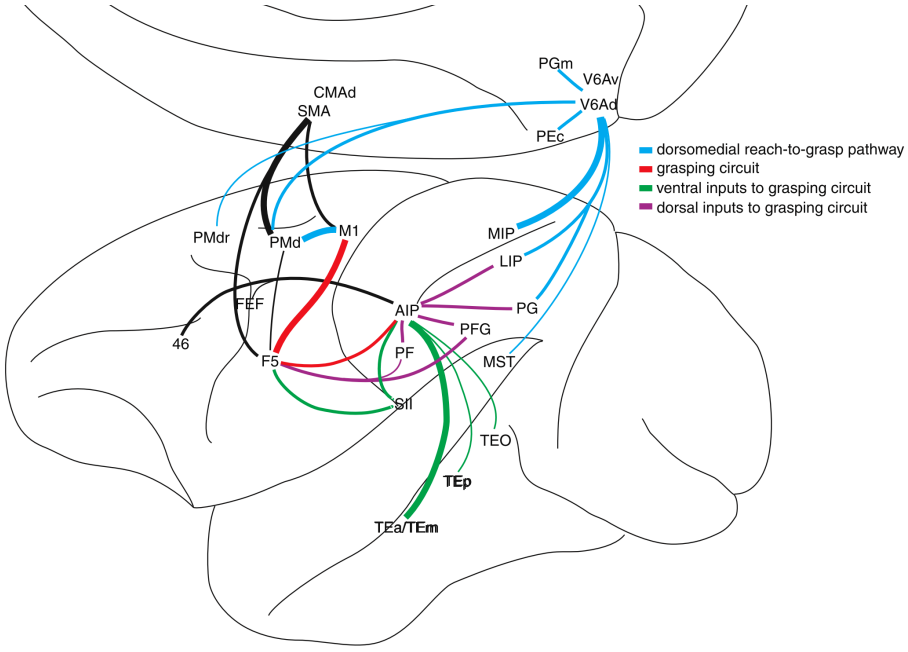

Figure 1.2 Schematic representation of the anatomical connections in the cortical prehension system of non-human primates. Adapted from Davare et al. (2011).

This brain system (Fig. 1.2) comprises a widespread network of frontal (e.g., prefrontal, premotor, primary motor, supplementary motor), parietal

(e.g., superior, inferior, posterior parietal, intraparietal, supramarginal), and temporal (e.g., superior, posterior, middle temporal) areas that, at different stages of movement generation, interact during the planning and execution of reaching and grasping movements. Given the central importance played by the prehension system in the present thesis, the following paragraphs will describe the studies concerning planning and execution of reaching and grasping movements, and what is known about the properties that are coded in these brain regions, in greater detail.

1.3 Preparatory neural activity in primates encodes movement properties

As mentioned above, movement planning must logically and causally precede the moment of execution. Before we perform any object-directed action, a motor goal must be formed and some movement parameters (e.g., direction, speed, amplitude, trajectory) specified, encoded in the firing of posterior parietal and premotor neurons of our brain. Evidence coming from neurophysiological studies confirmed this intuitive assumption. In several classical experiments, monkeys performed reaching or grasping movements while the electrical activity of single cells, or neuronal populations, was recorded in frontal (Rizzolatti and Camarda, 1988; Cisek and Kalaska, 2004, 2005, Raos, 2004, 2005; Afshar et al., 2011) or parietal areas of the monkey prehension system (Murata et al., 2000; Andersen and Buneo, 2002; Cui and Andersen, 2007, 2011; Kuang et al., 2016).

Typically, the delayed-movement paradigm is used to examine movement planning and execution: each trial starts with a fixation period of

baseline activity, usually in complete darkness to prevent unwanted visual stimulation. Next, the primate receives a cue instructing to prepare either one or multiple specific movements (e.g., reach, saccade), or movement directions (e.g., left, right). After a brief memory period a second cue appears specifying the actual target or action that, following a *"Go"* cue, has to be performed. At the *"Go"* cue the monkey moves the specified effector to the target, holds the position and, if the answer was correct, gets rewarded, before returning to the initial position.

Several studies using this paradigm observed that during the delay period, before the *"Go"* cue, neuronal firing rates increased in correspondence to the selection of certain movement features (Crammond and Kalaska, 2000; Cisek and Kalaska, 2004, 2005; Cisek, 2006; Cui and Andersen, 2007, 2011; Fig. 1.3).

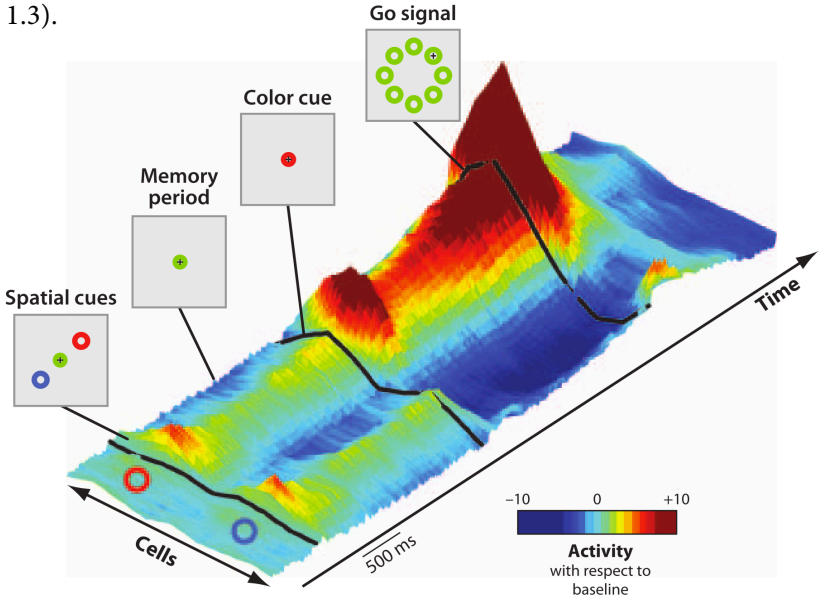

Figure 1.3 Neural population activity with respect to baseline in the primate dorsal premotor cortex during a delayed-movement reaching task. Diagrams on the left show the stimuli presented to the monkey at different stages of an example trial. Adapted from Cisek and Kalaska (2010).

When information for selecting one feature over the other became available to the monkey, the neural representation of the chosen feature was strengthened, while that of the unchosen feature was suppressed. In other words, these results show that pre-movement brain activity is predictive about some aspects of the subsequent behavior, advancing our understanding of the neural mechanisms for action selection and movement preparation.

Depending on the experimental design, the features encoded in neuronal firings for prehension movements could be spatial targets (Cisek and Kalaska, 2005), movement effectors (Cui and Andersen, 2007), or grip types (Raos, 2004). Additionally, experiments that included the possibility for the monkey to choose which effector to move (in contrast to being instructed to use a specific effector) found that pre-movement spike trains in parietal regions reflected the movement plans regardless of an internal choice or an external instruction (Cui and Andersen, 2007, 2011; Andersen and Cui, 2009).

Collectively, these observations shared between neurophysiological studies led to the conclusion that in monkeys preparatory brain signals across a network of frontal and parietal regions (i.e., the prehension system) represent relevant information about planned movements. Importantly, this information can be extracted and analyzed to understand what movement, or movement sequence (Pesaran et al., 2008), the monkey is going perform. In other words, it became possible to predict complex sensorimotor behaviors as arm or eyes movements on the basis of these changes in neural activity preceding movement onset (Andersen and Cui, 2009; Andersen and Buneo, 2002; Cisek and Kalaska, 2010).

However, until recent years, the ability to decode planning-related cortical signals to predict object-directed movements remained mostly confined to invasive neural recordings in non-human primates (Townsend et al., 2011). How and where specific movement plans are encoded in the human brain remained important yet unanswered questions.

1.4 Neuroimaging evidence for movement planning in humans

Previous functional magnetic resonance imaging (fMRI) experiments on movement planning in humans used slight variations of the delayed-movement paradigm introduced for neurophysiological studies in non-human primates (e.g., different cue modalities, delay period durations, task rules). However, due to technical difficulties intrinsic to the technique (i.e., limited space in the scanner and the need to reduce head-motion artifacts), early attempts to address movement preparation did not focus on prehension movements. Rather, these initial studies used simple button presses performed with the index and middle fingers of the right hand (Toni et al., 2001; Thoenissen et al., 2002; Cavina-Pratesi, 2006). Yet, in agreement with monkey studies, these studies reported widespread planning-related activations across a network involving not only frontal and parietal, but also extrastriate and mediotemporal regions. Furthermore, these results suggested a dissociation in the strategic roles played by posterior parietal and premotor frontal regions during the delay period of associative visuomotor tasks. While activity in parietal regions has been demonstrated to reflect stimulus-response (S-R) associations for multiple potential responses allowed by the task (Cavina-Pratesi, 2006), frontal regions have been

proposed to contain specific preparatory responses for the most likely movement (Thoenissen et al., 2002), leading to the preparation of the required motor program.

Later neuroimaging research extended these findings by investigating perceptuo-motor interactions during planning with different actions. Using reaching (Bernier et al., 2012; Gertz and Fiehler, 2015), grasping (Verhagen et al., 2008) or saccadic eye movements (Pertzov et al., 2011), these studies contributed to our understanding of the complex parieto-frontal cortical interactions that subserve visuomotor processing.

A study by Beurze and colleagues (2009) adopted a clever design to examine the planning of both hand and eye movements (i.e., reaches and saccades). In a two-stage delayed-movement paradigm, two successive visual cues instructed participants to prepare either which effector to use (eyes, right hand) or the spatial target location (left, right). The order of visual cues was randomized throughout the experiment so that in some trials the planning of the effector was independent of movement direction, and vice versa for the remaining trials. The researchers then examined which regions are selectively activated during the planning of an effector or a target location. Despite reporting a large overlap in the parieto-frontal network involved in planning eye and hand movements (i.e., limited effector specificity with clear target selectivity), they observed that the degree to which these brain areas responded more to target or effector information depended on the stage of movement generation (Fig. 1.4).

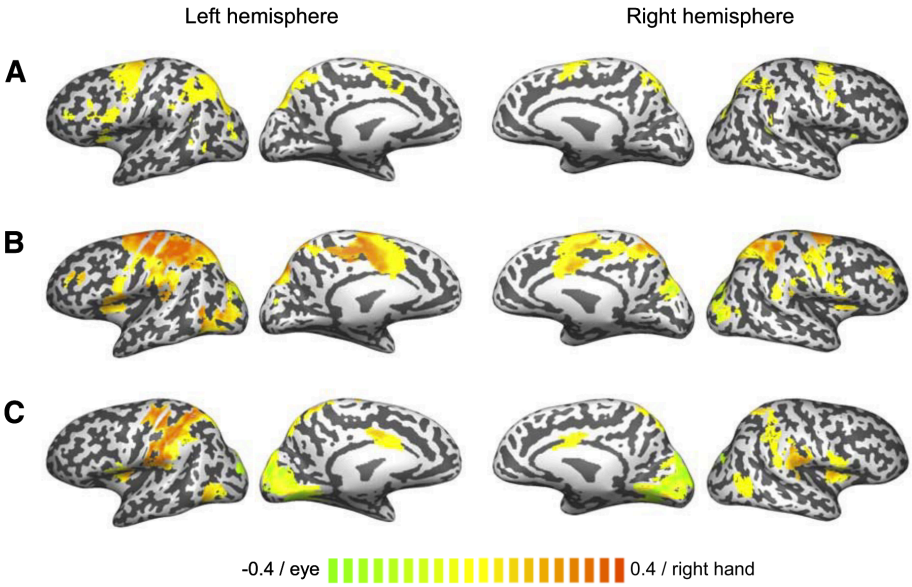

Figure 1.4 Effector specificity (saccades/eye vs. reaches/hand) in three stages of movement generation. **A:** first phase, effector cue in isolation: no significant effector specificity. **B:** second phase, combination of effector and target cues: effector selectivity in the neural circuitry involved in movement planning. **C:** movement execution stage: effector selectivity increases. Adapted from Beurze et al. (2009).

During an early planning delay, when only partial information was available (i.e., either target or effector), spatial target selectivity was predominant. During a later planning delay, when information for the actual plan was complete, they found intraparietal and the dorsal premotor regions selective to both target location and movement effector.

Whereas findings like this provided important insights into several functional aspects of the human parieto-frontal prehension network, successive studies tried to take the characterization of brain activity during movement planning one step further. They did so by starting to ask qualitatively different kinds of research questions and by utilizing a new

approach to look at the data that recent advances in fMRI analysis methods allowed.

1.5 A novel approach for fMRI studies on movement preparation

All of the neuroimaging studies referred to so far shared the same methodological limitations that are characteristic of standard fMRI analyses. Indeed, until the early 2010s, most neuroimaging studies on movement preparation typically used univariate approaches to analyze fMRI data. Borrowing from a different field of Cognitive Neuroscience (i.e., vision research, Haxby et al., 2001; Kamitani and Tong, 2005), more recent neuroimaging studies on sensorimotor control have begun adopting a method that promised to improve the sensitivity of conventional fMRI analysis while providing a new way to look at brain imaging data: multivariate pattern analysis (MVPA; for recent reviews, Haxby, 2012; Haxby et al., 2014). Univariate analyses of fMRI data assess differences in activation amplitude at the single voxel level (from here the term univariate), or, by averaging across voxels, within a region. By contrast, multivariate approaches preserve and exploit the information contained within the fine-scale spatially-distributed patterns of voxels activity to test which brain regions encode different conditions (i.e., have a neural representation of those conditions) (Fig. 1.5). The goal of univariate methods is to determine whether stimuli or tasks differ in terms of the amplitude of the blood-oxygen level dependent (BOLD) signal.

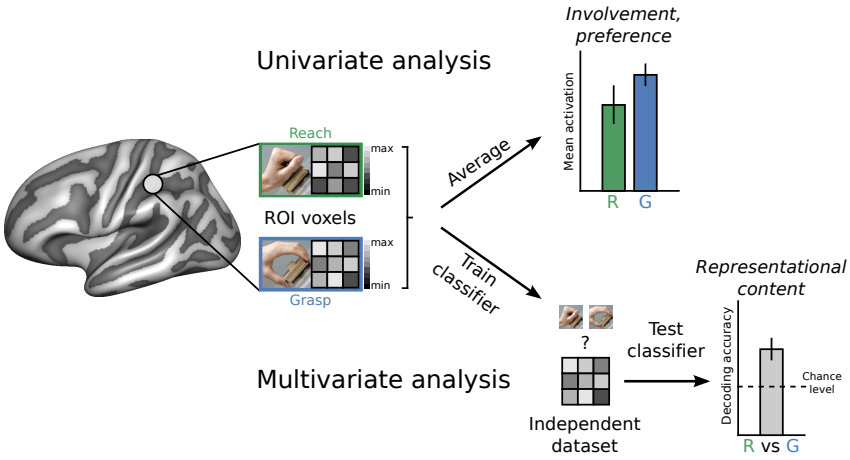

Figure 1.5 Main differences between univariate and multivariate analysis of fMRI data. The left side of the figure represents the differently active voxels (fMRI activity scale on gray levels) within a hypothetical region of interest (ROI) for reaching and grasping. The right side of the figure exemplifies the distinction between univariate (differences in mean activation, top) and multivariate analysis (classification of multi-voxel spatial patterns, bottom). Averaged activation indicates involvement or preference for a condition, pattern classification reveals the representational content of that ROI (i.e., that the ROI contains information about the condition).

To this aim, separately for each individual voxel in the brain, a general linear model (GLM) analysis estimates the BOLD amplitude (i.e., the Beta estimates) for different experimental conditions (e.g., reach vs grasp in Fig. 1.5). If the relative voxel activation for one condition (e.g., grasp) is consistently and significantly greater than the other condition (e.g., reach), then that voxel is deemed to show a preference for grasp in comparison to reach. By identifying clusters of individual active voxels within particular areas of the brain, univariate GLM analyses allow researchers to show which regions are recruited, or preferentially involved, for one among competing tasks.

However, one of the critical problems with this functional mapping approach is that, focusing solely on whether a region's averaged signal amplitude is higher or lower for one condition than another, it does not consider the information potentially contained in the relationships between multiple voxels within a voxel-population (i.e., the spatial patterns that these voxels form). Disregarding this kind of information, conventional GLM analyses may be less sensitive to subtle diffrences between conditions, such as movement plans for reaching and grasping.

MVPA has at least two advantages compared to more common univariate GLM analyses. First, by examining the informational content encoded in voxel activation patterns, it allows to make inferences about the underlying neural representations for different experimental manipulations. Second, by considering even voxels that show weak but consistent differences between conditions, MVPA provides higher sensitivity in discriminating between conditions that show similar mass-univariate effects (i.e., similar activations; Oosterhof et al., 2016).

One particular instance of MVPA methods (i.e., decoding analysis) consists of using classifiers (i.e., machine-learning algorithms such as support-vector-machines, SVMs, or linear discriminants, LDs) to discriminate between classes of stimuli on the basis of differences in the elicited spatial patterns of responses across multiple voxels. First, only a subset of the entire fMRI dataset is used to train the classifier to distinguish the voxel patterns that represent the different conditions. Next, the classifier is presented with the remaining, independent, subset of the data to test whether it can classify (i.e., decode) the learned associations between voxel patterns and conditions better than chance. The purpose of this analysis is to

determine whether the representational content elicited by two or more experimental conditions is encoded in a given brain region.

Importantly, whereas univariate methods aim at addressing questions about the involvement or preference of a brain region for certain stimuli or tasks, MVPA gave rise to a whole new set of research questions (Mur et al., 2009): how are hidden processes like intentions, goals and decisions represented in the brain? Which brain regions encode specific movements, effectors, or movement properties? Is it possible to decode movement plans by examining patterns of brain activity before movement onset, and thus predict upcoming behaviors? The answers to questions like these provided key insights into sensorimotor research and narrowed the gap between human neuroimaging and monkey neurophysiology.

1.6 Decoding motor intentions in the human parieto-frontal network

To recapitulate, while primate studies contributed to the intuition that preparatory neural activity encodes movement plans (Cisek and Kalaska, 2010), human neuroimaging studies showed that cortical parietofrontal networks involved in hand and arm movements are highly distributed, highly overlapping, and possibly organized along sensory or effector-dependent gradients (Filimon, 2010). MVPA of fMRI data proved to be a powerful analytical tool to uncover subtle differences in overlapping activations distributed across multiple voxels, and to access the cognitive contents (i.e., the neural representations) of the human mind (Haxby et al., 2014). Not much time passed before the study of prehension movements

took advantage of the recent advances in human neuroimaging methods that MVPA offered.

The first non-invasive attempt to decode upcoming object-directed actions using planning-related brain signals in humans was provided by Gallivan et al. (2011). The first challenge that the authors had to face concerned separating the brain activity associated with planning from the one elicited by execution of visually-guided reach or grasp movements towards a single centrally-located object. To do so, they used a modified version of the classical delayed-movement task. At the beginning of each trial an auditory instruction indicated to the participants which of the three hand movements to prepare (*"grasp* [the] *top"* part of the object with a pincher grip, *"grasp* [the] *bottom"* part of the object with a whole-hand grip, or *"touch"* the side of the target object with the knuckles). After a fixed 10 seconds delay (the planning phase), a *"beep"* sound prompted the subjects to perform the instructed action (execution phase). Using a univariate group-contrast (planning phase > baseline), the authors defined 14 regions of interest (ROIs) within the well-documented left-lateralized parieto-frontal network (Fig. 1.6) that are involved in movement planning.

Subsequent pattern classification analysis revealed that upcoming movements could be reliably predicted from the preparatory brain signals of the planning phase in a number of ROIs, including the intraparietal sulcus (IPS), the superior parieto-occipital cortex (SPOC), the dorsal and ventral premotor cortex (PMd, PMv), and the primary motor cortex (M1).

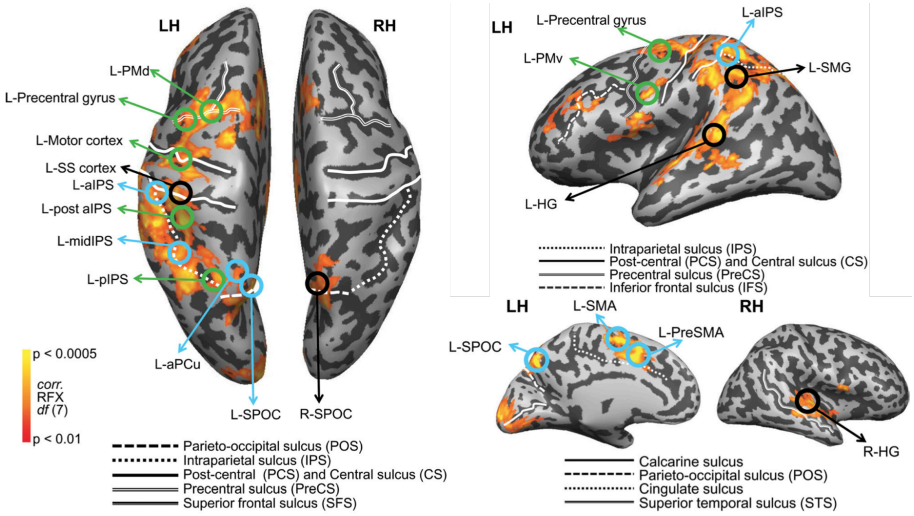

Figure 1.6 Decoding of object-directed movement intentions across the parieto-frontal network. Voxels that exhibited larger responses (i.e., activation) during movement planning than baseline are shown in orange/yellow. General locations of selected ROIs are outlined in circles and color coded according to the pairwise discriminations they can decode during the planning phase: *green*, all pairwise discriminations; *blue*, grasp versus touch; *black*, no decoding. Adapted from Gallivan et al. (2011a).

This innovative study was quickly followed up by two publications by the same group in which, using a very similar paradigm and analysis methods, they showed that more information could be extracted from human preparatory activity in fronto-parietal networks. Namely, they were able to decode not only the type of upcoming movements (reach vs. grasp), but also the intended spatial directions (left vs. right) of planned reaches and saccades (Gallivan et al., 2011b), and which limb (ipsilateral vs. contralateral arm) would be used for subsequent reach or grasp movements (Gallivan et al., 2013b). From a theoretical standpoint, the pattern classification approach used in these studies supports the idea that predictive movement information is contained in the spatial patterns of preparatory responses

within parieto-frontal regions, even, and crucially, in absence of differences in signal amplitude. Furthermore, these results offered a new understanding of previous notions (Filimon, 2010) on how frontal and parietal regions in the human brain contribute to the planning of object-directed prehension movements. First, by dissociating distributed overlapping networks for different actions; second, by identifying which areas carry the most discriminating signals for different sensorimotor functions (e.g., planning the movement direction, type, or effector).

However, despite these remarkable achievements, this approach to the study of movement planning has some limitations. First, one potential issue shared by most experiments on movement preparation (Toni et al., 2001; Mars et al., 2008; Pertzov et al., 2011; Bernier et al., 2012) lies in the use of instructed movements. By only having an instructed condition, it becomes hard for experimenters to disentangle the various components that coexist during a planning phase that is both artifical and disproportionately long compared with the natural course of events. Motor preparation always co-occurs and intermingles with the sensory processing of a visual or auditory instruction during the typical S-R mapping (Andersen & Cui, 2009). This is problematic because the brain activity measured during planning could in fact reflect a combination of movement preparation and other overlapping sensory or cognitive processes, undermining the specificity and accuracy of results, as well as the scope of the conclusions one may derive.

Second, another potentially important limitation concerns the use of the delayed-movement framework to elucidate the neural mechanisms of movement planning. During the delay period (i.e., the planning phase), subjects are not only preparing a movement, but are also withholding the

response, waiting for the right moment to execute (Ames et al., 2014). Indeed, long and fixed (i.e., non-jittered) planning delays tend to introduce brain activity unrelated to movement preparation (e.g., event anticipation, mind wandering, etc.). Consequently, it is poorly understood to what degree delay-related brain signals specifically reflect movement preparation. Moreover to what extent previous results obtained with delayed-movement paradigms can be generalized to contexts without a delay is unclear.

In my PhD I tried to address these issues related to movement preparation with the intent to better characterize the neural representations of movement plans observed within the human prehension system. The first fMRI study (Study I, Chapter 2) examined the problem related to instructed movements, whereas the second fMRI study (Study II, Chapter 3) addressed the problem related to delayed movements.

Chapter 2.

Study I: Decoding internally and externally driven movement plans

Giacomo Ariani[1], Moritz F. Wurm[1], Angelika Lingnau[1,2,3]

[1]Center for Mind/Brain Sciences (CIMeC), University of Trento, Via delle Regole 101, 38100 Mattarello (TN), Italy

[2]Department of Cognitive Sciences, University of Trento, Corso Bettini, 31, 38068 Rovereto (TN), Italy

[3]Department of Psychology, Royal Holloway University of London, TW20 0EX Egham, Surrey, UK

The work reported in the following chapter was published as:

Ariani G, Wurm MF, Lingnau A (2015) Decoding Internally and Externally Driven Movement Plans. *The Journal of Neuroscience*, October 21, 2015 • 35(42):14160–14171.

Acknowledgments

We are grateful to Jens Schwarzbach and Seth Levine for comments on the design and the manuscript, to Nick Oosterhof for advice on MVPA, and to Jens Schwarzbach for setting up the Arduino for response collection. This research was supported by the Provincia Autonoma di Trento and the Fondazione Cassa di Risparmio di Trento e Rovereto.

Author contributions

G.A., and A.L. designed research; G.A. and A.L. performed research; G.A. and M.W. analyzed data; and G.A., M.W., and A.L. wrote the manuscript.

2.1 Abstract

During movement planning, brain activity within parieto-frontal networks encodes information about upcoming actions that can be driven either externally (e.g., by a sensory cue) or internally (i.e., by a choice/decision). Here we used multivariate pattern analysis (MVPA) of functional magnetic resonance imaging (fMRI) data to distinguish between areas that represent (1) abstract movement plans that generalize across the way in which these were driven, (2) internally-driven movement plans, or (3) externally-driven movement plans. In a delayed-movement paradigm, human volunteers were asked to plan and execute three types of non-visually guided right-handed reaching movements towards a central target object, using a precision grip, a power grip, or touching the object without hand preshaping. On separate blocks of trials, movements were either instructed via color cues (Instructed condition), or chosen by the participant (Free-Choice condition). Using region-of-interest (ROI)-based and whole-brain searchlight-based MVPA, we found abstract representations of planned movements that generalize across the way these movements are selected (internally- vs externally-driven) in parietal cortex, dorsal premotor cortex and primary motor cortex contralateral to the acting hand. In addition, we revealed representations specific for internally-driven movement plans in contralateral ventral premotor cortex, dorsolateral prefrontal cortex, supramarginal gyrus, and in ipsilateral posterior parieto-temporal regions, suggesting that these regions are recruited during movement selection. Finally, we observed representations of externally-driven movement plans in bilateral supplementary motor cortex and a similar trend in pre-supplementary motor cortex, suggesting a role in stimulus-response mapping.

Key words: decoding; fMRI; free choice; movement planning; movement selection; MVPA

Significance statement

The way the human brain prepares the body for action constitutes an essential part of our ability to interact with our environment. Previous studies demonstrated that patterns of neuronal activity encode upcoming movements. Here we used multi-variate pattern analysis of human fMRI data to distinguish between brain regions containing movement plans for instructed (externally-driven) movements, areas involved in movement selection (internally-driven), and areas containing abstract movement plans that are invariant to the way these were generated (i.e., that generalize across externally- and internally-driven movement plans). Our findings extend our understanding of the neural basis of movement planning, and have the potential to contribute to the development of brain-controlled neural prosthetic devices.

2.2 Introduction

In daily life we continuously select which movements to plan and execute. Parieto-frontal regions have been implicated in the planning, execution and online control of eye and hand movements in a number of human (Binkofski et al., 1999; Connolly et al., 2002; Tunik et al., 2005; Beurze et al., 2009; Cavina-Pratesi et al., 2010; Filimon, 2010; Gallivan et al., 2011b, 2013b, 2011a; Glover et al., 2012; Barany et al., 2014; Leoné et al., 2014; Brandi et al., 2014; Fabbri et al., 2014; Gallivan and Culham, 2015) and monkey (Hoshi and Tanji, 2006; Andersen and Cui, 2009; Fattori et al., 2010; Afshar et al., 2011; Townsend et al., 2011; Lehmann and Scherberger, 2013) studies. Furthermore, pre-movement activity in both parietal and frontal regions has been shown to encode different hand configurations (Murata et al., 2000; Raos, 2004, 2005; Begliomini et al., 2007; Tunik et al., 2007; Fluet et al., 2010; Gallivan et al., 2011b; Verhagen et al., 2013).

Movements can be planned either on the basis of external cues in our environment (externally-driven), or in the absence of such cues (internally-driven). While it has been reported that the same parieto-frontal areas involved during externally-driven movements are recruited during internally-driven movements in monkeys (Cisek and Kalaska, 2005, 2010; Cui and Andersen, 2007; Pesaran et al., 2008), no previous study directly compared the planning of internally- and externally-driven movements in humans. Studies that compared externally- and internally-driven movements did not intend to separate movement planning from execution (Oliveira et al., 2010; Zhang et al., 2012; Bode et al., 2013). By contrast, studies separating between planning and execution focused on externally-driven movements and thus did not allow distinguishing between internally-

and externally-driven movements (Beurze et al., 2009; Gallivan et al., 2011a, 2011b, 2013b; Pertzov et al., 2011; Bernier et al., 2012).

Here we aimed to distinguish between brain regions representing abstract movement plans that are neither tied to specific external cues nor to internally-driven decisions, and brain regions representing movement plans specific for internally-driven or externally-driven movements (Fig. 2.1A). We asked participants to perform a delayed-movement task in which they had to plan and execute one of three different movements (i.e., reach to grasp with a precision grip, with a power grip, or reach to touch) toward a single centrally-located object (Fig. 2.1B). On each trial, a visual cue either instructed to plan a specific movement as instructed by the cue (Instructed condition, i.e., externally-driven), or it indicated to select and plan one of the three movements (Free-Choice condition, i.e., internally-driven; Fig. 2.1C). We used support-vector-machine (SVM)-based multivariate pattern analysis (MVPA) of fMRI data to compare the decoding of upcoming externally- and internally-driven movements. To examine abstract representations of movement plans that generalize across the planning conditions, we used cross-condition classification, i.e., training a classifier to distinguish between upcoming movements on the basis of externally-driven trials, and testing on internally-driven trials, and vice versa.

We reasoned that areas containing abstract movement plans should show movement selectivity that generalize across the planning condition. By contrast, areas involved in action selection should show movement selectivity in the Free-Choice but not in the Instructed condition. Finally, areas involved in the processing of sensory cues and/or the mapping between

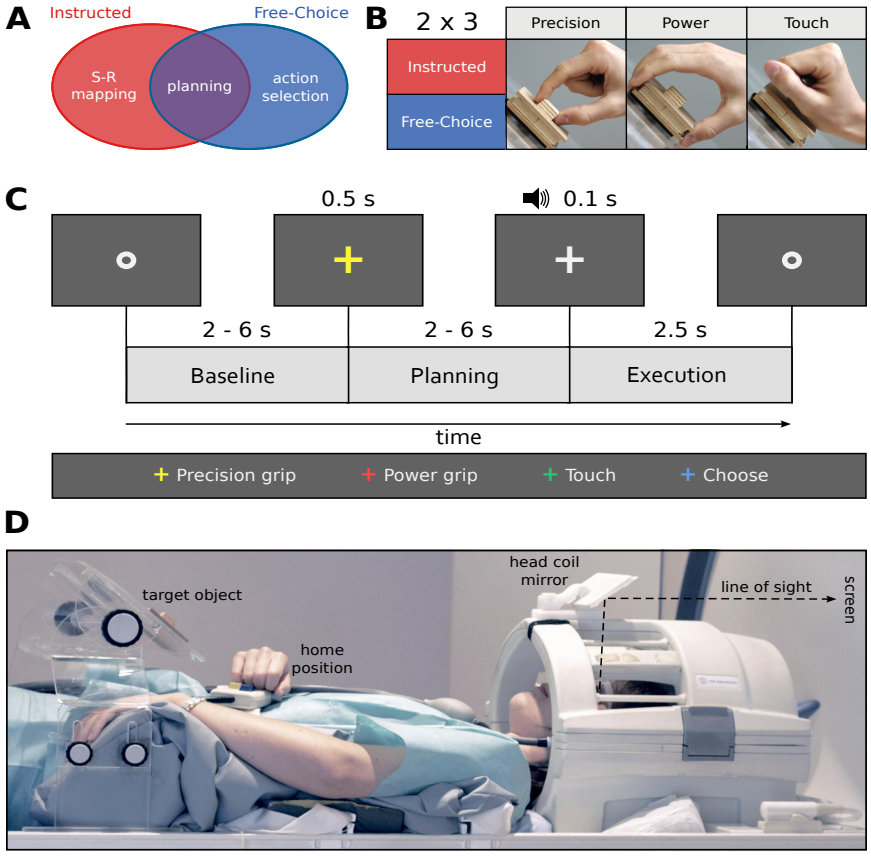

Figure 2.1 Experimental question, design, timing and setup. **A.** Schematic representation of the research question. **B.** 2x3 mixed factorial design: Planning condition (Instructed, Free-Choice), blocked, and Movement type (precision grip, PRG: two fingers only, index and thumb; power grip, PWG: whole hand open; touch, TCH: hand closed in a fist, without hand preshaping), randomized. **C.** Example trial with timing (Instructed block, PRG). Each trial began with participants fixating a dot (Baseline) for a variable amount of time randomly selected from a geometric distribution (p = 0.3, 2000 - 6000 ms). This interval was followed by a color fixation cross (500 ms) either instructing which movement to plan (Instructed blocks), or indicating to freely select one of the movements (Free-Choice blocks). The Planning phase consisted of a a jittered ISI (independently chosen from the same geometric distribution). After this delay, an auditory cue (100 ms) provided the GO-signal to start the movement (Execution phase, 2500 ms). In the Instructed condition the color of the fixation cross corresponded to one of the three movements. In the Free-Choice condition the cue always had the same, non-informative, color (in this example, blue). **D.** Lateral view of a participant with the right hand at the home position. Participants saw the screen through a mirror attached to the head coil (line of sight illustrated by black dashed line). This setup ensured that participants neither saw the target object nor their own movements.

such cues and the corresponding movements should show movement selectivity in the Instructed, but not in the Free-Choice condition.

2.3 Materials and Methods

2.3.1 Participants. Twenty-five right-handed volunteers (12 males, 13 females; mean age: 27.2 years; age range: 21-54 years) took part in the study. All participants were neurologically intact and had either normal or corrected-to-normal vision. The experimental procedures were approved by the ethics committee at the University of Trento. Participants gave written informed consent and were paid for their participation. Seven participants were subsequently excluded from data analysis: one due to technical problems with video recordings (see *Setup*), one due to not completing the experimental session, and five due to severe head motion. Rapid (i.e., taking place within one volume) head motion was detected on the basis of the 3 translation and rotation parameters resulting from 3D motion correction (cut-off criterion: > 1 mm for translation, > 1 degree for rotation). Overall, 18 participants were included in the successive analyses.

2.3.2 Setup. Visual stimuli (i.e., fixation cross and fixation dot) were back-projected onto a screen (frame rate: 60 Hz; screen resolution: 1024 × 768 pixels; mean luminance: 109 cd/m^2) via a liquid crystal projector (OC EMP 7900, Epson Nagano, Japan). Participants viewed the screen binocularly through a mirror mounted on the head coil (Fig. 2.1D). The screen was visible as a rectangular aperture of 17.8° x 13.4°. The auditory go-signal was delivered via MR-compatible headphones.

Participants performed unimanual (right hand only) reach-to-grasp movements (Fig. 2.1B) toward a single, centrally located object (according to each participant's sagittal midline) mounted on top of a workspace that consisted of a transparent plexiglas board attached to the scanner bed above the waist of the participant (Fig. 2.1D). The target object consisted of two custom-made square pieces of wood, glued on top of each other (Fig. 2.1D). To exclude uncontrolled visual stimulation by the sight of the own hands and the object, or systematic eye movements towards the object, participants were scanned in a conventional fMRI configuration (i.e., horizontally, without tilting the head towards the body; Fig. 2.1D) and were instructed to maintain fixation throughout the experiment. This precluded direct viewing of their own limbs, or the target object, while performing the task without visual feedback.

An MR compatible response button (Lumina LP 400, Cambridge Research Systems), attached to a custom belt around the waist, was pressed by the participant with the knuckles when at rest (home position, Fig. 2.1D). A microcontroller board (Arduino Uno) connected to the Lumina Controller positioned outside the magnet room was used to signal the release of that button. This time stamp was used to measure movement onset time.

To enable movements as comfortable as possible, the position of the workspace and the response button were adjusted individually to match each participant's arm length (mean distance hand-object: 16.6 cm). Head and trunk movements were minimized by stabilizing the head and the upper right arm with foam blocks and cushions.

To monitor movement execution, we recorded each experimental session using an MR-compatible digital video camera (VP-D15i; Samsung

Electronics) mounted on a tripod in a corner of the MR room (outside the 0.5-mT line). Stimulus presentation, response collection, and synchronization with the scanner were controlled using "ASF" (Schwarzbach, 2011), based on the Matlab Psychtoolbox-3 for Windows (Brainard, 1997).

2.3.3 Design. We used a mixed design with the factors *planning condition* (Instructed, Free-Choice) and *movement type* (precision grip, PRG; power grip, PWG; touch, TCH; Fig. 2.1B). *Planning condition* was blocked, *movement type* was randomized within blocks. In Instructed blocks, each movement type occurred equally often (3 times), and the color of the fixation cross indicated which movement to perform. In Free-Choice blocks, participants were instructed to choose one of the three movement types with no restrictions.

2.3.4 Procedure. To temporally isolate the neural processes associated with movement planning from movement execution, we used a delayed-movement paradigm (Andersen and Buneo, 2002; Beurze et al., 2009; Gallivan et al., 2011a, 2011b, 2013b; Fig. 2.1C). Each trial started with a grey fixation dot lasting for a variable amount of time that served to alert participants of the upcoming trial. The duration of the fixation dot was chosen from a geometric distribution (p = 0.3; 2000 - 6000 ms, in steps of 500 ms). The fixation dot was followed by a colored fixation cross for 500 ms, either instructing the type of movement to perform (Instructed condition), or indicating to select one of the movements (Free-Choice condition). The colored fixation cross was followed by a jittered inter-

stimulus-interval (ISI; Planning phase) independently chosen from a geometric distribution with the same parameters as described above. At the end of the delay period an auditory signal (duration: 100 ms, frequency: 350 hz, amplitude: 0.6) provided the GO-cue to start the movement (Execution phase, 2500 ms), and to return to the home position after completion of the movement. Participants were asked to keep the hand still and relaxed in the *home* position throughout all the phases of the trial apart from the Execution phase. Reaction times were defined as the time when the response button was released time-locked to the GO-cue.

While in the Instructed condition different color cues corresponded to different movement types, the cue always had the same, non-informative, color in the Free-Choice condition. We used two sets of color-cue assignments that were balanced across participants. Each participant completed a single experimental session consisting of a practice session outside the scanner (~20 min), the structural scan (~5 min), and 10 functional runs (~6 min each). Each functional run started and ended with 15 sec rest and contained 4 blocks of trials (2 blocks per planning condition) separated by 15 sec rest each. Between the second and the third block a longer rest period (25 sec) allowed participants to relax their right arm, wrist and hand. The order of block types (I = Instructed; F = Free-Choice) was pseudo-randomized such that the first two (or second two) blocks could never be of the same type (i.e., IFIF, FIFI, IFFI, or FIIF). Each block (~60 sec) consisted of 9 trials, for a total of 360 trials per participant. For the Instructed condition, after excluding error trials, we had an average of 58.70 (range: 50-60) repetitions per movement type and planning condition per participant. For the Free-Choice condition, the number of trials per

movement type depended on the choices of the participant, with an average of 59.68 (range: 35-81) repetitions per condition per participant (see *Multivariate pattern classification analysis* section for further details).

2.3.5 Data acquisition. Functional and structural data were collected using a 4T Bruker MedSpec Biospin MR scanner and an 8-channel birdcage head coil. Functional images were acquired with a T2*-weighted gradient-recalled echo-planar imaging (EPI) sequence. Acquisition parameters were a TR (time to repeat) of 2000 ms; voxel resolution, 3 x 3 x 3 mm; TE (time to echo), 33 ms; flip angle (FA), 73°; field of view (FOV), 192 x 192 mm; gap size, 0.45 mm. We used 28 slices, acquired in ascending interleaved order, slightly tilted to run approximately parallel to the calcarine sulcus. The number of volumes acquired in the main experiment for each functional run varied according to the length of variable delay periods (range: 178-183 volumes). Before each functional run, we performed an additional scan to measure the point-spread function (PSF) of the acquired sequence, which served for distortion correction, expected with high-field imaging (Zaitsev et al., 2004). To be able to coregister the low-resolution functional images to a high-resolution anatomical scan, we acquired a T1-weighted anatomical scan (magnetization-prepared rapid-acquisition gradient echo; TR: 2700 ms; voxel resolution: 1 x 1 x 1 mm; TE: 4.18 ms; FA: 7°; FOV: 256 x 224 mm; 176 slices; generalized autocalibrating partially parallel acquisition with an acceleration factor of 2; inversion time: 1020 ms).

2.3.6 Data analysis.

Behavioral analyses. We measured reaction time (RT) as the time to release the response button (see *Procedure*) with respect to the auditory GO-cue. Moreover, we analyzed video recordings of the experimental sessions to ensure that participants performed the movements correctly, and to know which movements were performed during the Free-Choice condition. Trials were considered errors either when performed incorrectly (i.e., incorrect hand preshaping; temporal anticipation: RT < 100 ms; reaction time timeout: RT > 1500 ms) or, in the Instructed condition only, when participants executed a movement that was different from the one instructed by the cue. Using the videos, we also counted the number of correct trials per movement type, of particular importance for the Free-Choice condition. Next, to potentially detect participants that showed stereotyped selections (i.e., cognitive strategies) or excessively frequent movement choices, we created a transition matrix that showed the number of times each movement followed any other (3-by-3 matrix, *trial_n* x *trial_n+1*). This allowed us to calculate a measure of randomness (i.e., entropy) for movement selection in Free-Choice trials (separately per participant and run), the Shannon's Entropy (Uncertainty) index (Shannon, 1948):

$$H(X) = -\sum_{i=1}^{n} p(x_i)\, log_b\, p(x_i)$$

where X is a random variable with n outcomes $\{x_1, ..., x_n\}$, and $p(x_i)$ is the probability mass function of the outcome x_i. Shannon's Entropy index (H)

ranges from 0 to $log_2 n$, where n is the number of states or possible outcomes.

fMRI data analysis.

Preprocessing. Data were preprocessed and analyzed using BrainVoyager QX 2.8.0 (BrainInnovation, Maastricht, The Netherlands) in combination with the BVQX Toolbox and custom software written in Matlab R2012b (MathWorks, Natick, MA, U.S.A.). To correct for distortions in geometry and intensity in the echo planar imaging (EPI) images, we applied distortion correction on the basis of the PSF (see *Data acquisition;* Zeng and Constable, 2002). To avoid T1 saturation, we discarded the first 4 volumes. The first volume of the first functional run of each participant was aligned to the high-resolution anatomy (6 rigid-body transformation parameters). Next, we performed 3D motion correction (trilinear interpolation for estimation and sinc interpolation for resampling) using the first volume of the first run of each participant as reference, followed by slice timing correction (ascending interleaved even-odd order) and high-pass temporal filtering (3 cycles per run). Spatial smoothing was applied with a Gaussian kernel of 8 mm full-width half maximum (FWHM) for univariate analysis only. For successive group analysis, both functional and anatomical data were transformed into a common Talairach space, using trilinear interpolation.

Univariate analysis (GLM). To localize brain areas preferentially involved in movement preparation, we computed a group random-effects (RFX) general linear model (GLM) analysis in the volume. To avoid making assumptions about the shape of the HRF during the Planning phase, we used a

deconvolution analysis, estimating the amplitude of the BOLD signal separately for each predictor and time point (TR). We created six (2 planning conditions x 3 movement types) predictors both for the Planning and Execution phases, and 1 predictor modelling the baseline between the first and second half of each run, leading to 13 (predictors) x 8 (time points) = 104 predictors. This led to independent estimates of the BOLD amplitude for each condition and time point resulting from the deconvolution analysis. Parameters from 3D motion correction (translation and rotation) and regressors for error trials (modelled separately for each time point) were also included in the model as predictors of no interest. For each voxel, the average of the estimated beta-value at the 3rd and 4th time points (i.e., 4 to 8 sec after the onset of the planning cue) was used both for uni- and multivariate analyses (for a similar procedure, see Eisenberg et al., 2010).

We aimed to identify regions of interest (ROIs) commonly reported to be involved in the planning and execution of prehension movements (see Beurze et al., 2009; Gallivan et al., 2011a, 2011b, 2013b; Fabbri et al., 2014; for a review see Turella and Lingnau, 2014). To do so, we contrasted the Planning phase against the Baseline [Planning > Baseline] (Fig. 2.2), collapsing across the two planning conditions. The resulting volumetric statistical map was corrected for multiple comparisons using a False-Discovery-Rate (FDR) < 0.05 and projected on the group-averaged surface mesh for visualization (Fig. 2.2A).

ROI definition. To identify individual ROIs objectively, we followed a similar procedure as recently used by Oosterhof, Tipper, and Downing (2012a). In brief, we first manually outlined the activations individuated through the

RFX-GLM contrast [Planning > Baseline] on the group-averaged surface mesh (for details on the creation of the group-averaged surface mesh, see *Brain segmentation, mesh reconstruction, and cortex-based alignment*), roughly circumscribing the ROIs around known anatomical landmarks (see also Gallivan et al., 2011a, 2011b, 2013b). Specifically, we used the following criteria:

- *Primary motor cortex (M1)*: around the hand-knob area in the anterior bank of the central sulcus;
- *Dorsal premotor cortex (PMd)*: at the junction of the superior frontal sulcus and the precentral sulcus;
- *Ventral premotor cortex (PMv)*: slightly inferior and posterior to the junction of the inferior frontal sulcus and the precentral sulcus;
- *Anterior intraparietal sulcus (aIPS)*: on the anterior segment of the intraparietal sulcus, at the junction with the postcentral sulcus;
- *Middle intraparietal sulcus (mIPS)*: on the middle segment of the intraparietal sulcus, not overlapping with aIPS;
- *Posterior intraparietal sulcus (pIPS)*: on the posterior segment of the intraparietal sulcus, not overlapping with mIPS;
- *Superior parietal lobule (SPL)*: the anterior portion of the superior parietal lobule, superior to the IPS and slightly posterior to the postcentral sulcus;
- *Supramarginal gyrus (SMG)*: the anterior portion of the supramarginal gyrus, slightly posterior to the postcentral sulcus and superior to the lateral sulcus;

- *Dorsolateral prefrontal cortex (dlPFC)*: on the anterior portion of the middle frontal gyrus, around Brodmann area (BA) 46 (Badre and D'Esposito, 2009);
- *Supplementary motor area (SMA)*: on the medial wall of the superior frontal gyrus, anterior to the medial end of the central sulcus, posterior to the vertical projection of the anterior commissure;
- *Presupplementary motor area (preSMA)*: on the anterior segment of the cingulate sulcus, slightly anterior to the vertical projection of the anterior commissure;
- *Posterior superior temporal gyrus (pSTG)*: the posterior portion of the superior temporal gyrus, inferior to the supramarginal gyrus;
- *Posterior middle temporal gyrus (pMTG)*: the posterior portion of the middle temporal gyrus.

Next, we projected these marked activation patches from the surface back to the volume. Within each of them, we looked for individual peak voxels coming from the single-subject GLM contrasts [Planning > Baseline], computed as described above. We defined individual ROIs, separately for each participant, as spheres (8 mm radius) centered around each individual peak voxel (for a summary of the Talairach coordinates of individual ROIs, see Table 1). To examine classification performance in regions that are not expected to show predictive power, we additionally included a non-brain control ROI outside the skull of the brain near the right frontal cortex (same size and shape as before, and identical location for all participants).

Table 2.1 TAL coordinates (x, y, z rounded mean and standard deviation across participants) of individual peak voxels for the ROIs identified by the group contrast [Planning > Baseline].

Region	**x**	**y**	**z**	**SD x**	**SD y**	**SD z**
L-M1	-33	-25	50	2,7	2,7	2,4
L-PMd	-25	-11	48	3,1	3,3	4,0
L-PMv	-46	3	27	4,5	2,3	5,1
L-aIPS	-39	-34	39	3,5	3,6	2,2
L-mIPS	-35	-45	40	2,7	3,5	2,1
L-pIPS	-30	-57	42	2,5	2,8	2,8
L-SPL	-31	-51	54	2,9	5,5	2,9
L-SMG	-56	-28	29	2,3	5,0	4,8
L-dlPFC	-36	34	28	3,4	3,3	2,8
L-SMA	-7	-3	50	1,5	2,6	4,4
L-preSMA	-8	4	41	1,7	3,6	2,5
R-pIPS	30	-50	42	2,3	3,3	2,5
R-pSTG	53	-39	13	3,9	2,7	3,0
R-pMTG	51	-51	4	3,4	5,2	3,7
R-SMA	6	-4	51	2,3	3,1	2,8
R-preSMA	7	7	39	1,6	3,3	2,3
Out of brain	51	53	56	0	0	0

Abbreviations: L-M1, left primary motor cortex; L-PMd, left dorsal premotor cortex; L-PMv, left ventral premotor cortex; L-aIPS, left anterior intraparietal sulcus; L-mIPS, left middle intraparietal sulcus; L-pIPS, left posterior intraparietal sulcus; L-SPL, left superior parietal lobule; L-SMG, left supramarginal gyrus; L-dlPFC, left dorsolateral prefrontal cortex; L-SMA, left supplementary motor area; L-preSMA, left pre-supplementary motor area; R-pIPS, right posterior intraparietal sulcus; R-pSTG, right posterior superior temporal gyrus; R-pMTG, right posterior middle temporal gyrus; R-SMA, right supplementary motor area; R-preSMA, right pre-supplementary motor area.

Multivariate pattern classification analysis. We ran both ROI- and searchlight-based MVPA using support-vector-machines (SVM) as implemented in LIBSVM (Chang and Lin, 2011). The ROI analysis served to test whether we could decode planned movements in the regions identified individually by the functional contrast [Planning > Baseline] as described above. In addition, to rule out that we missed potentially important regions in the ROI analysis, we carried out a whole-brain surface-based searchlight analysis (Oosterhof et al., 2011; see also *Further observations* in the Discussion). For the MVPA we estimated beta weights using the same design matrices as in the univariate analysis, except for the following: because participants freely selected which movements to plan and execute in the Free-Choice condition, the number of trials per movement type in this condition was not fully balanced. To prevent classification on the basis of the number of trials instead of the spatial patterns of brain activity, we balanced the number of trials per movement type in the Free-Choice and the Instructed condition by levelling to the minimum number of repetitions in either condition within each run, and discarding the trials in excess (randomly selected among the total). Beta maps containing the mean of the beta estimates of the 3rd and 4th timepoint for each predictor of interest (13,

see *Univariate analysis*), individual spherical ROI (133 voxels) and run (10) were created for each participant. These maps were then *z*-transformed and normalized into multivoxel patterns of *t*-values (beta estimates divided by their standard error) that we used as input for the classifier. This procedure resulted in 10 multivoxel patterns of *t*-values per planning condition (one per experimental run). Classification accuracies were computed using a *leave-one-run-out* cross-validation method, i.e., the classifier was trained using data from 9 patterns and tested on the data from the remaining pattern. Note that while for the within-condition decoding all 10 patterns came from the same condition, the classifier was trained with 9 patterns from one planning condition (e.g., Free-Choice) and tested on one pattern from the other planning condition (e.g., Instructed) for the cross-condition decoding. Training and testing was repeated for 10 iterations, using all possible combinations of train and test patterns. The average across these 10 iterations constituted the mean decoding accuracy per participant and ROI.

To decode upcoming hand movements from preparatory brain activity patterns, multiple binary classifiers were trained to discriminate between two movements within each of the three possible pairs of movements (i.e., precision grip vs power grip, precision grip vs touch, and power grip vs touch) during the Planning phase, separately for the Instructed and the Free-Choice condition. Classification accuracies from the three binary classifiers were successively combined to produce an average accuracy per ROI.

To test for representations of planned movement types independent of the planning condition, we carried out cross-condition decoding, i.e., training the classifier on discriminating movement pairs in one condition (e.g., precision grip vs power grip in the Instructed condition) and testing

the performance of the classifier to distinguish between the same pair of movements in the other planning condition (e.g., precision grip vs power grip in the Free-Choice condition), and vice versa. As before, the mean of the three binary classifiers was computed to produce one accuracy score per ROI. Results from the two cross-condition decoding analyses (i.e., train on Instructed condition, test on Free-Choice condition, and vice versa) were also averaged. Finally, we carried out the same within-condition decoding analysis described above for the Execution phase, but, given that no differences were expected after the movement had started, we collapsed across planning conditions.

To assess statistical significance of the decoding accuracy, we entered the individual (N = 18) classification accuracies (averaged across the three binary classifiers) into two-tailed one-sample t-tests across participants against chance decoding (50%), separately for each ROI. Furthermore, to directly compare our main conditions of interest we performed post-hoc two-tailed paired samples t-tests between planning conditions for each ROI. Statistical results were corrected for multiple comparisons (number of ROIs x number of tests) using the False-Discovery-Rate (FDR) method (Benjamini and Yekutieli, 2001).

Brain segmentation, mesh reconstruction, and cortex-based alignment (CBA). To create high quality 3D brain reconstructions, we gathered, when available, multiple anatomical scans from each participant collected in different experiments carried out at the Center for Mind/ Brain Sciences, which we aligned and averaged (min: 1, max: 13 scans). Individual surface meshes for each hemisphere were reconstructed along the border between

grey and white matter. Next, individual reconstructions of each hemisphere were used to generate individual spherical surfaces for each participant that were then morphed to a template surface (a standard sphere). A coarse-to-fine moving target approach with four coarse-to-fine levels of smoothing was then used to extract multiscale surface curvature maps that reflect the gyral and sulcal folding patterns (Fischl et al., 1999; Goebel et al., 2006). This information allowed us to align the individual standardized spherical surfaces of all participants to a group-averaged spherical surface. Transformation matrices resulting from the cortex-based alignment of individual spherical surfaces to the group-averaged spherical surface were then used to align individual functional maps before entering group statistics. Finally, using the curvature maps from CBA, we combined (i.e., averaged) the individual reconstructions of folded surfaces of all participants (N = 18) to create one group mesh for each hemisphere. Group-averaged left and right hemisphere meshes were used to display statistical maps resulting from both uni- and multivariate group-analyses.

Surface-based Searchlight SVM-MVPA. The spherical searchlight (8 mm radius) was restricted to the surface by only including voxels from -1 to 3 mm along the grey/white matter boundary. Decoding procedures were very similar to the ones used for the ROI-based MVPA. For each hemisphere, we first created mesh time courses from the volume time courses. Next, we used mesh time courses to generate whole-brain *t*-maps (20 per participant: 2 hemispheres x 10 runs), and finally we ran pairwise classifications on the *t*-maps as described above. Decoding results of the spherical searchlight were assigned to the central voxel. Individual surface accuracy maps were

projected onto the group-averaged cortical surface mesh (see *Brain segmentation, mesh reconstruction, and cortex-based alignment*) and then anatomically aligned using the transformation parameters derived from cortex-based alignment. We successively performed a two-tailed one-sample *t*-test across individual cortical maps to identify vertices where classification was significantly greater than chance (50%). Statistical *t*-maps were thresholded at $p < 0.01$ and corrected for multiple comparisons ($p < 0.05$) using a cluster-size algorithm (Forman et al., 1995) based on Monte Carlo simulations (1000 iterations) as implemented in Brain Voyager 2.8.0. For each hemisphere, we generated *t*-maps and decoding accuracy maps separately for the Instructed condition, the Free-Choice condition, and across planning conditions.

2.4 Results

2.4.1 Behavioral results

Reaction times (RTs). Participants responded slightly faster in the Instructed [602.12 ± 18.67 ms] compared to the Free-Choice condition [605.51 ± 18.65 ms; $F(1,17) = 8.37$, $p < 0.01$]. However, RTs did not differ between movement types [$F(2,34) = 0.42$, $p < 0.65$], and the interaction between planning condition and movement type was not significant [$F(2,34) = 2.66$, $p < 0.08$].

Error rates (ERs). Participants were generally accurate in performing the delayed-movement task. Overall error rates were very low: 2.15% of all the trials in the Instructed condition, and 0.54% in the Free-Choice condition.

The fact that error rates were lower in the Free-Choice compared to the Instructed condition was expected given that, while errors in the Free-Choice condition only concerned kinematics, timing, or hand preshaping of the movements, errors in the Instructed condition also included executing a movement that was different from the instructed movement type.

Shannon's Entropy in Free-Choice trials. To examine whether the movements selected in successive trials followed a regular pattern, we calculated a measure of randomness for movement selection in Free-Choice trials, defined as Shannon's Entropy index (Shannon, 1948; see *Materials and methods*). A low entropy index ($0 < H < 1$) indicates that one of the outcomes was chosen more often than others, or that the participant used a stereotyped transition pattern (e.g., 1 2 3, 1 2 3, etc.). By contrast, a high entropy index ($H > 1.5$) indicates that it is very hard to predict the next outcome on the basis of the previous outcomes. In our study, the mean entropy index per participant was 1.53, which is close to the maximum entropy level for three alternatives ($H = 1.584$). This analysis indicates that participants did not choose movements in a systematic, predictable way. As an example, this is a sequence chosen in the two consecutive blocks of one run by a representative participant: 2,1,2,3,2,2,1,1,3 and 2,1,2,3,2,3,1,2,2 (1 = precision grip, PRG; 2 = power grip, PWG; 3 = touch, TCH).

2.4.2 Univariate RFX-GLM results. To identify brain regions preferentially recruited during movement planning, we carried out a univariate random effects general linear model (RFX-GLM) contrast [Planning > Baseline] (Fig. 2.2A).

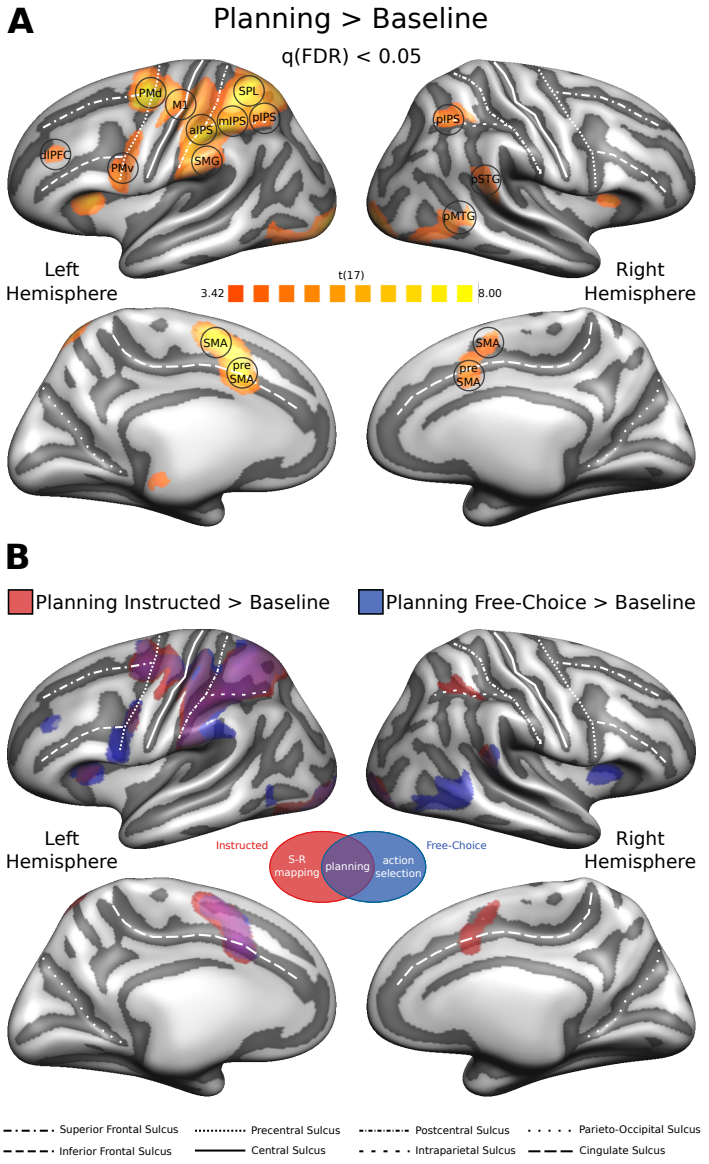

Figure 2.2 Univariate RFX-GLM analysis. **A.** The univariate contrast [Planning > Baseline] collapsing across planning conditions. The statistical RFX group-map (N = 18) was corrected for multiple comparisons using a false discovery rate q(FDR) < 0.05 and projected on the group-averaged inflated surface mesh for visualization. Individual spherical ROIs (black circles) were defined as spheres (8 mm radius) around individual peak voxels resulting from single-subject statistical maps (see Table 1). **B.** Univariate contrast [Planning > Baseline], separately for each Planning condition ([Planning Instructed > Baseline], red; [Planning Free-Choice > Baseline], blue). Purple areas denote the overlap between the two statistical group maps.

Note that this contrast is unbiased with respect to comparisons between the Instructed and Free-Choice Planning condition, or between different movement types. The resulting statistical map was used to define 16 group-ROIs: left primary motor cortex (L-M1); left dorsal and ventral premotor cortex (L-PMd, and L-PMv, respectively); left anterior, middle and posterior intraparietal sulcus (L-aIPS, L-mIPS, and L-pIPS, respectively); left superior parietal lobule (L-SPL); left supramarginal gyrus (L-SMG); left dorsolateral prefrontal cortex (L-dlPFC); left supplementary motor area (L-SMA); left pre-supplementary motor area (L-preSMA); right posterior intraparietal sulcus (R-pIPS); right posterior superior temporal gyrus (R-pSTG); right posterior middle temporal gyrus (R-pMTG); right supplementary motor area (R-SMA); and right pre-supplementary motor area (R-preSMA; for details on the definition of individual ROIs, see the section *Univariate analysis (GLM) and ROI definition* and Table 2.1). Additionally, we contrasted the Planning phase against the Baseline separately for the two planning conditions ([Planning Instructed > Baseline]; [Planning Free-Choice > Baseline], Fig. 2.2B). Overall, the statistical maps for the Instructed and Free-Choice planning condition looked very similar, in particular in the left hemisphere, and the direct comparison [Planning Instructed > Planning Free-Choice] did not reveal any significant univariate effects.

2.4.3 Multivariate results.

ROI-based MVPA. In the ROI-based MVPA we tested whether upcoming movements could be decoded on the basis of patterns of preparatory brain activity within regions recruited during movement planning. To this end, for each ROI and planning condition we ran two-tailed one-sample *t*-tests (FDR

corrected for multiple comparisons) on the mean decoding accuracy across participants (N = 18) against chance (50%). Figure 3 shows the mean classification accuracy in each ROI for averaged pairwise comparisons of movement types in four types of ROIs: (1) During the Planning phase, i.e., before any movement occurred, we found significant decoding of movement type both within (red and blue bars) and across (yellow bars) planning conditions in L-mIPS, L-pIPS, L-PMd, L-SPL, L-aIPS and L-M1, suggesting abstract representations of planned movements that generalize across planning condition (i.e., Instructed vs Free-Choice; Fig. 2.3A). (2) In R-pIPS, L-dlPFC, R-pSTG, L-PMv and R-pMTG we were able to predict upcoming movements for the Free-Choice planning condition, but not for the Instructed planning condition (Fig. 2.3B). In L-SMG we found a similar trend (p = 0.044) that did not survive FDR correction for multiple comparisons. (3) In L-SMA we obtained above chance decoding for the Instructed, but not for the Free-Choice planning condition (Fig. 2.3C). R-SMA (p = 0.018), L-preSMA (p = 0.033) and R-preSMA (p = 0.026) showed trends in the same direction that did not pass FDR correction. (4) As expected, decoding of movement type was not possible (i.e., chance performance for all experimental conditions) in the non-brain control region outside the brain (Fig. 2.3D).

To further examine the nature of our effects, we performed post-hoc two-tailed paired samples t-tests on the mean decoding accuracy between the two planning conditions for each ROI. After FDR correction for multiple comparisons (q < 0.05), these tests revealed a significant effect in L-PMv ($t(17)$ = -4.44, p = 0.0004), indicating that decoding was significantly higher for Free-Choice compared to Instructed planning in this region.

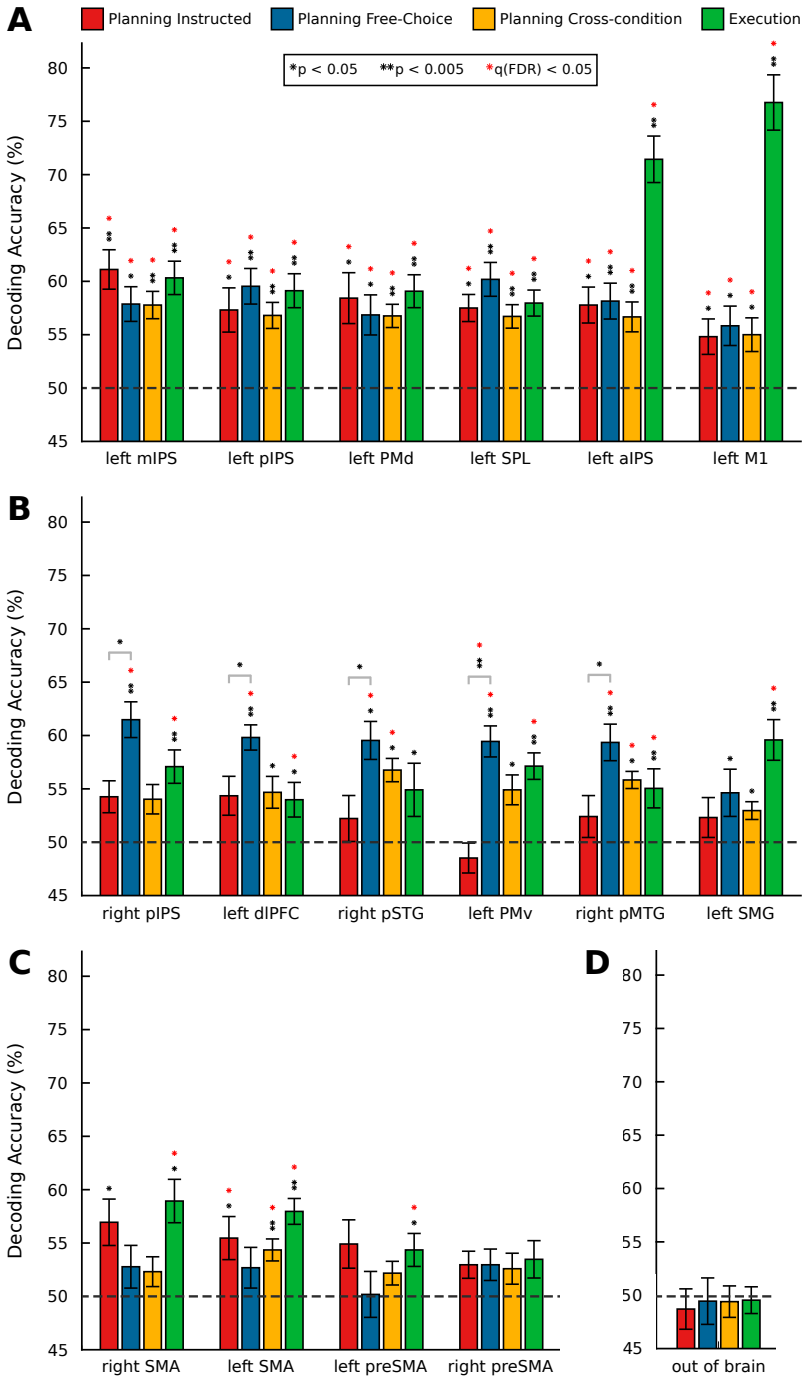
A
Planning Instructed
Planning Free-Choice
Planning Cross-condition
Execution
*p < 0.05 **p < 0.005 *q(FDR) < 0.05
Decoding Accuracy (%)
left mIPS
left pIPS
left PMd
left SPL
left aIPS
left M1
B
right pIPS
left dlPFC
right pSTG
left PMv
right pMTG
left SMG
C
right SMA
left SMA
left preSMA
right preSMA
D
out of brain

Figure 2.3 ROI-based MVPA. Mean percentage decoding accuracies for movement type resulting from multiple binary classifiers. SVM classification accuracies for the three possible discriminations between movement pairs were averaged to produce a unique score per ROI and planning condition. Red bars, Planning Instructed; blue bars, Planning Free-Choice; yellow bars, Planning cross-condition (see Methods); green bars, Execution (collapsing across Planning conditions). Statistical significance was assessed via one-sample *t*-tests (two-tailed) against 50% chance. Results were FDR-corrected for multiple comparisons (number of ROIs x number of tests). Significance levels: one black asterisk, uncorrected $p < 0.05$; two black asterisks, uncorrected $p < 0.005$; one red asterisk, FDR corrected $q < 0.05$. **A.** Regions where we found both significant within- and cross-condition decoding. **B.** Regions where we observed significant effects (or trends) for the Free-Choice, but not for the Instructed Planning task. **C.** Regions where we observed significant effects (or trends) for the Instructed, but not for the Free-Choice Planning task. **D.** Control non-brain region outside the brain.

Post-hoc comparisons that did not survive FDR correction for multiple comparisons include R-pIPS ($p = 0.016$), L-dlPFC ($p = 0.027$), R-pSTG ($p = 0.042$) and R-pMTG ($p = 0.045$).

Finally, during the Execution phase (Fig. 2.3, green bars), we were able to decode upcoming movements in all the ROIs, with the exception of R-pSTG (trend at $p = 0.043$), R-preSMA ($p = 0.063$) and the non-brain control region. Not surprisingly, we observed the highest decoding accuracy during the execution phase in the left (contralateral) primary motor cortex (L-M1), followed by the left aIPS.

Searchlight-based MVPA. To identify additional regions beyond our ROIs that potentially represent information about upcoming movements, we conducted a whole-brain searchlight-based MVPA on the surface (Fig. 2.4, Fig. 2.5). Figure 2.4 shows the performance of the classifier across the two planning conditions superimposed on the group-averaged inflated surface mesh.

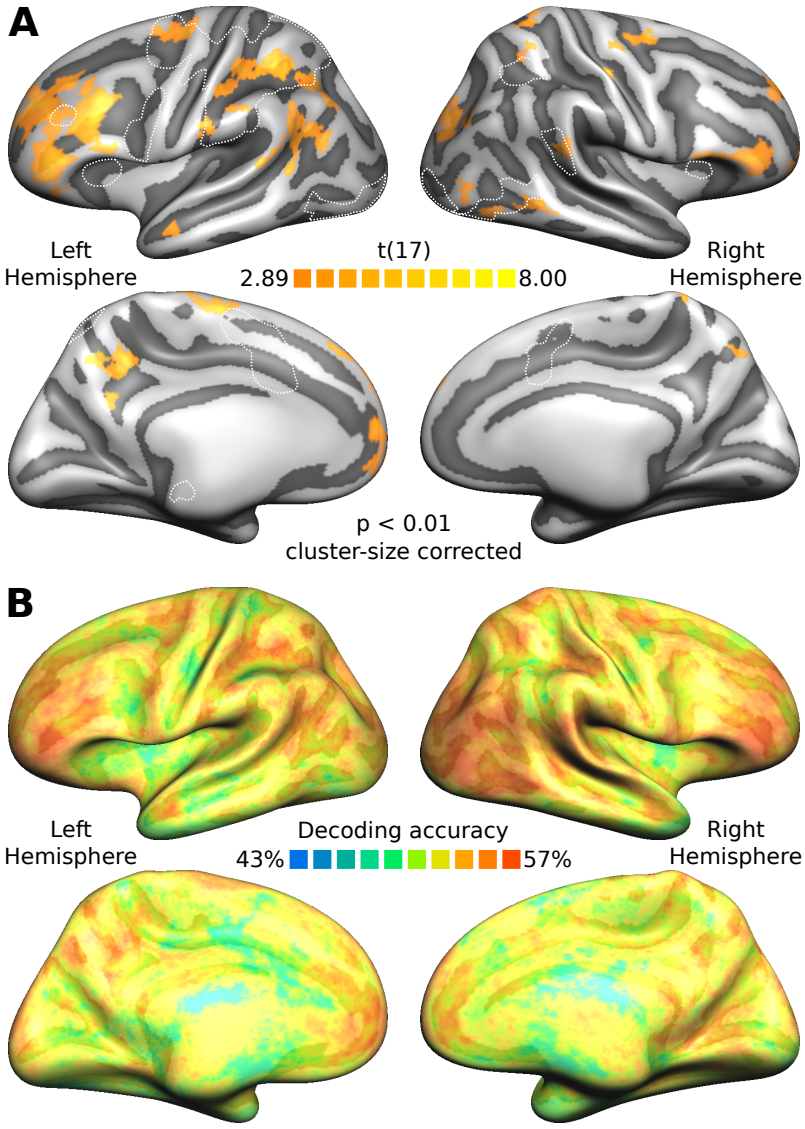

Figure 2.4 Searchlight SVM-MVPA: cross-condition decoding. The spherical searchlight (8 mm radius) was restricted to the surface (-1 to 3 mm). Decoding procedures were very similar to the ones used for the ROI-based MVPA (see Materials and Methods section). **A.** Group *t*-map (thresholded at $p < 0.01$ and then cluster-size corrected) for the cross-condition decoding projected on the group-averaged surface mesh. White dashed lines indicate the outlines of the statistical map revealed by the univariate contrast [Planning > Baseline]. **B.** Group accuracy map (%) for cross-condition decoding.

The cross-condition decoding *t*-map (Fig. 2.4A) revealed significant clusters in left orbitofrontal (L-OFC) and fronto-polar cortex (L-FP), L-dlPFC, posterior dorsal L-SMA, L-PMd, left anterior superior temporal sulcus (L-aSTS), L-IPS, inferior L-SPL, L-pSTG, L-SMG, left angular gyrus (L-AnG) and the left precuneus (L-preCu). In the right hemisphere, this analysis revealed significant clusters in R-FP, R-PMd, R-SPL, right superior parieto-occipital cortex (R-SPOC), R-pSTG, R-MTG and right lateral occipital gyrus (R-LOG).

Figure 2.5A shows the within-condition-decoding *t*-maps with cluster-size correction (p = 0.05) for multiple comparisons (red, Instructed; blue, Free-Choice) and their overlap (purple). Overall, significant clusters for Instructed and Free-Choice Planning appeared in neighboring but mostly non-overlapping locations (except for the left anterior fronto-median cortex, bilateral superior dlPFC and pSPL), and generally more widespread for the Free-Choice in comparison to the Instructed condition, especially in frontal (FP, dlPFC, PMd) and parietal (IPS, pIPL, pSPL) areas. For the Free-Choice planning condition we obtained significant clusters in the left hemisphere in the anterior fronto-median cortex and L-OFC, L-FP, L-dlPFC, L-PMv, L-PMd, L-aIPS, L-pSPL, L-SPOC, L-AnG. In the right hemisphere, this analysis revealed significant clusters in R-FP, superior R-dlPFC, R-aIPS, R-SMG, R-pSTG, R-pIPS, the right posterior inferior parietal lobule (R-pIPL), R-pSPL, R-SPOC, and, medially, the right cuneus (R-Cu) and R-preCu. For the Instructed planning condition we obtained significant clusters in the left hemisphere in the superior L-dlPFC, the anterior fronto-median cortex (slightly anterior to L-SMA and superior to L-preSMA), L-PMd, L-SMG, L-pSPL, and L-LOG.

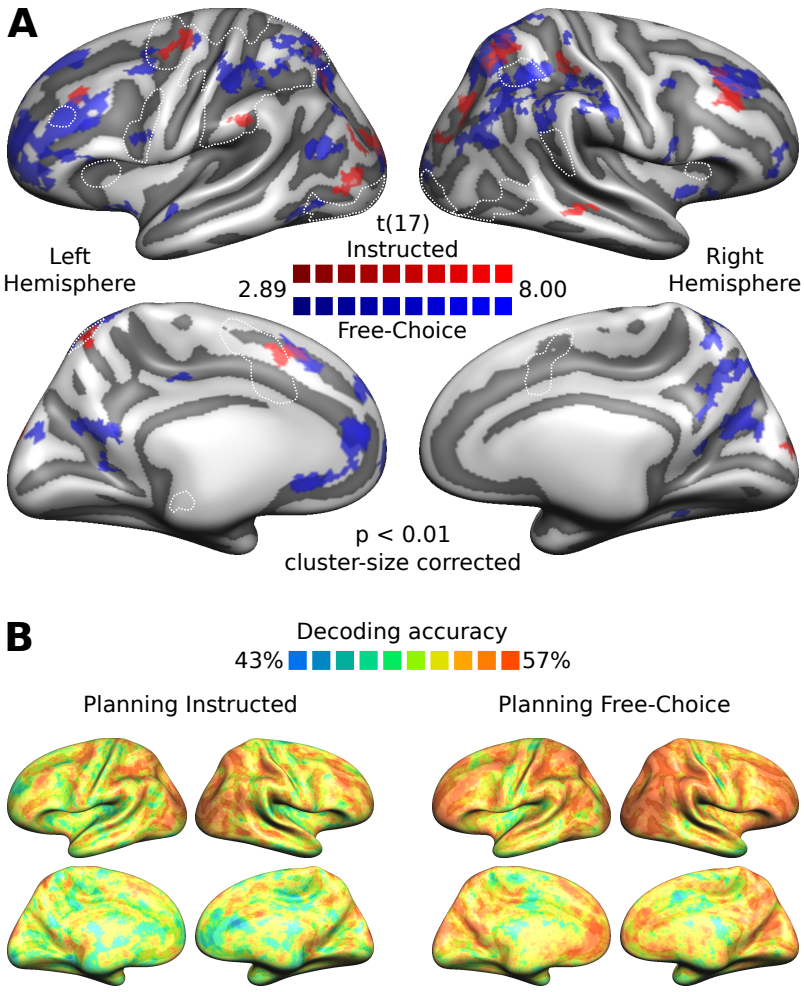

Figure 2.5 Searchlight SVM-MVPA: within-condition decoding. **A.** Group *t*-maps (thresholded at $p < 0.01$ and then cluster-size corrected), separately for each planning condition (red, Instructed; blue, Free-Choice), projected on the group-averaged surface mesh. **B.** Group decoding accuracy maps (%) separately for each planning condition (Planning Instructed, left; Planning Free-Choice, right). All other conventions are the same as in Fig. 2.4.

For the right hemisphere, we obtained significant clusters in the superior R-dlPFC, the anterior R-SPL (right above R-aIPS), R-MTG (extending to the

superior temporal sulcus), R-pSPL and R-SPOC. When using a more conservative threshold of $p < 0.001$ (not shown here), only clusters in L-dlPFC, L-PMd, L-IPS, for the cross-condition decoding, and in bilateral dlPFC, pSPL, L-aIPS, and R-pIPS for the Free-Choice planning condition survived (i.e., no clusters for Instructed planning condition).

Figures 2.4B and 2.5B illustrate mean decoding accuracies for the cross-condition (Fig. 2.4B) and within-condition (Fig. 2.5B) decoding. These figures show both significant and sub-threshold clusters of decoding accuracy to complement the information present in the searchlight *t*-maps. Although we observed slight discrepancies between the ROI-based and searchlight-based MVPA results in some regions (L-M1, L-aIPS, L-mIPS, L-SMG, R-pMTG, R-pSTG), overall searchlight results appear to be largely in line with ROI results in several frontal (L-dlPFC, L-PMd, L-PMv, bilateral SMA and preSMA) and parietal (L-pIPS, R-pIPS, L-SPL) regions (for a comparison of the two MVPA approaches see section *Further observations* in the Discussion).

2.5 Discussion

Frontal and parietal regions recruited during movement planning encode information about upcoming movements (Andersen and Buneo, 2002; Cisek and Kalaska, 2005; Cui and Andersen, 2007). Here we aimed to distinguish between areas representing abstract movement plans, areas involved in movement selection, and areas involved in the mapping between arbitrary sensory cues and the corresponding responses. We obtained three key results (summarized in Fig. 2.6): (1) contralateral (i.e., left) SPL and IPS, PMd and

M1 discriminate between planned movements irrespective of the planning condition (i.e., both within and across internally- and externally-driven movements); (2) contralateral (i.e., left) PMv, dlPFC, SMG and ipsilateral (i.e., right) pIPS, pSTG, and pMTG encode internally-driven but not externally-driven movement plans. (3) Bilateral SMA, possibly supported by pre-SMA, encodes the processing of externally-driven movement plans.

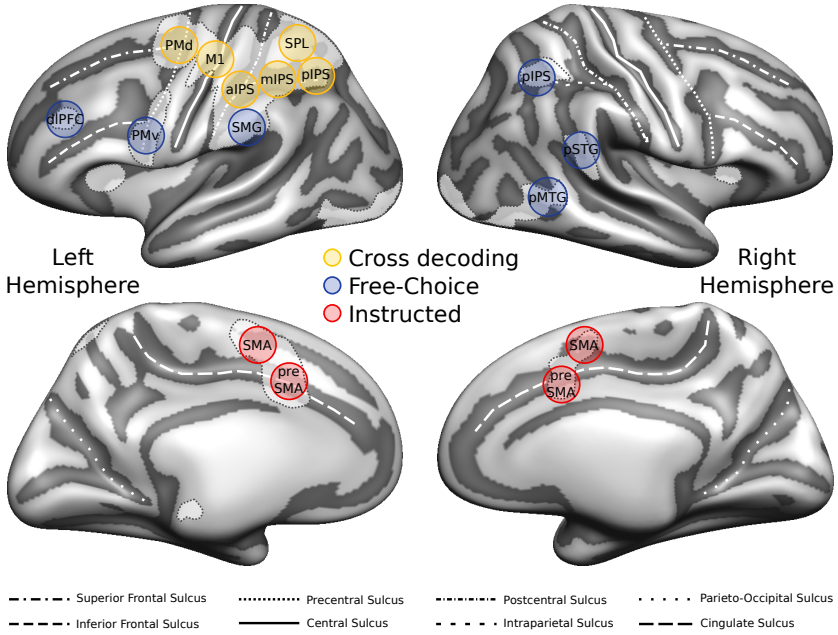

Figure 2.6 Summary of decoding results for the Planning phase. Circles superimposed on the group-averaged surface mesh represent examples of individual spherical ROIs color-coded according to the results of the ROI MVPA (significant cross-condition decoding, yellow; preferential decoding for Free-Choice planning, blue; preferential decoding for Instructed planning, red). White-shaded areas with dashed outlines indicate the statistical map revealed by the univariate contrast [Planning > Baseline].

2.5.1 Areas representing abstract movement plans

We obtained significant within-condition decoding of movement plans for both planning conditions, as well as significant cross-condition decoding, in the left (i.e., contralateral to the moving limb) SPL, pIPS, mIPS, aIPS, PMd and M1 (Fig. 2.3A, Fig. 2.6). Our results are in line with studies showing that premotor regions are sensitive to arbitrary instructing cues (i.e., which movement to perform, or which effector to use; Hoshi and Tanji, 2000, 2006, 2007), while also participating in action selection, when movements are freely chosen (Cisek and Kalaska, 2005; Pesaran et al., 2008; Beudel and De Jong, 2009; Klaes et al., 2011). Our results thus show that contralateral parieto-frontal regions represent abstract movement plans that are invariant to the way these are generated rather than being tied to simple stimulus-response mapping (Hartstra et al., 2011, 2012) or movement decisions.

Movement plans can be abstract in a number of different ways. For instance, Gallivan et al. (2013a, 2013b) observed that bilateral posterior parietal cortex (PPC), PMd, posterior fusiform sulcus (pFs) and fusiform body area (FBA) contain representations of upcoming movements that generalize across the effector (left vs right hand). These studies provide further evidence for abstract representations of movement plans in frontal, parietal and ventral stream areas.

During movement execution, aIPS and M1 have been shown to represent handwriting movements generalizing across letter scale (Kadmon Harpaz et al., 2014). During movement observation, a number of recent studies revealed abstract action representations that generalize across viewpoint and modalities (Oosterhof et al., 2012a), and the object on which these actions are performed (Wurm and Lingnau, 2015; Wurm et al., 2016), in aIPS and

lateral occipitotemporal cortex (LOTC). Further research is required to determine to which degree abstract movement representations are shared across planning, observation, and execution.

2.5.2 Areas involved in action selection

We were able to decode upcoming movements in the Free-Choice, but not in the Instructed condition in contralateral (left) PMv, dlPFC, SMG and ipsilateral (right) pIPS, pSTG, and pMTG (Fig. 2.3B, Fig. 2.6). The dorsolateral pathway has been historically associated with grasping movements (Jeannerod et al., 1995; Luppino et al., 1999; for a recent review see Turella and Lingnau, 2014). Our results extend these findings by revealing areas preferentially representing the selection rather than the planning of movements.

In contrast to studies that found significant decoding for instructed movements in PMv (Gallivan et al., 2011a, 2013b), we were able to decode upcoming movements in PMv for internally-driven but not for externally-driven movements, suggesting a more prominent role in action selection (i.e., deciding which movement to perform). It is possible that these inconsistencies are due to methodological differences. As an example, in contrast to the studies by Gallivan et al. (2011a, 2013b), participants in the current study neither saw the object nor their own hand throughout the experiment. Likewise, our planning phase was substantially shorter than the planning phase used by Gallivan et al. (2011a, 2013b). It is therefore possible that PMv represents both internally- and externally-triggered movement plans, depending on the availability of sensory cues and/ or time for movement planning.

We were able to decode internally-triggered movement plans in pMTG, a portion of the LOTC. LOTC is recruited during the processing of a variety of visual stimuli, e.g., basic and biological motion, tools, body parts and actions, but also has been implicated to host action concepts (for a recent review, see Lingnau and Downing, 2015). In addition, and perhaps more surprising, LOTC has been demonstrated to be recruited during the planning and control of actions (Astafiev et al., 2004; Johnson-Frey et al., 2005; Verhagen et al., 2008; Kühn et al., 2011; Gallivan et al., 2013a, 2015; Kilintari et al., 2014). Integrating various kinds of information from the dorsal (e.g., visuo-spatial, motoric) and the ventral stream (e.g., semantics), LOTC might be an optimal site of convergence to create a link between perceiving, understanding and interacting with the environment (Lingnau and Downing, 2015). Moreover, LOTC and the dorsal stream might exchange information about upcoming movements and/ or anticipated sensory consequences of selected actions (Verhagen et al., 2008; Kühn et al., 2011; Gallivan, 2014; Lingnau and Downing, 2015). Finally, some studies suggest that, in contexts that lack visual feedback, occipito-temporal regions could play a role in motor imagery, dynamically updating representations of the moving limbs (Astafiev et al., 2004; Kühn et al., 2011; but see Orlov et al., 2010).

2.5.3 Areas involved in stimulus-response associations

We were able to decode externally-triggered movement plans in left SMA, with a similar trend in the right SMA and left preSMA (Fig. 2.3C, Fig. 2.5A), in agreement with previous studies (Hoshi and Tanji, 2004; Mars et al., 2008; Gallivan et al., 2011a, 2011b, 2013b; Hartstra et al., 2012). This suggests a

role for the fronto-median cortex in stimulus-response mapping, possibly in a broader network that includes also posterior parietal and premotor regions (Fig. 2.5). However, other studies have also linked SMA activity to voluntary action selection (Lau et al., 2004; Zhang et al., 2012, 2013) or self-initiated movements (Cunnington et al., 2002, 2003; Fried et al., 2011). Further work will be required to define the specific role of the SMA and preSMA, and possibly also posterior parietal and premotor regions, in stimulus-response mapping and movement planning.

2.5.4 Further observations

The univariate contrast [Planning > Baseline] revealed a more widespread recruitment of the contralateral in comparison to the ipsilateral hemisphere (Fig. 2.2), whereas the searchlight MVPA revealed significant clusters in both hemispheres (Fig. 2.4, 2.5). It thus appears that, despite weak activation, the hemisphere ipsilateral to the moving limb (in our study: the right hemisphere) also contains information about planned movements (see also Gallivan et al., 2013b; Leoné et al., 2014). This apparent inconsistency is likely due to the fact that MVPA relies on differences between activation patterns that can occur in the absence of amplitude differences (e.g., Kriegeskorte et al., 2006; Haxby, 2012).

We found significant cross-condition decoding in regions that only show significant within-condition decoding for one of the two planning conditions (Free-Choice: R-pSTG, R-MTG; Instructed: L-SMA; Fig. 2.3). At first glance, this result might look implausible: if a region codes movement plans independent of the task, then it should also reveal decoding in both tasks alone. There are, however, theoretical reasons that can explain this

pattern of results. If condition A tends to evoke more consistent patterns in comparison to condition B, condition A might improve cross-condition decoding. If condition A is used for the training dataset, the classifier can more easily learn to distinguish the patterns. Likewise, if condition A is used for the testing dataset, even if the classifier was trained on condition B, it is more likely to guess correctly. In other words, training on more consistent patterns and testing on less consistent patterns (or vice versa) would produce better results than just training and testing within the same inconsistent pattern (see also Oosterhof et al., 2012b).

While the ROI- and the searchlight-based MVPA overall reveal converging results, the ROI analysis tended to be more sensitive than the searchlight analysis, in line with previous studies (Oosterhof et al., 2012b; Wurm and Lingnau, 2015). This is likely due to methodological differences between the two approaches (see also Etzel et al., 2013a). In particular, the use of individual ROIs is less affected by individual differences in functional brain topography. By contrast, the searchlight approach is not limited to ROIs defined a priori, but requires stricter criteria to produce significant results: first, the exact same voxels in group space have to show significant decoding in the majority of participants. Second, given the number of voxels in the brain, correcting for multiple comparisons is a much harder problem for searchlight-based MVPA. Given the pros and cons of both approaches, we present both analyses to provide the reader with a more complete picture of the results.

In conclusion, our results extend the existing literature on movement planning, distinguishing between regions containing abstract movement plans that are invariant to the way these were generated (externally vs

internally driven), areas involved in movement selection, and areas containing movement plans for instructed movements.

Chapter 3.

Study II: Time-resolved MVPA reveals shared representations for delayed and non-delayed movement planning in human primary motor cortex

Giacomo Ariani[1], Nikolaas N. Oosterhof[1], Angelika Lingnau[1,2,3]

[1]Center for Mind/Brain Sciences (CIMeC), University of Trento, Via delle Regole 101, 38100 Mattarello (TN), Italy

[2]Department of Cognitive Sciences, University of Trento, Corso Bettini, 31, 38068 Rovereto (TN), Italy

[3]Department of Psychology, Royal Holloway University of London, TW20 0EX Egham, Surrey, UK

The work reported in the following chapter was prepared for submission to *The Journal of Neuroscience* in October 2016.

Acknowledgments

This work was supported by the Provincia Autonoma di Trento and the Fondazione Cassa di Risparmio di Trento e Rovereto. We are thankful to Jens Schwarzbach for setting up the Arduino for response collection. The authors declare no conflicts of interest.

Author contributions

G.A., N.N.O., and A.L. designed research; G.A. performed research; G.A. and N.N.O. analyzed data; G.A., N.N.O., and A.L. wrote the manuscript.

3.1 Abstract

Different contexts require us either to react immediately, or to wait for the right moment. Previous studies that aimed at dissociating movement preparation and execution typically used delayed-movement paradigms. However, whether results obtained studying delayed movements can be generalized to the planning and execution of immediate movements remains unclear. In the present functional magnetic resonance imaging (fMRI) study we used a slow event-related design to directly compare delayed (delayed task), non-delayed (non-delayed task) and suppressed (no-go task) reaching and grasping movements. To examine how neural representations evolved throughout movement planning, execution and suppression, we performed time-resolved multivariate pattern analysis (MVPA). We were able to decode planned movements in contralateral parietal and premotor areas. Executed movements were best discriminated in widespread bilateral networks of motor, premotor and somatosensory areas. Finally, we found significant decoding across delayed and non-delayed tasks in contralateral primary motor cortex. Our results provide new insights into the dynamics of the prehension network and suggest early neural representations of movement plans in the primary motor cortex that are shared between delayed and non-delayed contexts.

Key words: movement planning, delayed-movement paradigm, immediate movements; neural decoding; time-resolved fMRI-MVPA

Significance statement

Our actions vary with context: some demand immediate reaction, other allow time to fully prepare before moving. Previous studies on motor planning used delayed-movement tasks and focused on delayed movements. Here we used time-resolved MVPA of fMRI data to follow how movement classification (1) generalized across delayed motor plans and non-delayed movements, and (2) evolved throughout the planning phase. By revealing a common neural code for motor plans across delay conditions and by elucidating the temporal dynamics of movement decoding, our results extend the current understanding of how the human parieto-frontal prehension network represents planned hand movements.

3.2 Introduction

Different contexts require different actions. While certain situations demand immediate action (e.g., suddenly crossing the street to chase after a leaving bus), others require to withhold our movements until the right moment (e.g., waiting at the traffic lights before crossing the street to the bus stop). Finally, some situations require getting ready but then to refrain from moving at all (e.g., not crossing the street to chase the bus when seeing an approaching car). How does the human brain exercise control on our actions in different contexts?

Unlike motor reflexes, even relatively simple voluntary movements need to be prepared before they are executed (Haggard, 2005, 2008). Understanding how specific brain areas contribute to movement planning requires being able to dissociate neural preparation from movement activity. To do so, previous monkey (Cisek and Kalaska, 2004, 2005; Baumann et al., 2009; Hwang and Andersen, 2009; Fluet et al., 2010; Afshar et al., 2011; Cui and Andersen, 2011; Townsend et al., 2011) and human studies (Toni et al., 2001; Thoenissen et al., 2002; Mars et al., 2008; Baumann et al., 2009; Beurze et al., 2009; Gallivan et al., 2009, 2011a, 2011b, 2013a, 2013b, 2013d, 2016a, 2016b; Lindner et al., 2010; Heed et al., 2011; Pertzov et al., 2011; Leoné et al., 2014; Ariani et al., 2015; Gertz and Fiehler, 2015) typically adopted delayed-movement paradigms in which movements are planned and withheld in memory for a certain amount of time before being released following a trigger cue. Such studies not only revealed a number of frontal and parietal regions recruited during movement planning of arm and hand actions, but also that preparatory activity in some of these regions can be used to decode upcoming movement properties (for a review see Gallivan

and Culham, 2015), implicating these regions in reach and grasp generation. However, only few human studies have directly compared this context with situations where no preparation time was allowed. Critically, this work either focused on action execution and online motor control only, neglecting the planning component (Cohen et al., 2009), or did not find differences between delayed and immediate movements (Himmelbach et al., 2009). Thus whether results obtained with delayed-movement paradigms in humans can be generalized to contexts without a delay remains unclear.

To address this question, we carried out an fMRI experiment in which prehension movements had to be performed under three conditions. In the *delayed task*, there was a jittered delay between planning and execution. To further disencourage movement anticipation, and to ensure that neural responses to movement planning were not always followed (and thus systematically contaminated) by movement execution, delayed trials had an equal probability to end with an instruction to execute (*delayed task*) or to suppress the movement (*no-go task*). In the *non-delayed task*, participants had to execute the movement with no additional time to plan.

We asked two main questions: (1) Are there shared neural representations for delayed and non-delayed motor plans? (2) How do movement representations evolve throughout the planning phase delay? Additionally, our design allowed us to explore whether regions recruited during movement suppression still carry information about the previously formed and then inhibited motor plans. To examine the time course of movement planning and execution, we performed multivariate pattern analysis (MVPA) of fMRI data with a "volume-by-volume" time-resolved approach (i.e., decoding separately for each acquired volume). To test

whether neural patterns obtained during the planning phase of delayed movements show similarities with those obtained for non-delayed movements, we performed cross-condition decoding: i.e., training a classifier on delayed movement planning and using independent data from non-delayed execution for testing (and vice versa).

3.3 Materials and Methods

3.3.1 Participants. We recruited twenty-four right-handed volunteers (11 males, 13 females; mean age: 28.21 years; age range: 18-38 years). All participants were neurologically intact and had either normal or corrected-to-normal vision. Participants gave written informed consent and were paid 30 € for their participation. The experimental procedures were approved by the ethics committee at the University of Trento.

3.3.2 Setup. Visual stimuli were back-projected to a screen (frame rate: 60 Hz; screen resolution: 1280 × 1024 pixels) via a liquid crystal projector (OC EMP 7900, Epson Nagano, Japan). Participants viewed the screen binocularly through an angled mirror mounted on the head coil (Fig. 3.1A). Auditory cues were delivered via standard MR-compatible headphones. Participants were scanned in a conventional fMRI configuration (i.e., lying horizontally, without tilting the head towards the body) and were required to maintain fixation (Fig. 3.1A). This setup prevented uncontrolled visual feedback from the sight of their own limbs and the target object, or systematic eye movements towards limbs or the target object, while performing the task.

The workspace consisted of a transparent plexiglas board attached to the scanner bed at waist level (Fig. 3.1A-3.1B). We instructed participants to perform unimanual right-handed movements towards a custom-made target object placed on the workspace and located centrally with respect to the participant's sagittal midline. Whenever at rest, participants were required to keep their right hand in a fist resting on the keys (home position) of a button box (Lumina LP 400, Cambridge Research Systems) attached to a custom-made belt around their waist. A microcontroller board (Arduino Uno) connected to the Lumina Controller positioned outside the magnet room was used to signal the release of the keys at movement onset. This time stamp was used to define and measure reaction times (RTs). To enable movements as comfortable as possible, the position of the workspace and the button box were adjusted individually to match each participant's arm length (mean distance hand-object: 15.88±2.25 cm). Head and trunk movements were minimized by stabilizing the head and the upper right arm with foam blocks and cushions. To control for task execution we recorded each experimental session using an MR-compatible digital video camera (VP-D15i; Samsung Electronics) placed on a tripod in a corner of the scanner room (outside the 0.5 mT line). Stimulus presentation, response collection, and synchronization with the scanner were controlled using ASF (Schwarzbach, 2011), based on the Matlab Psychtoolbox 3 for Windows (Brainard, 1997).

3.3.3 Experimental design and timing. To compare delayed, non-delayed and suppressed movement plans, we used a slow event-related design with factors movement (reach-to-touch, T; reach-to-grasp, G; Fig. 3.1B) and task

(delayed, D; non-delayed, ND; no-go, NG; Fig. 3.1C). Both factors were pseudo-randomized within each experimental run. A brief change in brightness of the grey fixation cross (alert cue, 500 ms) informed participants about the beginning of each trial and an upcoming cue. In the delayed task (Fig. 3.1C, first row), the alert cue was immediately followed by a change in color of the fixation cross (color cue, 500 ms) instructing which of the two movements to prepare (e.g., green fixation cross = reach-to-touch; yellow fixation cross = reach-to-grasp). We asked participants to start preparing for the instructed movement right after the presentation of the color cue (planning phase), and then to wait until the go cue (darkening of the fixation cross) to execute the movement. A variable delay from 8 to 14 seconds (in steps of the TR, 2 s) preceded the go cue. Delay durations (i.e., 8 s, 10 s, 12 s, 14 s) were equally distributed within each run (4 trials per delay duration, or, one trial per factorial combination of movement, 2, task, 2, and delay, 4). The dark fixation lasted for 2s, ensuring enough time to start and complete the instructed movement to the target object (execution phase). After movement completion, participants were instructed to keep their hand on the target object until the fixation cross returned to the initial grey color (go-back cue), and then to return to the home position (see *Setup*). In the non-delayed task (Fig. 3.1C, second row), following the alert cue, an auditory cue (*'beep'*, 500 ms) simultaneous to the go cue indicated which movement to perform (e.g., high-pitch sound = reach-to-touch; low-pitch sound = reach-to-grasp). For this task participants were asked to prepare and execute movements immediately (i.e., no delay between auditory instruction and go cue), and to remain on the target object until the go-back cue.

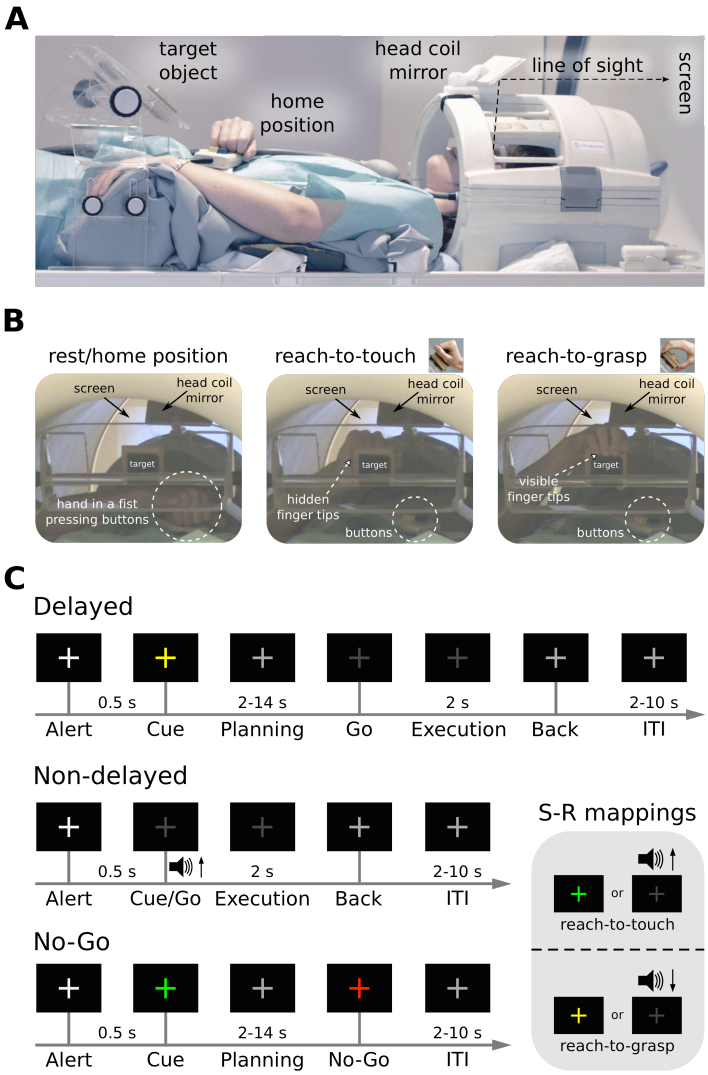

Figure 3.1 Experimental setup, design and timing. **A.** View of the setup from the side. Unimanual right-handed movements were performed towards a target object mounted on a plexiglas workspace positioned at waist level. The wooden graspable object was composed of two small cuboids glued to each other (2x2x1 and 7x7x2 cm). Participants lied horizontally and maintained fixation on a screen that was visible binocularly through a mirror attached to the head coil (line of sight illustrated by black dashed line). This setup prevented visual feedback from the target object, or the participants' own movements. **B.** Screenshots from video recordings to illustrate movement types. Whenever at rest participants were required to keep their right hand in the home position (closed in a fist and pressing the response buttons, left panel; see also A). The two movement types were reach-to-touch (no hand preshaping, central panel) and reach-to-grasp (whole-hand grip, right panel). **C.** Task types with respective trial timing.

Note that the reason to use, respectively, visual and auditory cues for the delayed and non-delayed task was to prevent cross-decoding based on shared low-level features. Finally, during no-go trials (Fig. 3.1C, third row), the planning phase was followed by a no-go cue (a red fixation cross, 500 ms), indicating to suppress the previously instructed movement and to remain as still as possible in the home position while waiting for the next trial to start. To keep participants focused throughout the experiment and to prevent psychological effects of task habituation or event anticipation with increasing number of trials, we also included a small proportion of catch trials (~15%, 4 per run, 2 per movement) for the delayed condition only, in which the delay duration was noticeably shorter (from 2 s to 6 s, in steps of 2 s, randomly sampled from a geometric distribution with p = 0.3). We subsequently excluded these trials from successive analyses.

Each run started and ended with 12 s rest and contained 4 repetitions per factorial combination of movement x task, plus catch trials (i.e., 24 + 4 = 28 trials per run; 280 trials per participant). The stimulus-response (S-R) mappings between cues (i.e., colors and sounds) and movements were counterbalanced across subjects. Trial randomization and inter-trial-interval (ITI) jittering were determined by Optseq2 (Greve, 2002; *Optseq Home Page*, available online at: http://surfer.nmr.mgh.harvard.edu/optseq). Each experimental session consisted of: training outside the MR scanner and setup preparation (~25 min), structural scan (~5 min), main experiment (10 functional runs, ~7 min each), for a total of ~100 min per participant. At the end of the session, participants filled out a post-session questionnaire asking them about movement verbalization during the tasks. Moreover, separately for each of the three tasks, we asked them to rate during which phase of the

trial they had the strongest subjective impression to actively plan the instructed movement.

3.3.4 Data acquisition. Functional and structural data were collected using a 4T Bruker MedSpec Biospin MR scanner and an 8-channel birdcage head coil. Functional images were acquired with a T2*-weighted gradient-recalled echo-planar imaging (EPI) sequence. Acquisition parameters were a TR (time to repeat) of 2000 ms; voxel resolution, 3 x 3 x 3 mm; TE (time to echo), 28 ms; flip angle (FA), 73°; field of view (FOV), 192 x 192 mm; gap size, 0.45 mm. We used 30 slices, acquired in ascending interleaved order, slightly tilted to run approximately parallel to the calcarine sulcus. The number of volumes acquired in the main experiment for each functional run varied according to the length of variable delay periods (range: 190-200 volumes). Before each functional run, we performed an additional scan to measure the point-spread function (PSF) of the acquired sequence, which served for distortion correction, expected with high-field imaging (Zaitsev et al., 2004). To be able to coregister the low-resolution functional images to a high-resolution anatomical scan, we acquired a T1-weighted anatomical scan (magnetization-prepared rapid-acquisition gradient echo; TR: 2700 ms; voxel resolution: 1 x 1 x 1 mm; TE: 4.18 ms; FA: 7°; FOV: 256 x 224 mm; 176 slices; generalized autocalibrating partially parallel acquisition with an acceleration factor of 2; inversion time: 1020 ms).

3.3.5 Data analysis.

Behavior. Reaction times (RTs) were measured as the time to release the response buttons (see *Setup*) with respect to the go cue. Video recordings of

the experimental sessions were analyzed offline to ensure that participants had performed the movements correctly. Trials were considered errors either when performed incorrectly (i.e., imprecise hand preshaping; temporal anticipation: RT < 100 ms; reaction time timeout: RT > 1500 ms) or when participants executed a movement that was different from the one instructed by the visual or auditory cues.

fMRI preprocessing. Data were preprocessed and analyzed using BrainVoyager QX 2.8.0 (BrainInnovation, Maastricht, The Netherlands) in combination with the NeuroElf v1.0 toolbox and custom software written in Matlab R2012b (MathWorks, Natick, MA, U.S.A.). To correct for distortions in geometry and intensity in the echo planar imaging (EPI) images, we applied distortion correction on the basis of the PSF (see *Data acquisition;* Zeng & Constable, 2002). To avoid T1 saturation, we discarded the first 4 volumes of each run. The first volume of the first functional run of each participant was aligned to the high-resolution anatomy (6 rigid-body transformation parameters). Next, we performed 3D motion correction (trilinear interpolation for estimation and sinc interpolation for resampling) using the first volume of the first run of each participant as reference, followed by slice timing correction (ascending interleaved even-odd order) and high-pass temporal filtering (3 cycles per run). Spatial smoothing was applied with a Gaussian kernel of 3 mm full-width half maximum (FWHM) for univariate and multivariate analyses. For successive group analysis, both functional and anatomical data were transformed into Talairach space, using trilinear interpolation.

Brain segmentation and surface mesh reconstruction. We used BrainVoyager to reconstruct individual surface meshes for each hemisphere of each subject along the border between grey and white matter. Next, separately for the left and right hemisphere, we combined the individual reconstructions of folded surfaces of all participants (N = 24) using cortex-based alignment as implemented in BrainVoyager QX 2.8.0. Group-aligned left and right hemisphere meshes were used to display statistical maps resulting from both uni- and multivariate second-level analyses.

Univariate RFX-GLM analysis. To examine brain responses during the three tasks, we ran a group random-effects (RFX) general linear model (GLM) analysis (N = 24; Fig. 3.3). We created six predictors, one for each factorial combination of movement x task. Additionally, for tasks with a delay (i.e., delayed and no-go), we created separate predictors for movement planning (time-locked to the instructing cue) and movement execution/suppression (time-locked to the go/no-go cue), leading to a total of 10 predictors of interest (delayed planning/execution of touch/grasp, no-go planning/execution of touch/grasp, non-delayed execution of touch/grasp). Each predictor was modeled with a standard duration of 1 s and convolved with the canonical hemodynamic response function (HRF). In addition, catch trials, error trials and 3D motion correction parameters (3 translations and 3 rotations) were included in the model as nuisance regressors. To identify brain regions involved in the preparation of prehension movements irrespective of whether the movement plan was subsequently executed or not we contrasted the planning phase of both go and no-go trials (collapsed across the two movement types) against the implicit baseline (Fig. 3.3A).

Similarly, to identify brain regions recruited during movement planning and execution, we contrasted the execution phase in the non-delayed task (collapsed across both movement types) against baseline (Fig. 3.3B). Finally, to examine whether there are any brain regions that respond more strongly during no-go trials in comparison to go trials, we computed the contrast delayed no-go vs delayed go trials (Fig. 3.3C). The resulting volumetric statistical maps were corrected for multiple comparisons using Threshold Free Cluster Enhancement (TFCE, corrected $p < 0.05$, montecarlo permutations for 10000 iterations) as implemented in the CoSMoMVPA toolbox for Matlab/GNU Octave (Oosterhof et al., 2016), and projected on the group-averaged surface mesh for visualization purposes.

ROI definition. We defined regions of interest (ROIs) on the basis of both anatomical and functional criteria using a similar procedure as in Ariani et al., 2015. First, on the group-averaged surface mesh we manually outlined bilateral ROIs around anatomical landmarks known to be involved in movement planning (Fig. 3.2), using the following anatomical criteria:

- *Dorsolateral prefrontal cortex (dlPFC)*: on the anterior portion of the middle frontal gyrus, around Brodmann area (BA) 46 (Badre & D'Esposito, 2009);
- *Ventral premotor cortex (PMv)*: slightly inferior and posterior to the junction of the inferior frontal sulcus and the precentral sulcus (Gallivan et al., 2011a);

- *Dorsal premotor cortex (PMd)*: at the junction of the superior frontal sulcus and the precentral sulcus;
- *Supplementary motor area (SMA)*: on the medial wall of the superior frontal gyrus, anterior to the medial end of the central sulcus, posterior to the vertical projection of the anterior commissure;
- *Primary motor cortex (M1)*: around the hand-knob area in the anterior bank of the central sulcus;
- *Anterior intraparietal sulcus (aIPS)*: on the anterior segment of the intraparietal sulcus, at the junction with the postcentral sulcus;
- *Superior parietal lobule (SPL)*: the middle portion of the superior parietal lobule, superior to the IPS and posterior to the postcentral sulcus;
- Superior parieto-occipital cortex (SPOC): the posterior portion of the superior parietal lobule (Brodmann area 7b), located medially, superior to the IPS and anterior to the parieto-occipital sulcus (Scheperjans et al., 2008; Gallivan et al., 2011b);
- *Lateral occipito-temporal cortex (LOTC)*: portion of the middle temporal gyrus (MTG), inferior to the superior temporal sulcus (STS) and anterior to the lateral occipital sulcus (LOS) (Lingnau and Downing, 2015).

Next, we projected these marked patches from the surface back to the volume. Within each of them, we looked for individual peak voxels resulting from the single-subject GLM contrasts [planning + execution > baseline x 2], computed as described above. Finally, we defined individual ROIs, separately for each participant, as spheres (10 mm radius, ~230 voxels) centered

around each individual peak voxel (for Talairach coordinates of individual ROIs, see Table 3.1).

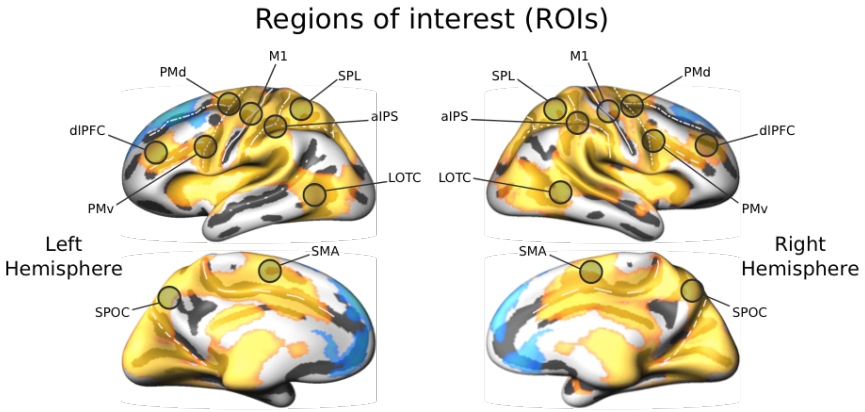

Figure 3.2 Regions of interest (ROIs). Black circles represent approximate locations of group-defined ROIs involved in movement generation. Actual ROIs used in the ROI-MVPA were defined, individually for each participant, as spheres (10mm radius) around individual peak voxels coming from single-subject statistical maps of the univariate contrast [delayed planning + non-delayed execution > baseline x 2] (collapsing across movement types). For additional details, see Materials and Methods section and Table 3.1. All the other figure conventions are the same as in Fig. 3.

Table 3.1 TAL coordinates (x, y, z rounded mean and standard deviation across participants) of individual peak voxels for the regions of interest (ROIs) identified by the group contrast [delayed planning + non-delayed execution > baseline x 2].

Region	x	y	z	SD x	SD y	SD z
L-dlPFC	-34	33	32	4,7	4,1	3,5
R-dlPFC	31	35	32	3,1	3,8	3,6
L-PMv	-44	1	30	4,6	2,8	3,6

R-PMv	40	2	33	4,2	2,4	2,3
L-PMd	-27	-11	52	3,9	3,1	4,0
R-PMd	27	-10	52	3,2	4,0	4,7
L-SMA	-4	-11	53	1,0	3,5	2,9
R-SMA	6	-5	52	2,3	2,8	2,6
L-M1	-33	-24	50	2,3	2,9	1,9
R-M1	35	-22	50	2,8	3,1	2,3
L-aIPS	-39	-35	38	3,5	3,5	2,3
R-aIPS	35	-37	40	3,8	3,7	2,6
L-SPL	-27	-55	55	2,8	4,4,	3,3
R-SPL	29	-52	57	1,7	5,6	3,3
L-SPOC	-6	-71	43	2,7	3,0	3,9
R-SPOC	8	-70	43	2,7	3,1	4,5
L-LOTC	-43	-63	4	3,3	2,3	2,9
R-LOTC	49	-54	3	4,3	3,2	3,7

Abbreviations: L-, left hemisphere; R-, right hemisphere; dlPFC, dorsolateral prefrontal cortex; PMv, ventral premotor cortex; PMd, dorsal premotor cortex; SMA, supplementary motor area; M1, primary motor cortex; aIPS, anterior intraparietal sulcus; SPL, superior parietal lobule; SPOC, superior parieto-occipital cortex; LOTC, lateral occipito-temporal cortex.

Time-resolved ROI-MVPA. To track the temporal unfolding of decoding of movement type for different brain regions and tasks, we used a time-resolved decoding approach (Soon et al., 2008; Bode and Haynes, 2009;

Linden et al., 2012; Gallivan et al., 2013c) for both ROI- and searchlight-based MVPA. The ROI analysis (Fig. 3.4-3.6) was intended to test previously reported regions known to play a role during movement planning and execution. The whole-brain searchlight analysis (Fig. 3.7-3.8) was carried out to prevent missing potentially important regions not covered in the ROI analysis. Both analyses were performed in volume space. To implement the time-resolved ROI-MVPA we repeated the following steps separately for each run of each participant and ROI. First, for each voxel included in the ROI, we normalized the raw volume time-course (VTC) by demeaning it. Next, for each factorial combination of movement x task, we extracted N volumes starting from the onset of the condition (N = 5 for delayed planning, N = 7 for all the other conditions), separately for each run and participant. For each classification pair (e.g., reach-to-touch vs reach-to-grasp, within the planning phase) this procedure resulted in a dataset matrix of samples [N volumes (e.g., 7) x movements (2) x runs (10)] x features [N voxels in the ROI] for each subject, task and ROI. In each matrix, the rows constituted the different multi-voxel patterns of fMRI data (i.e., vectors of mean BOLD values with a length equal to the number of voxels in the ROI). Classification accuracies were computed separately for each volume (i.e., movements (2) x runs (10) = 20 patterns) using a leave-one-run-out cross-validation method: a linear discriminant analysis (LDA) classifier was trained on 18 patterns (2 movements x 9 runs) and tested on the data from the remaining run (2 patterns, one per movement type). Training and testing was repeated for 10 iterations, using all possible combinations of train and test runs. The average across these 10 iterations constituted the mean classification accuracy of the two movements per participant per ROI. To

test for representations of planned movements across delay conditions (delayed, non-delayed), we carried out cross-condition decoding: we trained the classifier on discriminating between reaching and grasping in one task (e.g., delayed planning) and tested the performance of the classifier to distinguish between reaching and grasping in the other task (e.g., non-delayed execution), and vice versa. Results from the two cross-condition decoding analyses were successively averaged to produce one score per cross-condition decoding. To assess statistical significance of the decoding accuracy, separately for each ROI, we performed one-sample *t*-tests on decoding accuracies across participants against chance decoding (50%) at each time-point. We note that 50% is chance level because the cross-validation scheme was balanced, i.e., for each fold the training and test set both used the same number of patterns for each of the movement types. Statistical results were corrected for multiple comparisons (number of ROIs x time-points) using TFCE ($p < 0.05$, 10000 iterations) as implemented in CoSMoMVPA.

Time-resolved searchlight-MVPA. Decoding procedures for the time-resolved whole-brain searchlight analysis in the volume were nearly identical to the ones used for the ROI analysis. The main difference was that we used a spherical searchlight (~250 voxels) approach instead of predefined ROIs and decoding results for each searchlight were assigned to the central voxel. Resulting group mean decoding accuracy maps at each time-point were then projected onto the group-aligned cortical surface mesh (see *Brain segmentation and surface mesh reconstruction*) for visualization purposes (Fig. 3.7-3.8, top rows). To identify voxels where classification was

significantly greater than chance (50%) we performed a two-tailed one-sample *t*-test across individual whole-brain maps. Statistical *t*-maps were then corrected for multiple comparisons using TFCE (1000 iterations). For descriptive purposes (i.e., to show statistical trends) we thresholded the uncorrected *t*-maps at t = 2 and marked significant clusters that survived TFCE correction with black outlines (Fig. 3.7-3.8, bottom rows). Cluster-based TFCE was done using a neighborhood in which clusters could form along the spatial dimensions (i.e., voxels sharing an edge) but not along the temporal dimension. This means that inferences about significance can be made at the single volume level along the temporal dimension, but not at the single voxel level (i.e., only at the cluster level) along the spatial dimension. We created whole-brain *t*-maps and decoding accuracy maps at each time-point, separately for the three tasks (within-condition decoding), and for the decoding across delayed planning and non-delayed execution (cross-condition decoding). Overall, the novel methods used in this study provided two main advantages with respect to conventional MVP analyses: (1) thanks to the time-resolved MVPA we were able to show how movement planning evolves during the delay period; (2) using raw time-course data as input for the classifier (e.g., instead of beta-weights or *t*-values coming from a GLM) made our findings less dependent on assumptions about the shape of the hemodynamic response function (HRF).

3.4 Results

3.4.1 Behavior. Participants responded faster in the delayed (660.48 ± 11.54 ms) in comparison to the non-delayed task (905.54 ± 12.83; $t(23) = -$

9.58, $p < 0.0001$). Error rates were comparable for the delayed (7.39% ± 1.48) and non-delayed task (6.25% ± 1.55; signed-rank $z(23) = 0.78$, $p = 0.43$). In the no-go task participants made an average of 0.42% ± 0.18 'false start' errors. From the post-session questionnaires we obtained a mean rating of 3.63 ± 1.21 for movement verbalization during the planning phase (on a scale from 1 = "not at all" to 6 = "quietly naming"). Additionally, 13/24 participants reported to have actively planned the instructed movements "Right after the presentation of the color cue"; 7/24 "Within a couple of seconds following the presentation of the color cue"; and 4/24 "Right after the presentation of the Go cue".

3.4.2 fMRI.

Univariate RFX-GLM analysis. A univariate RFX-GLM analysis was used to identify brain regions recruited during movement planning, execution and suppression (for details, see Materials and Methods, *Univariate RFX-GLM analysis*). First, the contrast [delayed planning > baseline] (Fig. 3.3A) revealed a widespread bilateral network of frontal, parietal and temporal regions, in line with previous studies (Gallivan et al., 2011a, 2011b; Ariani et al., 2015). Second, the contrast [non-delayed execution > baseline] (Fig. 3.3B) revealed a network of areas comparable to that involved in movement planning. As expected, in comparison to the statistical map resulting from the contrast [delayed planning > baseline], the statistical map resulting from the contrast [non-delayed execution > baseline] was more widespread and showed considerably stronger effects in primary motor and auditory areas (likely due to the auditory cues instructing which movement to perform in this task). Third, the contrast [delayed no-go > delayed go] (Fig. 3.3C) did

not reveal any areas that survived TFCE (at a more liberal threshold, this contrast revealed dorso-medial prefrontal areas, not shown in Fig. 3.3C). As expected, the reverse contrast [delayed go > delayed no-go] showed a widespread network of areas comparable to those recruited during movement planning and execution.

To define a set of group-ROIs known to be recruited during movement planning and execution for the time-resolved within- and cross-condition decoding analysis, we computed the contrast [delayed planning + non-delayed execution > baseline x 2] (Fig. 3.2). Note that we chose this contrast to prevent biasing the decoding analysis towards planning or execution related areas, which is relevant in particular for the cross-decoding analysis. At the same time, this contrast does not introduce any bias towards one of the two movement types (or the contrast between the two) and thus prevents circular analysis (Kriegeskorte et al., 2009). On the basis of this contrast, we selected 18 bilateral frontal, parietal and temporal ROIs, individually for each participant (see *ROI definition* and Table 3.1): left and right dorsolateral prefrontal cortex (dlPFC); left and right ventral premotor cortex (PMv); left and right dorsal premotor cortex (PMd), left and right supplementary motor area (SMA); left and right primary motor cortex (M1); left and right anterior intraparietal sulcus (aIPS); left and right superior parietal lobule (SPL); left and right superior parieto-occipital cortex (SPOC); left and right lateral occipito-temporal cortex (LOTC).

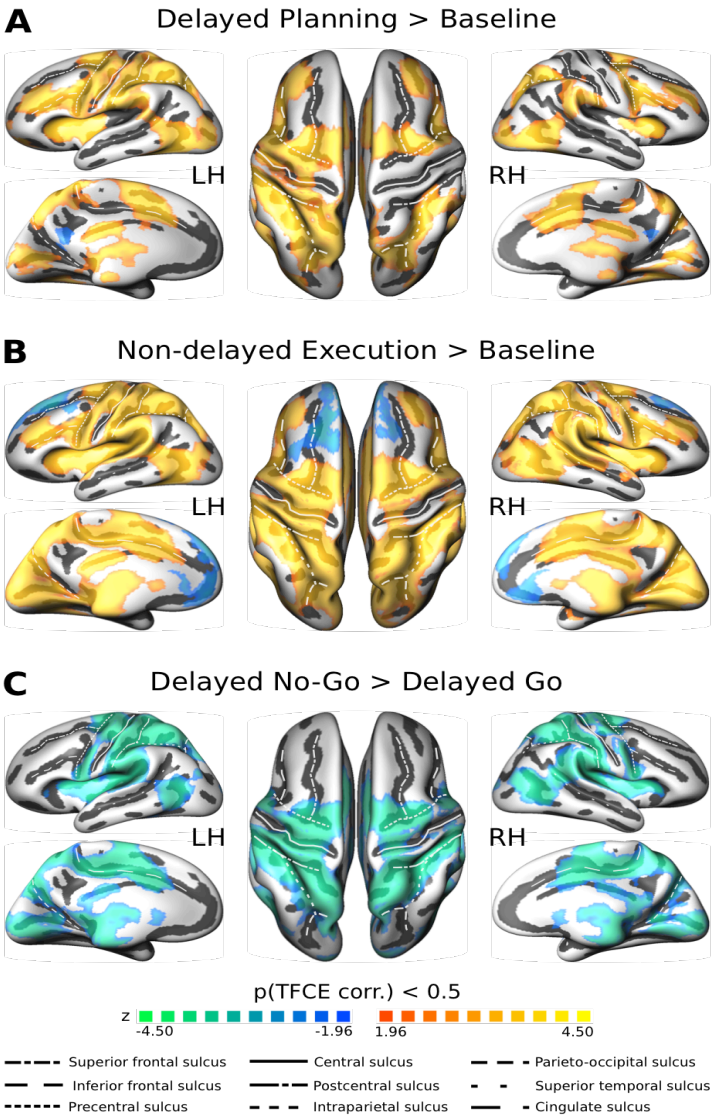

Figure 3.3 Univariate RFX-GLM analysis (N = 24). **A.** Univariate contrast [delayed planning > baseline], collapsing across movement types and go/no-go trials. **B.** Univariate contrast [non-delayed execution > baseline], collapsing across movement types. **C.** Univariate contrast [delayed no-go > delayed go], collapsing across movement types. All statistical group-maps were corrected for multiple comparisons using Threshold Free Cluster Enhancement (TFCE) as implemented in CoSMoMVPA (Oosterhof et al., 2016), thresholded at $p < 0.05$ and projected on the group-aligned inflated surface mesh for visualization purposes. White lines on the surface meshes denote main brain sulci as landmarks (see legend at the bottom of the figure).

Time-resolved ROI-MVPA. We ran the ROI-MVPA with a time-resolved approach (i.e., classification performed separately at each acquired volume, starting from the onset of an event) to follow the temporal unfolding of movement decoding for the different tasks in selected brain regions (Fig. 3.4-3.6). For each ROI in Figures 4-6, the overlapping line plots represent the classification accuracy of movement type (expressed in percentage correct) at each time-point for the different conditions. On the left column, the x-axis is time-locked to the onset of the visual/auditory instructing cue (0-2 s/vol. 1). The yellow line refers to decoding for delayed planning (collapsed across go and no-go trials), the bright green line to decoding for non-delayed execution and the blue line to the cross-condition decoding (i.e., training the classifier on delayed planning using non-delayed execution for testing, and vice versa). On the right column, the x-axis is time-locked to the go/no-go cue (0-2 s/vol. 1). The dark green line refers to decoding for delayed execution, and the red line to decoding for delayed suppression (i.e., after the no-go cue). The bright green line plot is identical to the one presented in the left column and serves for ease of comparison between decoding results across conditions. Figure 3.4 shows the results in bilateral frontal motor regions, Figure 3.5 in bilateral parietal sensorimotor regions, and Figure 3.6 in bilateral fronto-temporal ventral stream regions. During the planning phase of delayed trials (i.e., yellow line plots) we observed significant decoding of movement type in L-PMd at 4-6s (vol. 3; Fig. 3.4), L-aIPS at 2-4 s (vol. 2; Fig. 3.5), and L-SPL at 8-10 s (vol. 5; Fig. 3.5). Other trends that did not survive correction for multiple comparisons were found in L-M1 at 6-8 s (vol. 4; Fig. 3.4), bilateral aIPS at 6-8 s (vol. 4; Fig. 3.5), L-SPOC at 4-8 s (vol. 3-4; Fig. 3.5) and bilateral LOTC at 6-8 s (vol. 4; Fig. 3.6).

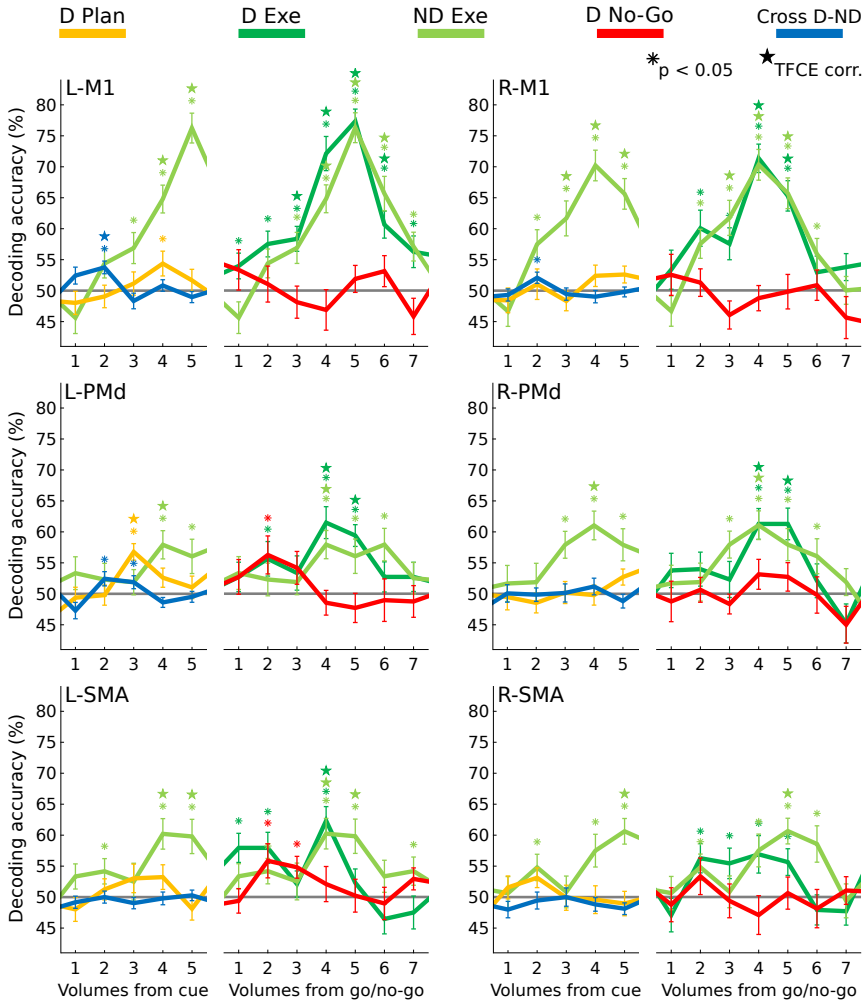

Figure 3.4 Time-resolved ROI-MVPA in bilateral frontal motor regions. Mean percentage decoding accuracy of movements at each time-point (Volume = TR = 2 s) in selected ROIs (for details see Fig. 3.2 and Table 3.1). For each ROI, line plots on the left panel are time-locked to the onset of the visual instructing cue in the delayed task (D Plan, yellow), the auditory instructing cue in the non-delayed task (ND Exe, bright green), or both instructing cues for the cross-condition decoding (Cross D-ND, blue). On the right panel, line plots are time-locked to the onset of the go cue for the delayed execution (D Exe, dark green) and the non-delayed execution (ND Exe, bright green), or the onset of the no-go cue for the no-go task (D No-Go, red). The bright green line (identical on the two panels of each figure) was intended to facilitate direct comparison across conditions. Error bars represent within-subject standard error of the mean (SEM). Statistical significance was assessed via one-sample *t*-tests against 50% chance (grey horizontal line in each ROI plot) at each time-point separately. Results were corrected for multiple comparisons (number of time-points x number of ROIs) using TFCE (asterisk = uncorrected $p < 0.05$; star = TFCE corrected at $p < 0.05$).

Results for delayed and non-delayed execution (i.e., dark and bright green line plots) were very similar: significant decoding starting as early as 4-6 s (vol. 3) and continued until as late as 10-12 s (vol. 6) in most motor and sensorimotor areas (bilateral M1, PMd, SMA, and aIPS). Comparable trends were obtained in bilateral SPL and R-LOTC.

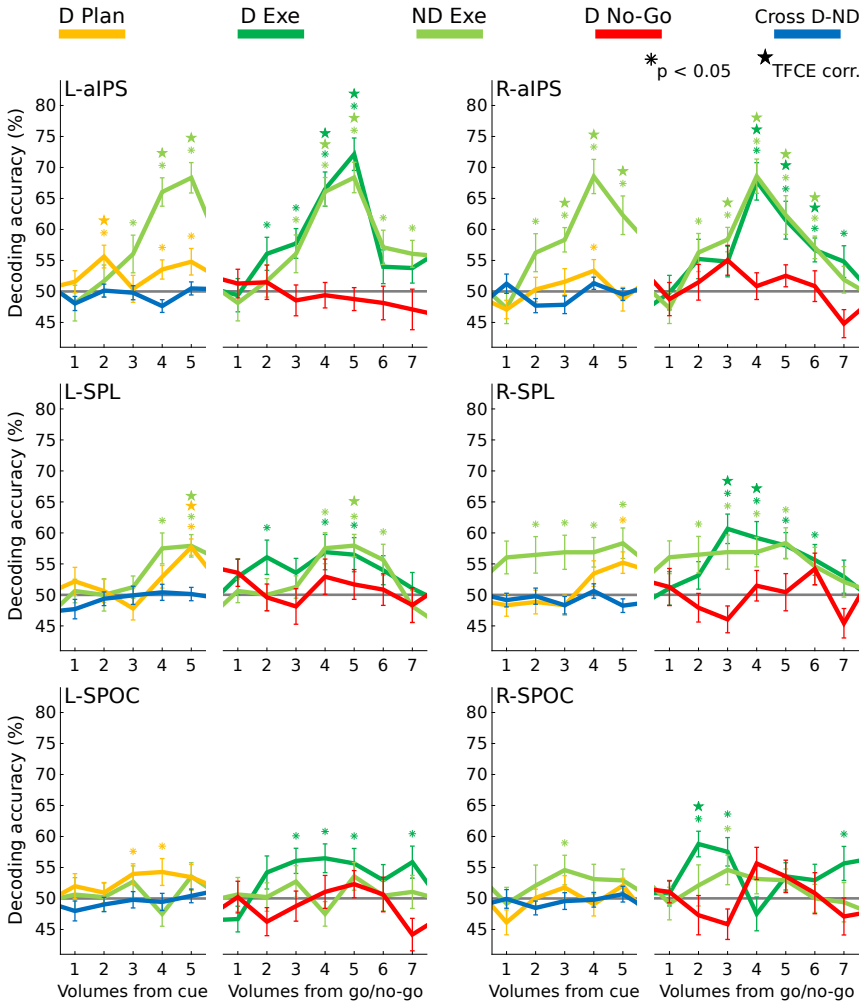

Figure 3.5 Time-resolved ROI-MVPA in bilateral parietal sensorimotor regions. Legend and figure conventions are the same as in Fig. 3.4.

For the no-go task (i.e., red line plots) we observed some trends in L-PMd at 2-4 s (vol. 2), L-SMA at 2-6 s (vol. 2-3), and L-dlPFC at 2-4 s (vol. 2), but none of these survived correction for multiple comparisons.

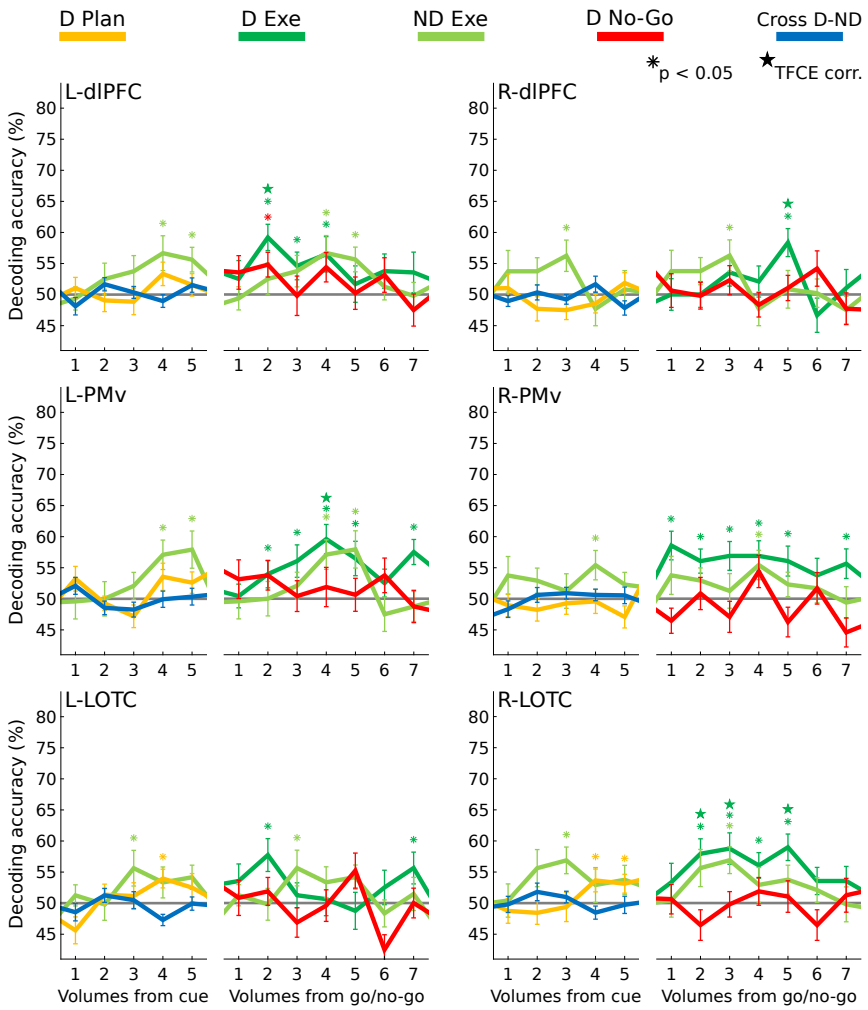

Figure 3.6 Time-resolved ROI-MVPA in bilateral fronto-temporal ventral stream regions. Legend and figure conventions are the same as in Fig. 3.4.

Regarding shared representations across delayed and non-delayed movement plans (i.e., blue line plots), we were able to decode movement types across delay conditions at 2-4 s (vol. 2) in L-M1. Similar trends were observed in R-M1 at 2-4 s (vol. 2) and L-PMd at 2-6 s (vol. 2-3), but these did not survive corrections for multiple comparisons.

Time-resolved searchlight-MVPA. The time-resolved searchlight-based MVPA (Fig. 3.7-3.8) was intended to provide a whole-brain overview of regions discriminating between reaching and grasping, including regions not specifically covered by the ROI analysis. Decoding results are in line with what we observed in the selected ROIs. Figure 3.7 shows mean classification accuracy maps (top) and group *t*-maps (bottom) at each time-point (i.e., volume/TR, time-locked to either visual or auditory cues) for delayed planning (collapsing go and no-go trials, Fig. 3.7A), non-delayed execution (Fig. 3.7B), and the cross-decoding of the two delay conditions (Fig. 3.7C).,Decoding results during delayed planning (Fig. 3.7A) showed some trends in L-PMd, bilateral aIPS and L-SPL 6-8 s after the onset of the instructing cue (vol. 4, the last time-point before the earliest go/no-go cue considering all the trials), although none of the clusters identified by the *t*-test against chance survived TFCE correction. Searchlight results for non-delayed execution (Fig. 3.7B) confirmed the results of the ROI-based MVPA: significant clusters emerged in bilateral somatosensory, sensorimotor and motor regions at 4-6 s (vol. 3) and reached the peak of classification accuracy at 8-10 s (vol. 5) in the left primary motor cortex (i.e., contralateral to the acting limb). Finally, for the cross-condition decoding (delayed planning on non-delayed execution, and vice versa, Fig. 3.7C) no clusters survived TFCE

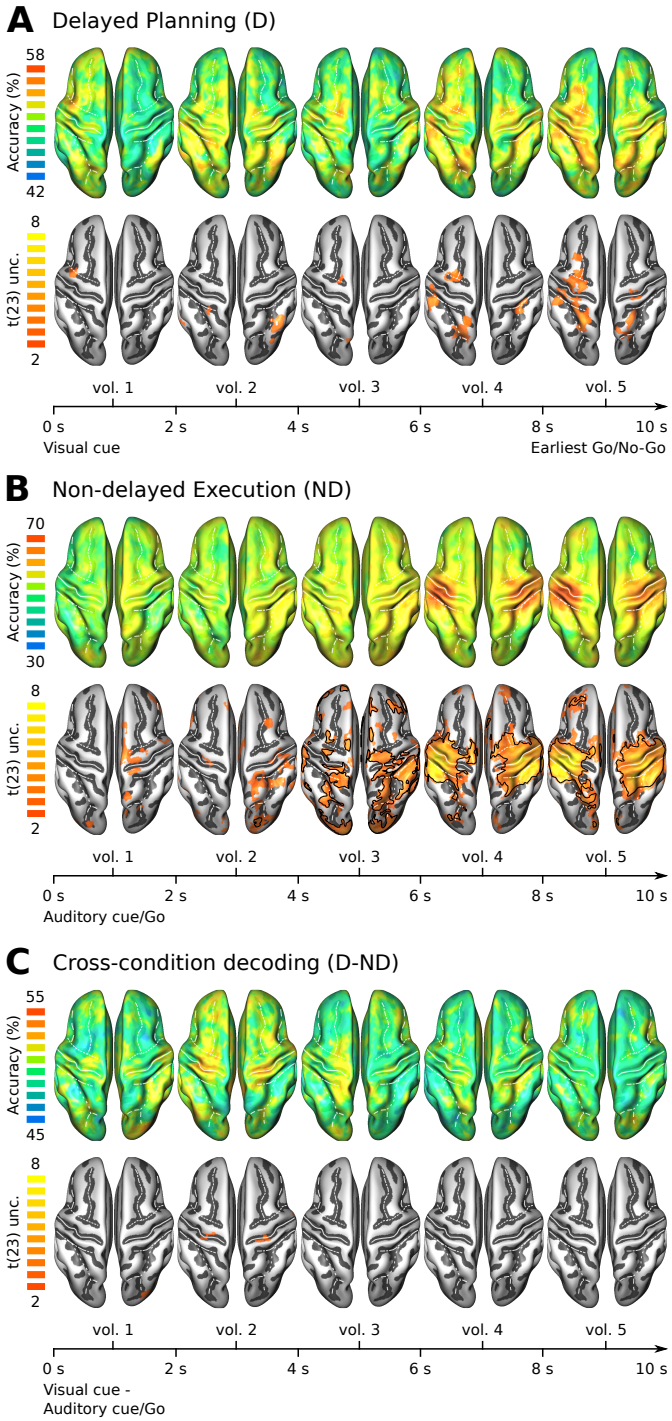
A
Delayed Planning (D)
58
Accuracy (%)
42
8
t(23) unc.
2
vol. 1
vol. 2
vol. 3
vol. 4
vol. 5
0 s
2 s
4 s
6 s
8 s
10 s
Visual cue
Earliest Go/No-Go
B
Non-delayed Execution (ND)
70
Accuracy (%)
30
8
t(23) unc.
2
vol. 1
vol. 2
vol. 3
vol. 4
vol. 5
0 s
2 s
4 s
6 s
8 s
10 s
Auditory cue/Go
C
Cross-condition decoding (D-ND)
55
Accuracy (%)
45
8
t(23) unc.
2
vol. 1
vol. 2
vol. 3
vol. 4
vol. 5
0 s
2 s
4 s
6 s
8 s
10 s
Visual cue -
Auditory cue/Go

Figure 3.7 Time-resolved whole-brain searchlight-MVPA for delayed and non-delayed tasks. Decoding procedures were identical to the ones used for the ROI-MVPA except for the use of a spherical searchlight (~250 voxels) approach (see *Materials and Methods*). Group (N = 24) mean decoding accuracy (in %, top) and uncorrected *t*-scores (bottom) whole-brain maps projected on the group-averaged surface mesh are shown at each time-point for each within-condition decoding and the cross-condition decoding. Accuracy maps, intended for descriptive purposes only, have different accuracy ranges across conditions. All *t*-maps are thresholded at $t = 2$. Clusters surviving TFCE correction for multiple comparisons ($p < 0.05$) are outlined in black. White lines on the surface meshes denote main brain sulci as in Fig. 3.2-3.3. **A.** Delayed Planning. Whole-brain maps are time-locked to the onset of the visual instructing cue (0-2 s/vol. 1). Due to jittered planning delays the earliest possible go or no-go signal was after 8 seconds (4 volumes). **B.** Non-delayed execution. Whole-brain maps are time-locked to the auditory instructing/go cue (0-2 s/vol. 1). **C.** Cross-condition decoding. Whole-brain maps are time-locked to both visual (for delayed planning) and auditory (for non-delayed execution) cues (0-2 s/vol. 1).

correction, but a trend in bilateral primary motor cortex (L-M1, R-M1) mirrored the effect found in the ROI-MVPA at 2-4 s (vol. 2). Figure 3.8 is a comparison of whole-brain mean accuracy maps (top) and group *t*-maps (bottom) for delayed execution (time-locked to the go cue, Fig. 3.8A) and delayed suppression (time-locked to the no-go cue, Fig. 3.8B). During delayed execution clusters discriminating reach-to-touch vs reach-to-grasp reached significance even earlier than during non-delayed execution, at 2-4 s (vol. 2) in bilateral posterior parietal, motor and premotor regions. Additionally, as anticipated by the ROI-MVPA results, thanks to the time-resolved decoding approach one can appreciate how, after gradually rising and peaking at 8-10 s (vol. 5), most regions no longer discriminated the movements (i.e., chance decoding) after 10-12 s (vol. 6). For delayed suppression (Fig. 3.8B) we did not find any significant clusters discriminating the previously planned movements. Similar to the results of the time-resolved ROI-MVPA, were were unable to reveal inhibitory brain signals carrying information about suppressed movement plans (i.e., after a no-go cue). Finally, comparing results during movement execution

separately for the delayed (Fig. 3.8A) and non-delayed (Fig. 3.7B) task, we noticed that the overall decoding seemed to evolve slightly more slowly for the non-delayed execution.

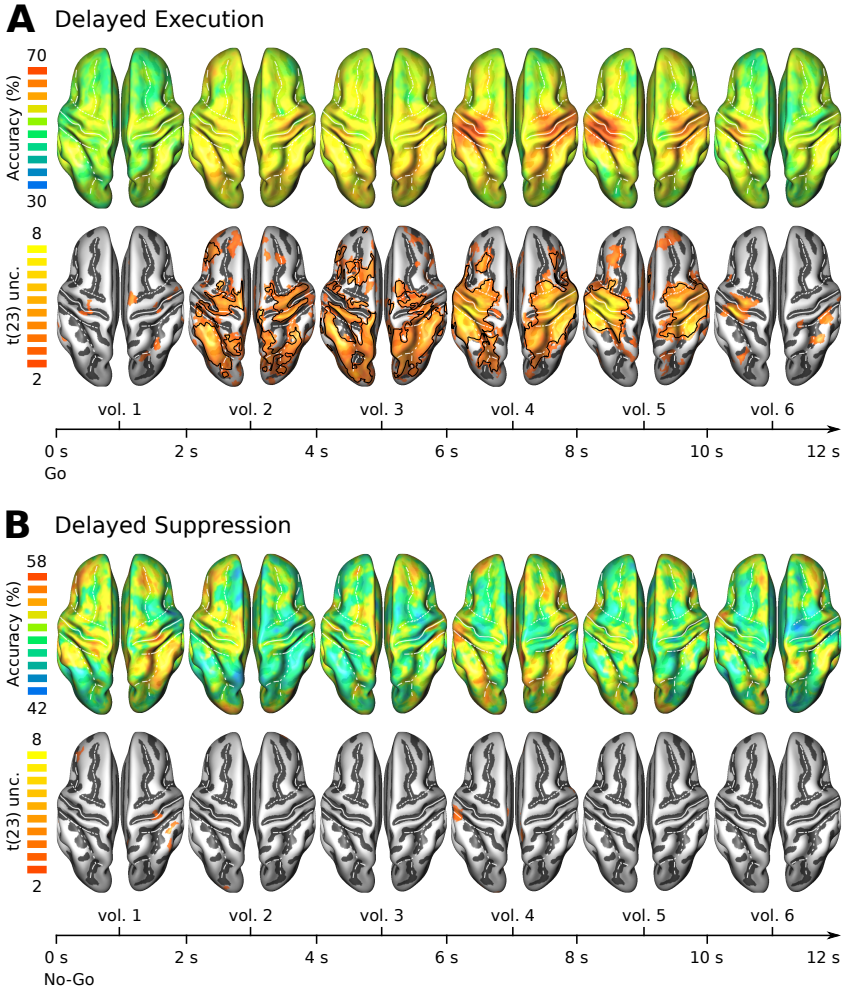

Figure 3.8 Time-resolved whole-brain searchlight-MVPA for delayed and no-go tasks. All figure conventions are the same as in Fig. 3.7. **A.** Delayed execution. Brain maps are time-locked to the onset of the Go cue (0-2s/vol.1) for delayed trials only. **B.** Delayed suppression. Brain maps are time-locked to the onset of the No-Go cue (0-2s/vol.1).

It is possible that in more realistic situations where we do not have to plan and withhold an action for several seconds movement representations result delayed in time (see vol. 1, 2, 3 in Fig. 3.7B), whereas under conditions with a delay already prepared patterns might be simply released from the first volume of the execution to the next (see vol. 1, 2 in Fig. 3.8A).

3.5 Discussion

Here we compared three tasks in which movements had to be planned, withheld, and then executed (delayed task: both planning and execution); immediately executed (non-delayed task: execution without planning); or planned, withheld, and then suppressed (no-go task: planning without execution). Thanks to the time-resolved MVPA, we were able to examine how movement representations evolve throughout different stages of planning, execution and suppression. Below we discuss the main findings.

3.5.1 Shared early neural representations for delayed and non-delayed movement plans

We obtained significant cross-condition decoding between delayed planning and non-delayed execution in the left primary motor cortex at 2-4 s (vol. 2; Fig. 3.4). In other words, in primary motor cortex, multi-voxel activity patterns during early stages of planning reach-to-touch and reach-to-grasp movements are similar to the patterns obtained at early stages of immediate movement execution (i.e., not preceded by a delay).

To the best of our knowledge, only two recent studies on macaques directly compared the planning of delayed and non-delayed arm movements

(Crammond and Kalaska, 2000; Ames et al., 2014). Both studies recorded from monkey PMd and M1 while macaques performed delayed and non-delayed reaching movements in separate blocks of trials. They found that neuronal responses to the instruction cue and the go cue (prior to movement onset) are highly similar across delay conditions, possibly constituting a neural correlate of early planning stages (e.g., response parameters selection). Our findings resonate with these observations, suggesting that human primary motor cortex contains similar information about upcoming hand movements regardless of the presence of a delay. Crucially, these neural representations of planned movements shared across delayed and non-delayed contexts occur early within their respective phases (vol. 2), soon after the occurrence of the cues, and before brain activity for planning and execution starts diverging both in terms of overall activation and spatial patterns of voxel activity.

One potential reservation could be that decoding is driven by the sensory properties of the instructing cues (e.g., stimulus-response mapping), but it should be noted that in the delayed task instructing cues for each movement type were visual (i.e., colors), whereas in the non-delayed task they were auditory (i.e., sounds). Therefore, unless primary motor cortex is shown to contain multi-modal (audio-visual) representations of sensory stimuli, we consider this explanation rather unlikely.

Another potential reservation when interpreting the significant cross-condition decoding in L-M1 at 2-4 s (vol. 2) lies in the fact that we obtained trends (Fig. 3.7), but no significant within-condition decoding, neither for delayed planning, nor for non-delayed execution (Fig. 3.4). A possible explanation for this seemingly discrepancy that is the fact that more trials

can be used for training and testing the classifier for cross-decoding (e.g., train on all delayed planning trials, and test on all non-delayed trials, and vice versa), whereas within-condition decoding has to rely on fewer trials (half as many, 40 vs. 80). Moreover, it is worth mentioning that previous studies using cross-decoding made similar observations, i.e., demonstrated the possibility of stronger cross-decoding than within-condition decoding (Gallivan et al., 2011b, 2013; Oosterhof et al., 2012; Ariani et al., 2015).

3.5.2 Movement planning: sustained or transient neural process?

Extending previous reports using more conventional MVPA (Gallivan et al., 2011a, 2013; Ariani et al., 2015), our time-resolved ROI-MVPA revealed decoding of hand movements during delayed planning in premotor (L-PMd) and parietal (L-aIPS) areas (Fig. 3.4-3.5). One might argue that these results might be partially driven by (1) decoding of the color cues or (2) by decoding of stimulus-response mapping rather than movement planning. Regarding the first point, our regions are not part of the inferior temporal neural networks typically associated with color perception, or knowledge about colors (Martin et al., 1995; Simmons et al., 2007). Regarding the second point, we recently compared internally- and externally triggered movements to address this issue and found abstract representations of planned hand movements (i.e., that did not depend on specific instruction cues) both in L-PMd and L-aIPS (Ariani et al., 2015). In agreement with previous studies (Cavina-Pratesi, 2006; Hartstra et al., 2012), this suggests that dorsal premotor and anterior intraparietal regions are indeed engaged in representing and preparing instructed movements.

Significant decoding appeared early within the planning delay (vol. 2 and vol. 3) and only lasted for one volume. This suggests, at least at the level of movement decoding, transient neural representations of motor plans in parieto-frontal regions. Other delayed-movement studies (Toni et al., 2001; Curtis et al., 2004; Lindner et al., 2010; Chapman et al., 2011; Gallivan et al., 2011b) have argued that planning is a sustained neural process that begins with an instructing cue and persists throughout the whole delay until the trigger.

Our results however are compatible with an alternative possibility: planning as a double transient process. Movement preparation in delayed-movement paradigms could occur once right after the instructing cue (i.e when information about the movement to plan first becomes available) and then again after the go cue (i.e., during RTs, when participants have to retrieve and release the motor plan; e.g., see Crammond and Kalaska, 2000; Pertzov et al., 2011; Confais et al., 2012). We do not exclude that during movement planning the brain could respond differently depending on task demands (i.e., on the experimental paradigm; see Mauritz and Wise, 1986). Studies with long, fixed, planning delays could elicit a more sustained brain response, whereas studies with short, jittered, delays could evoke a more transient response. Indeed, thanks to the use of jittered delays, catch trials, and randomized go/no-go conditions, the best behavioral strategy for our participants to handle the different tasks was to prepare to move as soon as possible. Subjective reports in post-session questionnaires filled right after each experimental session confirm this view (see last paragraph of *Behavior* in Results). Future studies will be needed to clarify this controversy.

3.5.3 *Unspecific suppression of movement plans*

Despite not being the main focus of this study, our design enabled us to examine also neural representations of suppressed movement plans. One possible outcome was that information about planned movements in multi-voxel patterns of fMRI activity is still present after a No-Go cue, meaning that some brain regions are involved in suppressing specific movement plans (i.e., that these inhibitory signals are movement specific). The alternative was that, regardless of the preceding movement plan, the No-Go cue would trigger unspecific suppression, similarly for different movement types, thus not allowing their decoding. Despite some trends in L-dlPFC (vol. 2), L-PMd (vol. 2) and L-SMA (vol. 2-3), we failed to obtain significant decoding of suppressed movement plans at any time-point or ROI. This outcome would be compatible with the view of unspecific suppression of movement plans, but care needs to be taken in interpreting this null-effect. For instance, it could be that due to poor spatio-temporal resolution fMRI is not a good method to answer this research question (Dubois et al., 2015). Furthermore, the lack of significant decoding could be due to a statistical power issue intrinsic to time-resolved MVPA (i.e., having many separate time-points and having to correct for multiple comparisons for all of them). Further work specifically focusing on the inhibitory aspect of motor control, and employing complementary research techniques, will help elucidating the neural dynamics and neural representations of movement suppression.

3.5.4 *Conclusions and future directions*

In agreement with previous work on non-human primates, we provided evidence for early shared representations between delayed and non-delayed

movement plans in humans. We also showed that movement representations do not necessarily remain constant throughout the planning phase, suggesting planning as a more transient process than previously hypothesized. Our findings were made possible by a time-resolved decoding approach that allowed us to examine the unfolding of movement representations across different stages of movement generation. Building on our current results, using complementary high-temporal-resolution techniques (e.g., multi-band fMRI, magneto-electroencephalography, M-EEG, and transcranial magnetic stimulation, TMS), future studies should try to clarify the relationship between delayed and non-delayed movement planning and further elucidate the neural dynamics of movement representations during planning, execution and suppression within the human prehension network.

Chapter 4.

Discussion and Future perspectives

4.1 Thesis recap

Movement planning constitutes the critical link from perceiving to interacting with the world. In the context of object manipulation, it has been suggested to consist of several intermediate, hierarchically-organized steps, including the identification of potential targets, the formation of abstract action goals, and the specification of concrete motor programs.

Early human neuroimaging studies built upon years of pioneering work on non-human primates (for reviews, Jeannerod et al., 1995; Rizzolatti and Luppino, 2001; Andersen and Buneo, 2002; Andersen and Cui, 2009; Cisek and Kalaska, 2010) to reveal several brain areas within parietal and frontal cortices involved in the planning, execution and control of hand (e.g., reaching, grasping) and eye movements (i.e., saccades) on the basis of specific motor goals (Gallivan and Culham, 2015). Although these regions were initially grouped by their specialization for certain effectors (Medendorp et al., 2005; Heed et al., 2011; Bernier et al., 2012; Leoné et al., 2014) or movement types (Begliomini et al., 2007; Brandi et al., 2014; Turella and Lingnau, 2014), the recent development of more complex and sensitive analytic tools such as MVPA (Haxby et al., 2014) has taken current fMRI

research one step beyond the original functional mapping approach. These studies have shown that a broad range of action-related information (e.g., which effector, grip type, movement sequence, wrist orientation, etc.) can be extracted from multivariate patterns of activity within widespread networks of brain regions across the whole cerebral cortex (Gallivan et al., 2011a, 2011b, 2013b, 2016b; Pistohl et al., 2012; Barany et al., 2014; Ariani et al., 2015; Nambu et al., 2015). Critically, even regions showing no activation amplitude differences between tasks or against a baseline have been demonstrated to contain enough information to allow above-chance decoding of particular planned and executed movements.

One of the key challenges that emerges from these more recent studies is to refine our understanding of the specific aspects of information that can be decoded. In other words, future work should try to identify the essential contributions given by these regions to the movement generation process.

In the present thesis, I aimed at addressing two important gaps in the field. First, given that research on planning has primarily focused on externally-triggered movements, I aimed to compare externally driven and internally driven movement plans (Study I, Chapter 2). This comparison allowed us to study planning-related brain activity devoid of co-occurring confounding sensorimotor processes, such as S-R mapping. Second, by comparing movement preparation for delayed and immediate movements (Study II, Chapter 3), I was able to address the issues related to the use of instrumental delays in delayed-movement tasks (e.g., unrelated brain activity), while still dissociating planning from execution.

Our approach included both univariate and multivariate analyses of fMRI data. That is, we looked at differences and similarities in both the coarse

amount of regional activation and the fine-grained spatial patterns of voxel activity elicited by the different experimental conditions. The univariate approach informed us about the regions recruited during the planning of prehension movements. By contrast, the multivariate approach revealed the spatial activity patterns within these regions that allowed us to discriminate different movement plans (i.e., the way movement plans are represented, or encoded, at the neural level).

4.1.1 Summary of main experimental findings

In Study I, we aimed at disentangling movement planning from overlapping delay-related neural computations. To do so, we compared an instructed (externally driven) condition with a free-choice (internally driven) condition that enabled us to investigate not only action selection, but also which areas represent movement plans in a more abstract way that is not tied to specific external cues, or internal decisions. Our decoding results revealed that a set of contralateral parieto-frontal brain regions (SPL, IPS, PMd, and M1) can discriminate planned movements across planning conditions. Conversely, other regions encoded planned movements only when these were internally (i.e., contralateral PMv, dlPFC, SMG, and ipsilateral pIPS, pSTG, pMTG) or externally (i.e., bilateral SMA, pre-SMA) driven. In addition to replicating and corroborating previous findings about parieto-frontal regions encoding instructed plans for prehension movements (Baumann et al., 2009; Fluet et al., 2010; Gallivan et al., 2011b; Leoné et al., 2014), these results suggest that neural representations in contralateral regions of the human prehension system reflect movement planning rather than arbitrary associations between stimuli and responses.

In Study II, we aimed at better characterizing the neural coding of movement plans for reaching and grasping by filtering out unrelated brain activity present in the planning phase of delayed-movement tasks (e.g., working-memory, decision-making, mental wandering, etc.). To do so, we asked which substrates and computations are shared between delayed and non-delayed movement planning, and whether decoding results obtained with delayed-movement tasks can be generalized to immediate movements. We compared three main experimental conditions: a delayed task (i.e., planning with execution), a non-delayed task (i.e., execution without planning), and a no-go task (i.e., planning without execution). Additionally we took advantage of time-resolved MVPA to explore the temporal unfolding of movement classification throughout the different stages of movement planning, execution and suppression. Using this approach, we were able to decode planned movements across delayed and non-delayed tasks in contralateral primary motor cortex (M1), revealing early shared representations between delayed and non-delayed movement plans. This suggests that human primary motor cortex contains similar information about upcoming hand movements regardless of the presence of a delay.

4.2 Searching for core representations of movement planning

Previous studies that investigated neural representations of movement planning within the human prehension system were based on delayed-movement paradigms and instructed movements (Eisenberg et al., 2011; Gallivan et al., 2011b; Pertzov et al., 2011; Leoné et al., 2014; Turella et al., 2016). For understandable pragmatic reasons, researchers usually presented

subjects with visual or auditory cues to guide their actions and then measure delay-related responses in relation to them. Indeed, movement preparation has proven hard to study experimentally. First, like other cognitive functions (e.g., memory, imagery, or attention), planning is a covert process, and as such cannot be directly observed, but only inferred from indirect measures (e.g., brain responses, or effects on subsequent behavior, reaction times, etc.). Second, particularly for human fMRI studies, which typically lack the temporal precision of neuronal recodings in monkeys, another source of difficulty is given by the temporal coupling between movement planning and execution. If planning is always immediately followed by execution (i.e., perfectly correlated), then it becomes hard to disentangle the respective contributions of each stage of movement generation to the measured brain effects.

In this respect, the use of instructed movements and instrumental delays has been quite successful, enabling researchers to study planning and execution in isolation from each other. Additionally, inserting a delay between the presentation of a visual or auditory instructing cue and the subsequent movement has the advantage of separating sensory and motor related brain responses.

This delayed-movement approach has provided important contributions to the study of sensorimotor control, both in humans and monkeys. For instance, previous work elucidated the neural correlates of movement preparation and execution for saccades and manual actions, such as reaching, grasping and tool use (Cisek and Kalaska, 2004; Afshar et al., 2011; Brandi et al., 2014; Turella and Lingnau, 2014). Other studies proposed organizing principles for this network of brain areas (Eisenberg et al., 2010;

Heed et al., 2011; Verhagen et al., 2013) and revealed specific sensorimotor contributions to movement planning by regions within the prehension system (Hoshi and Tanji, 2004, 2006; Medendorp et al., 2005; Verhagen et al., 2012; Zimmermann et al., 2016).

However, even when properly dissociated from execution, our ability to plan future actions remains a complex phenomenon, with close links to several other sensory and cognitive processes (e.g., visual perception, S-R mapping, memory, decision-making). For example, during visually-guided prehension movements, vision is required to select the object that will be the target of our action plan and to know our position in the environment relative to the object's own (i.e., the distance between us). On the other hand, during memory-guided prehension movements, we also need to remember the association between a cue and a response, as well as the spatial location of the target object in order to plan where to grasp for it.

One key aspect that the studies presented in this thesis have in common is the search for regions that (1) were specifically involved in movement preparation (i.e., univariate results) rather than in co-occurring brain computations, and (2) encoded representations of movement plans (i.e., multivariate results) distinctly from those of other overlapping delay-related brain processes. In other words, we tried to carve out what lies at the core of movement preparation, addressing factors often mixed up in previous paradigms.

First, to disentangle the S-R mapping and action selection components of the planning delay, we explored the relationship between movement planning and voluntary action by comparing internally and externally driven hand movements in Study I. Previous studies on internally driven actions

have typically opted for instructions that, keeping some aspects of a movement fixed while letting participants choose others, only partially determine the outcome of a task. Most frequently, subjects are requested to perform an action at a specified time but are allowed to select either a spatial target (Watanabe et al., 2006; Pastor-Bernier et al., 2012) or a moving effector (Oliveira et al., 2010; Bernier et al., 2012), a type of movement (Zhang et al., 2012) or movement sequence (Pesaran et al., 2008). Other studies instead entail the repetition of predefined actions (e.g., pressing a button), leaving the timing of execution up to the participants – whenever they "feel the urge to [move]" (Libet et al., 1983; Haynes, 2011; Soon et al., 2008). In our experiment, we gave participants the choice of which prehension movement to plan and execute. We hypothesized that areas representing chosen movements should reflect action selection processes. Conversely, areas representing instructed movements should reflect the association between sensory cues and the corresponding motor responses. Finally, this design allowed us to study areas representing movement plans across instruction conditions. These abstract neural representations should not depend on any component or process that is specific to either condition; rather, they should reveal what they have in common, thus better reflecting the core of movement planning.

Second, to further remove delay-related brain activity that was unspecific to movement preparation, in Study II we compared delayed and non-delayed movements, looking for shared neural representations across these conditions. We reasoned that while delayed movements are planned, withheld, and then released, non-delayed movements are planned and immediately executed (Ames et al., 2014). Therefore, by studying the shared

planning component of both movement types, we should be able to reveal the key regions and neural representations at the core of movement planning. On the one hand, we would remove delay-related brain activity that does not strictly pertain to planning (e.g., working-memory). On the other hand, we would remove execution-related brain activity that, in natural non-delayed movements, is always intermingled with planning and tends to overshadow the weaker planning-related brain responses.

Despite requiring a conceptually opposite approach by the participants (i.e., choosing and acting vs not-choosing and reacting to a stimulus), it seems reasonable to expect that planning an externally determined movement and a movement of choice present similarities at the neural level (Cisek and Kalaska, 2005; Cui and Andersen, 2007, 2011; Pesaran et al., 2008). Likewise, preparing to execute a movement immediately should at least partially intersect with preparing a movement and withholding in memory for some time before releasing it (Crammond and Kalaska, 2000; Ames et al., 2014). In support of these hypotheses, and in agreement with previous human and monkey studies, we confirmed that the same parieto-frontal network involved in movement planning also participates when actions are freely chosen or internally driven (Pesaran et al., 2008; Andersen and Cui, 2009; Cisek and Kalaska, 2010). Indeed, premotor, prefrontal and posterior parietal regions have been reported for a variety of motor tasks, from choosing a reaching target (Cisek and Kalaska, 2005; Scherberger and Andersen, 2007; Thura and Cisek, 2014) to selecting a limb for giving the response (Dirnberger et al., 1998; Beudel and De Jong, 2009; Garcia Dominguez et al., 2011). Similarly, we observed a large overlap in the brain regions recruited during movement planning for delayed and non-delayed

movements (Fig. 3.2A-B). Despite the overall stronger activation for non-delayed execution compared to delayed planning, a widespread bilateral network of frontal, parietal and temporal regions was involved during both conditions (Himmelbach et al., 2009).

Observing comparable brain activations for externally and internally driven movements (see univariate results), or between delayed and immediate movements, one might think that neural representations of planned movements do not substantially change with respect to the mode of action selection (i.e., internal vs. external), or the presence of an instrumental delay. However, our decoding results highlighted some differences between these experimental conditions, which seem to lead to a partially different conclusion. For instance, in Study I, we showed that internally driven movement plans are represented in a larger and more widespread network than externally driven movement plans (Fig. 2.5). This network included also regions that did not encode externally driven movements (Fig. 2.3B). On the other hand, we found trends for regions encoding externally but not internally driven movements (Fig. 2.3C). Moreover, only a subset of the regions showing univariate effects during planning encoded upcoming movements across instruction conditions (Fig. 2.4, Fig. 2.6). In Study II we found that several bilateral parieto-frontal areas of the brain contained representations of non-delayed movements (Fig. 3.7B), whereas fewer regions (particluarly in the contralateral hemisphere) seemed to encode delayed movement plans (Fig. 3.7A). With the exception of the contralateral primary motor cortex, where we found similar multi-voxel activity patterns during early motor preparation of delayed and immediate movements (Fig. 3.4), neural representations elicited by delayed

and non-delayed movement plans appeared to be quite different (i.e., no cross-condition decoding).

Collectively, these results suggest that not all the regions showing univariate activations during movement planning contain neural representations of the planned movements. Rather, we found that only regions in contralateral dorso-lateral parietal and frontal cortices encoded movement plans regardless of the way they were generated, and only the contralateral primary motor cortex contained neural representations that generalize across delayed and non-delayed movement plans. Our experimental manipulations ruled out the possibility that these neural representations reflected simple stimulus-response mapping (Hartstra et al., 2012) or movement decisions (Zhang et al., 2012). Overall our studies contributed to a better characterization of brain regions in the human parieto-frontal network, clarifying the kind of motor and non-motor representations previously lumped together under delayed planning of instructed prehension movements.

4.3 Exploring the temporal dynamics of movement decoding with fMRI

Functional magnetic resonance imaging is generally known for high spatial resolution but limited temporal precision (Sladky et al., 2011; Turner, 2016). The sluggishness of the hemodynamic blood-oxygen-level dependent (BOLD) response and the time needed to acquire each single brain volume (i.e., the repetition time, TR, usually about 2 seconds) make it generally difficult to infer neural processing taking place at a millisecond time-scale

(but see Ogawa et al., 2000). Nonetheless a certain amount of temporal information can still be extracted from fMRI datasets, particularly for behaviors and events extending over a few seconds. As already mentioned in the Introduction section of this thesis, in the context of neuroimaging research on movement planning, the delayed-movement paradigm (also known with the more general term delayed-match-to-sample, from studies on perceptual decision-making) can be thought of as an experimental device to spread out in time fast-occurring and largely overlapping brain computations (e.g., planning and executing, deciding and giving a response). In other words, by artificially creating separate trial phases for movement preparation and execution, it became possible to focus on either aspect of motor control temporally isolated from the other.

Typical univariate analyses in previous studies consisted of modeling the planning phase with a boxcar function lasting almost if not the entire delay-period duration (e.g., Toni et al., 2001; Cavina-Pratesi, 2006; Mars et al., 2008; Beurze et al., 2009; Heed et al., 2011; Gertz and Fiehler, 2015). This approach followed the assumption that, after the voluntary selection or external specification of a motor program, planning-related brain responses rise and remain sustained, basically invariant, over time. Even when analyzing fMRI datasets with more sensitive multivariate methods that allow decoding neural representations of planned movements, the standard approach was to feed machine-learning classifiers with the outcome of univariate analyses, often taking a windowed average of brain activity over several seconds of the planning phase (Gallivan et al., 2011a, 2011b, 2013a, 2013b, 2016b; Leoné et al., 2014). The clear trade-off is gaining more statistical power over losing information about temporal dynamics of

decodable information (e.g., motor plans). In other words, larger windows of averaged brain activity are more robust but allow for fewer time points to reconstruct the variations in decoding accuracy over time, and vice versa.

In our second study (Study II, Chapter 3) we tried to address this methodological aspect by adopting and further developing a novel MVPA approach. We took advantage of a time-resolved method in which movement classification was performed separately at each acquired volume. This allowed us to track how decoding accuracies evolved at different time points within the delay period. Previous studies with delayed-movement tasks and standard analysis methods suggested sustained brain activity throughout movement planning (Toni et al., 2001; Curtis et al., 2004; Lindner et al., 2010; Chapman et al., 2011; Gallivan et al., 2011b). Using time-resolved MVPA we observed that, at least at the level of decoding (in comparison to univariate analyses), neural representations of delayed hand movement plans appear to be less constant over time than previously hypothesized. Moreover, thanks to this method, we were able to compare delayed and immediate movements at various stages of movement generation. In the primary motor cortex, we obtained significant cross-condition decoding early within the respective phases of delayed planning and non-delayed execution, but not at later time points. This could suggest that neural representations of planned prehension movements are initially similar across delay contexts and then diverge when movements are actually executed in one condition but not (yet) in the other.

Overall, we took conventional MVPA methods one step further by providing further insight about the temporal dynamics of movement representations within the human prehension system. Previous fMRI studies

used similar methods to examine the flow of information from sensory stimuli to motor responses in the human brain (Soon et al., 2008, 2013; Bode and Haynes, 2009; Linden et al., 2012; Gallivan et al., 2013c). Our time-resolved MVPA differs from these previous studies in at least two important ways. First, we did not simply subdivide the delay period into arbitrary bins of time averaging windows of brain activity spanning over several seconds (e.g., Bode and Haynes, 2009; Linden et al., 2012). Rather, our analysis was truly performed volume-by-volume and the temporal resolution depended solely on the TR, that is, on the time for the fMRI scanner to collect one full brain volume. Second, instead of beta-weights or t-scores coming from a GLM (e.g., Leoné et al., 2014), we used volume-time-course data as input for the MVPA classifier. This carries the advantage that our findings are less dependent on specific assumptions regarding the expected shape of the hemodynamic response function (HRF). Overall, we believe that time-resolved MVPA constitutes a powerful tool for fMRI data analysis to substantially improve the temporal resolution of a technique that can already provide very good spatial information about neural representations of movement planning in the human brain.

4.4 Future directions

In the following section I am going to take into consideration three classes of limitations and caveats that might hinder the scope of our conclusions: limitations about (1) the technique, (2) the analysis methods, and (3) the task. At the same time I will discuss possible ways to address these issues. This is not intended to be a comprehensive list of the problems and solutions

for neuroimaging research on prehension movements, but rather an opportunity to hopefully foster new ideas and stimulate future studies. Finally, I will briefly address potential applications for this branch of research.

4.4.1 Limitations, possibilities, and open questions

Several limitations are intrinsic to the technique used in this thesis to collect data – fMRI shortcomings have been known for years (Logothetis and Wandell, 2004; Logothetis, 2008; Turner, 2016). As already mentioned, depending on the TR and on a hemodynamic response (in the order of seconds), the temporal resolution is quite poor for fast-occurring neuronal computations. The spatial resolution, with the size of voxels typically around 3x3x3 mm, is far from the cellular level. Moreover, fMRI is based on an indirect measure of neuronal activity (the hemodynamic BOLD response), which has been shown to correlate with local field potentials (LFP) of a given neuronal population, rather than the spiking activity (Logothetis et al., 2001; Logothetis, 2003). For instance, this could be problematic when comparing fMRI experiments and experiments in monkeys. Despite using the same tasks or stimulation conditions, BOLD fMRI could reveal significant activation in the absence of spiking activity, leading to results that are inconsistent with those from monkey neurophysiology.

Another factor to consider in neuroimaging research on movements is that experiments need to focus on actions that are compatible with the environment of the fMRI scanner (i.e., that can actually be performed while lying inside such a narrow space). This is one of the reasons why prehension movements have been investigated so extensively in recent years. In order to

limit the risk of signal artifacts, researchers conducting fMRI experiments have to be careful when studying actions that might trigger head motion by the participants. For the experiments described in this thesis, we used foam blocks and cushions to stabilize the shoulder and elbow of the moving arm. Furthermore we adjusted the distance from the target object according to each participant's arm length. This setup ensured that participants could perform reaching and grasping movements comfortably, while minimizing head and trunk movements.

A way to address these fMRI-related issues is to ask the same or similar research questions but using complementary techniques. Future studies could exploit the temporal resolution of magnetoencephalography (MEG; in the millisecond scale) to further investigate the temporal dynamics of movement planning with greater temporal precision (e.g., Hinkley et al., 2011; Turella et al., 2016). For example, such studies could focus on the shared representations that we observed across delayed and immediate movement plans and ask when exactly they emerge, or how long they last. The same could be done with electroencephalography (EEG; e.g., Ball et al., 1999; Llanos et al., 2013). It could be noted that MEG and EEG are very susceptible to movement artifacts, even more than fMRI, but ultimately every technique has its own characteristic strengths and limitations. This is why the best approach is to address the same topic from different angles, asking questions that are most suitable for each technique.

Among fMRI analysis methods, MVPA is a recent innovation, increasingly used as it proved to be effective at discriminating response patterns that are distributed at a fine spatial scale (i.e., decoding more subtle aspects of neural

representations). However, regardless of the approach or the specific method used, fMRI data analysis always relies on certain assumptions and comes with technical limitations (Smith et al., 2011; Etzel et al., 2013; Todd et al., 2013; Dubois et al., 2015). As an example, given the massive number of voxels that virtually fit within a brain volume (>100.000), one of the key problems with searchlight MVPA concerns low statistical power when correcting results for multiple comparisons. Indeed, it is important to be aware of all these different issues when looking at the results of neuroimaging studies, as they might be the cause of inconsistencies and thus lead to difficulties in interpretation.

Related to the experiments and analyses present in this thesis, it should be noted that we chose to focus particularly on the effects and contributions of the cerebral cortex. We thus neglected the role and importance of subcortical brain structures, or the cerebellum, in our studies. For us, this was motivated in part by technical choices (e.g., deciding whether to cover the entire cerebellum at the expense of a portion of the parietal lobe within a reasonably short TR) and in part by pragmatic reasons (e.g., focusing on the ROIs that are typically discussed in the literature). However this cortico-centric view of the brain appears to be a widespread tendency in the field of movement research, and as such it should at least be acknowledged, with the hope that future studies will further explore the neural correlates and representations of movement planning even in subcortical and cerebellar areas.

I believe that gradual advances in analysis methods will address and possibly solve, or at least improve, many of the current problems with MVPA of fMRI data. However one more aspect that was relevant to my PhD

project should be discussed. In accordance with previous work, we demonstrated that it is possible to decode planned movements from brain activity that precedes movement onset. One key challenge for future studies will have to be moving beyond simply decoding motor plans, or just revealing movement representations. Classification should be just the first step for this kind of analysis. Once we have shown that two planning conditions are discriminable on the basis of neural activity patterns we should ask: in what ways are they different? Or, how different are they from each other (e.g., see pattern information in Leoné et al., 2014)? How do these different representations specifically relate to subsequent behavior? In other words, how does the planning of one movement in one condition affect the way this movement will be executed differently from another condition? And again, what do these neural representations tell us about the underlying neural computations for movement planning? Open questions like these should be at the core of future developments in neuroimaging research on movements.

As mentioned in the introduction section of this thesis, movement planning is not a prerogative of prehension movements. Ideally, research on the preparation of reaching, grasping and eye movements should generalize to all kinds of possible actions, at least in terms of underlying principles (perhaps the specific regions recruited will slightly differ according to e.g., the effector used, Heed et al., 2011; Leoné et al., 2014). Just like we plan to grasp our smartphone, we can prepare for throwing a dart, climbing a rock, or kicking a ball. However, because the great majority of studies investigated the planning of reaching, grasping and saccades, this generalizability aspect

remains an open question. I think there is a need to include a wider range of ecologically-valid actions in the tasks of future experiments (e.g., Fabbri et al., 2016). While it is true that the boundaries of this range are often dictated by the technique used or by a specific research question, it would be informative to compare motor preparation of prehension with that of more complex and natural hand movements (e.g., writing, drawing, gesturing).

Another aspect of the tasks used to study movement planning, which to date remains unclear, concerns individual differences across participants, with particular emphasis on the influence of different strategies to handle different tasks. Do all people think of planning in the same way? When confronted with delayed-movement paradigms, do participants approach the delay period similarly? Could some manipulations, or experimental conditions, trigger a different planning strategy? In our two experiments we always administered post-session questionnaires to our participants, and one of the questions was about the strategy used to handle the task. Although we did not report major differences in the responses by participants, this is something that seems to be worth delving into in future research.

4.4.2 Potential practical applications

Several brain diseases and injuries (e.g., Parkinson's disease, amyotrophic lateral sclerosis, spinal cord injury, limb amputation) result in the loss of the ability to make purposeful and accurate movements, dramatically affecting the quality of life of these patients. Developing therapeutic interventions for such patients is a major area of research. Within the biomedical field, devices named brain-computer interfaces (BCIs) constitute a relatively recent invention. Also known as neural prostheses, BCI systems are built to

measure a patient's intention-related brain signals (e.g., with electrocorticography, ECoG), use them to decode a planned movement, and to convert this information into output commands capable of controlling external devices that range from computer cursors to robotic limbs, thus bypassing the compromised body parts (Andersen and Buneo, 2002; Hochberg et al., 2006; Schalk and Leuthardt, 2011). Knowledge about how movements and intentions are encoded in patterns of neural activity is at the basis of BCI technologies (Gallivan et al., 2011b). A deeper understanding of the cortical circuitry responsible for generating complex sensorimotor behaviors (e.g., prehension movements), and the identification of brain areas containing representations of motor plans for specific effectors (e.g., right hand, left hand) and contexts (e.g., internally driven, non-delayed), will be beneficial for the further development of ever more sophisticated, precise and effective neural prostheses (e.g., informing about optimal positioning for electrode arrays to capture appropriate intention-related signals). The hope is that, with the increasing number of studies on these topics, eventually this class of BCI devices will be able to reconstruct highly specific movement plans and thus restore the lost motor functionality for movement-impaired patient populations (e.g., Orsborn et al., 2014; Shenoy and Carmena, 2014; Shanechi et al., 2016).

4.5 Conclusions

This thesis explored how the human brain represents planned reaching and grasping movements in different behavioral contexts. In neuroimaging experiments using delayed-movement paradigms, delay-related neural

activity includes cognitive processes intermingled with movement preparation. The studies reported here aimed at clarifying this aspect, as well as the different roles of regions within parieto-frontal networks. Collectively, our results provided evidence for neural representations that, invariant to the mode of action selection, or the presence of a delay, more specifically reflect motor-related processes during movement planning. We also further improved a novel fMRI-MVPA method that allowed us to follow how these representations change throughout the stages of movement generation. Overall, our findings expand previous understanding of the regions implicated in movement planning and offer new insights into the dynamics of the human prehension system.

By addressing several open questions and limitations in this branch of research, I hope that my work will contribute to a deeper understanding of the cortical basis and neural representations of movement planning. The resulting knowledge might ultimately find application in the improvement of brain-controlled prostheses to assist movement-impaired patients. Beyond therapeutic possibilities, like for all basic research, the benefits of exploring how the nervous system generates purposeful movement are manifold, laying the theoretical foundations for discoveries and technological advances in various related fields.

References

Afshar A, Santhanam G, Yu BM, Ryu SI, Sahani M, Shenoy K V. (2011) Single-trial neural correlates of arm movement preparation. Neuron 71:555–564.

Ames KC, Ryu SI, Shenoy K V. (2014) Neural dynamics of reaching following incorrect or absent motor preparation. Neuron 81:438–451.

Andersen RA, Buneo CA (2002) Intentional maps in posterior parietal cortex. Annual Review of Neuroscience 25:189–220.

Andersen RA, Cui H (2009) Intention, Action Planning, and Decision Making in Parietal-Frontal Circuits. Neuron 63:568–583.

Ariani G, Wurm MF, Lingnau A (2015) Decoding Internally and Externally Driven Movement Plans. Journal of Neuroscience 35:14160–14171.

Astafiev SV, Stanley CM, Shulman GL, Corbetta M (2004) Extrastriate body area in human occipital cortex responds to the performance of motor actions. Nature neuroscience 7:542–548.

Badre D, D'Esposito M (2009) Is the rostro-caudal axis of the frontal lobe hierarchical? Nature reviews Neuroscience 10:659–669.

Ball T, Schreiber A, Feige B, Wagner M, Lücking CH, Kristeva-Feige R (1999) The Role of Higher-Order Motor Areas in Voluntary Movement as Revealed by High-Resolution EEG and fMRI. NeuroImage 10:682–694.

Barany DA, Della-Maggiore V, Viswanathan S, Cieslak M, Grafton ST (2014) Feature Interactions Enable Decoding of Sensorimotor

Transformations for Goal-Directed Movement. Journal of Neuroscience 34:6860–6873.

Bastian A, Schöner G, Riehle A (2003) Preshaping and continuous evolution of motor cortical representations during movement preparation. European Journal of Neuroscience 18:2047–2058.

Baumann MA, Fluet M-C, Scherberger H (2009) Context-Specific Grasp Movement Representation in the Macaque Anterior Intraparietal Area. The Journal of Neuroscience 29:6436–6448.

Begliomini C, Wall MB, Smith AT, Castiello U (2007) Differential cortical activity for precision and whole-hand visually guided grasping in humans. European Journal of Neuroscience 25:1245–1252.

Benjamini Y, Yekutieli D (2001) The control of the false discovery rate in multiple testing under depencency. The Annals of Statistics 29:1165–1188.

Bernier P-M, Cieslak M, Grafton ST (2012) Effector selection precedes reach planning in the dorsal parietofrontal cortex. Journal of neurophysiology 108:57–68.

Beudel M, De Jong BM (2009) Overlap and segregation in predorsal premotor cortex activations related to free selection of self-referenced and target-based finger movements. Cerebral Cortex 19:2361–2371.

Beurze SM, de Lange FP, Toni I, Medendorp WP (2009) Spatial and effector processing in the human parietofrontal network for reaches and saccades. Journal of neurophysiology 101:3053–3062.

Binkofski F, Buccino G, Stephan KM, Rizzolatti G, Seitz RJ, Freund HJ (1999) A parieto-premotor network for object manipulation: Evidence from neuroimaging. Experimental Brain Research 128:210–213.

Bode S, Bogler C, Haynes JD (2013) Similar neural mechanisms for perceptual guesses and free decisions. NeuroImage 65:456–465.

Bode S, Haynes JD (2009) Decoding sequential stages of task preparation in the human brain. NeuroImage 45:606–613.

Brainard DH (1997) The Psychophysics Toolbox. Spatial vision 10:433–436.

Brandi M, Wohlschla A, Sorg C, Hermsdo J (2014) The Neural Correlates of Planning and Executing Actual Tool Use. The Journal of neuroscience : the official journal of the Society for Neuroscience 34:13183–13194.

Cavina-Pratesi C (2006) Dissociating Arbitrary Stimulus-Response Mapping from Movement Planning during Preparatory Period: Evidence from Event-Related Functional Magnetic Resonance Imaging. Journal of Neuroscience 26:2704–2713.

Cavina-Pratesi C, Monaco S, Fattori P, Galletti C, McAdam TD, Quinlan DJ, Goodale MA, Culham JC (2010) Functional Magnetic Resonance Imaging Reveals the Neural Substrates of Arm Transport and Grip Formation in Reach-to-Grasp Actions in Humans. Journal of Neuroscience 30:10306–10323.

Chang C-C, Lin C-J (2011) LIBSVM: A library for support vector machines. ACM Transactions on Intelligent Systems and Technology 2:1–27.

Chapman CS, Gallivan JP, Culham JC, Goodale MA (2011) Mental blocks: fMRI reveals top-down modulation of early visual cortex when obstacles interfere with grasp planning. Neuropsychologia 49:1703–1717.

Cisek P (2006) Preparing for Speed. Focus on "Preparatory Activity in Premotor and Motor Cortex Reflects the Speed of the Upcoming Reach." Journal of Neurophysiology 96:2842–2843.

Cisek P, Kalaska JF (2004) Neural correlates of mental rehearsal in dorsal premotor cortex. Nature 431:993–996.

Cisek P, Kalaska JF (2005) Neural correlates of reaching decisions in dorsal premotor cortex: Specification of multiple direction choices and final selection of action. Neuron 45:801–814.

Cisek P, Kalaska JF (2010) Neural mechanisms for interacting with a world full of action choices. Annual review of neuroscience 33:269–298.

Cohen NR, Cross ES, Tunik E, Grafton ST, Culham JC (2009) Ventral and dorsal stream contributions to the online control of immediate and delayed grasping: A TMS approach. Neuropsychologia 47:1553–1562.

Confais J, Kilavik BE, Ponce-Alvarez A, Riehle A (2012) On the anticipatory precue activity in motor cortex. The Journal of neuroscience : the official journal of the Society for Neuroscience 32:15359–15368.

Connolly JD, Goodale M a, Menon RS, Munoz DP (2002) Human fMRI evidence for the neural correlates of preparatory set. Nature neuroscience 5:1345–1352.

Crammond DJ, Kalaska JF (2000) Prior information in motor and premotor cortex: activity during the delay period and effect on pre-movement activity. Journal of neurophysiology 84:986–1005.

Cui H, Andersen RA (2007) Posterior Parietal Cortex Encodes Autonomously Selected Motor Plans. Neuron 56:552–559.

Cui H, Andersen RA (2011) Different Representations of Potential and Selected Motor Plans by Distinct Parietal Areas. Journal of Neuroscience 31:18130–18136.

Culham JC, Danckert SL, DeSouza JFX, Gati JS, Menon RS, Goodale M a (2003) Visually guided grasping produces fMRI activation in dorsal but

not ventral stream brain areas. Experimental brain research Experimentelle Hirnforschung Expérimentation cérébrale 153:180–189.

Cunnington R, Windischberger C, Deecke L, Moser E (2002) The Preparation and Execution of Self-Initiated and Externally-Triggered Movement: A Study of Event-Related fMRI. NeuroImage 15:373–385.

Cunnington R, Windischberger C, Deecke L, Moser E (2003) The preparation and readiness for voluntary movement: a high-field event-related fMRI study of the Bereitschafts-BOLD response. NeuroImage 20:404–412.

Curtis CE, Rao VY, D'Esposito M (2004) Maintenance of Spatial and Motor Codes during Oculomotor Delayed Response Tasks. Journal of Neuroscience 24:3944–3952.

Davare M, Kraskov A, Rothwell JC, Lemon RN (2011) Interactions between areas of the cortical grasping network. Current Opinion in Neurobiology 21:565–570.

Dirnberger G, Fickel U, Lindinger G, Lang W, Jahanshahi M (1998) The mode of movement selection. Movement-related cortical potentials prior to freely selected and repetitive movements. Experimental Brain Research 120:263–272.

Dubois J, de Berker AO, Tsao DY (2015) Single Unit Recordings in the Macaque Face Patch System Reveal Limitations of fMRI MVPA. Journal of Neuroscience 35:2791–2802.

Eisenberg M, Shmuelof L, Vaadia E, Zohary E (2010) Functional organization of human motor cortex: directional selectivity for movement. J Neurosci 30:8897–8905.

Eisenberg M, Shmuelof L, Vaadia E, Zohary E (2011) The representation of visual and motor aspects of reaching movements in the human motor cortex. The Journal of neuroscience : the official journal of the Society for Neuroscience 31:12377–12384.

Etzel JA, Zacks JM, Braver TS (2013) Searchlight analysis: Promise, pitfalls, and potential. NeuroImage 78:261–269.

Fabbri S, Strnad L, Caramazza A, Lingnau A (2014) Overlapping representations for grip type and reach direction. NeuroImage 94:138–146.

Fabbri S, Stubbs KM, Cusack R, Culham JC (2016) Disentangling Representations of Object and Grasp Properties in the Human Brain. Journal of Neuroscience 36:7648–7662.

Fattori P, Raos V, Breveglieri R, Bosco A, Marzocchi N, Galletti C (2010) The Dorsomedial Pathway Is Not Just for Reaching: Grasping Neurons in the Medial {Parieto-Occipital} Cortex of the Macaque Monkey. The Journal of Neuroscience 30:342–349.

Filimon F (2010) Human cortical control of hand movements: parietofrontal networks for reaching, grasping, and pointing. The Neuroscientist : a review journal bringing neurobiology, neurology and psychiatry 16:388–407.

Fischl B, Sereno MI, Tootell RBH, Dale AM (1999) High-resolution intersubject averaging and a coordinate system for the cortical surface. Human Brain Mapping 8:272–284.

Fluet M-C, Baumann M a, Scherberger H (2010) Context-Specific Grasp Movement Representation in Macaque Ventral Premotor Cortex. Journal of Neuroscience 30:15175–15184.

Forman SD, Cohen JD, Fitzgerald M, Eddy WF, Mintun MA, Noll DC (1995) Improved Assessment of Significant Activation in Functional Magnetic Resonance Imaging (fMRI): Use of a Cluster-Size Threshold. Magnetic Resonance in Medicine 33:636–647.

Fried I, Mukamel R, Kreiman G (2011) Internally Generated Preactivation of Single Neurons in Human Medial Frontal Cortex Predicts Volition. Neuron 69:548–562.

Gallivan JP (2014) A Motor-Oriented Organization of Human Ventral Visual Cortex? The Journal of neuroscience : the official journal of the Society for Neuroscience 34:3119–3121.

Gallivan JP, Barton KS, Chapman CS, Wolpert DM, Randall Flanagan J (2015) Action plan co-optimization reveals the parallel encoding of competing reach movements. Nature communications 6:7428.

Gallivan JP, Bowman NAR, Chapman CS, Wolpert DM, Flanagan JR (2016a) The sequential encoding of competing action goals involves dynamic restructuring of motor plans in working memory. Journal of neurophysiology:jn.00951.2015.

Gallivan JP, Cavina-Pratesi C, Culham JC (2009) Is That within Reach? fMRI Reveals That the Human Superior Parieto-Occipital Cortex Encodes Objects Reachable by the Hand. Journal of Neuroscience 29:4381–4391.

Gallivan JP, Chapman CS, McLean DA, Flanagan JR, Culham JC (2013a) Activity patterns in the category-selective occipitotemporal cortex predict upcoming motor actions. European Journal of Neuroscience 38:2408–2424.

Gallivan JP, Culham JC (2015) Neural coding within human brain areas

involved in actions. Current Opinion in Neurobiology 33:141–149.

Gallivan JP, Johnsrude IS, Randall Flanagan J (2016b) Planning Ahead: Object-Directed Sequential Actions Decoded from Human Frontoparietal and Occipitotemporal Networks. Cerebral Cortex 26:708–730.

Gallivan JP, McLean DA, Flanagan JR, Culham JC (2013b) Where One Hand Meets the Other: Limb-Specific and Action-Dependent Movement Plans Decoded from Preparatory Signals in Single Human Frontoparietal Brain Areas. Journal of Neuroscience 33:1991–2008.

Gallivan JP, McLean DA, Smith FW, Culham JC (2011a) Decoding Effector-Dependent and Effector-Independent Movement Intentions from Human Parieto-Frontal Brain Activity. Journal of Neuroscience 31:17149–17168.

Gallivan JP, McLean DA, Valyear KF, Culham JC (2013c) Decoding the neural mechanisms of human tool use. eLife 2:e00425.

Gallivan JP, McLean DA, Valyear KF, Pettypiece CE, Culham JC (2011b) Decoding Action Intentions from Preparatory Brain Activity in Human Parieto-Frontal Networks. Journal of Neuroscience 31:9599–9610.

Garcia Dominguez L, Kostelecki W, Wennberg R, Perez Velazquez JL (2011) Distinct dynamical patterns that distinguish willed and forced actions. Cognitive Neurodynamics 5:67–76.

Gertz H, Fiehler K (2015) Human posterior parietal cortex encodes the movement goal in a pro-/anti-reach task. Journal of Neurophysiology 114:170–183.

Glover S, Wall MB, Smith AT (2012) Distinct cortical networks support the

planning and online control of reaching-to-grasp in humans. European Journal of Neuroscience 35:909–915.

Goebel R, Esposito F, Formisano E (2006) Analysis of functional image analysis contest (FIAC) data with brainvoyager QX: From single-subject to cortically aligned group general linear model analysis and self-organizing group independent component analysis. Human Brain Mapping 27:392–401.

Grafton ST (2010) The cognitive neuroscience of prehension: Recent developments. Experimental Brain Research 204:475–491.

Haggard P (2005) Conscious intention and motor cognition. Trends in Cognitive Sciences 9:290–295.

Haggard P (2008) Human volition: towards a neuroscience of will. Nature reviews Neuroscience 9:934–946.

Hartstra E, Kuhn S, Verguts T, Brass M (2011) The implementation of verbal instructions: An fMRI study. Human Brain Mapping 32:1811–1824.

Hartstra E, Waszak F, Brass M (2012) The implementation of verbal instructions: Dissociating motor preparation from the formation of stimulus-response associations. NeuroImage 63:1143–1153.

Haxby JV (2012) Multivariate pattern analysis of fMRI: The early beginnings. NeuroImage 62:852–855.

Haxby JV, Connolly AC, Guntupalli JS (2014) Decoding Neural Representational Spaces Using Multivariate Pattern Analysis. Annual review of neuroscience:435–456.

Haxby JV, Gobbini MI, Furey ML, Ishai A, Schouten JL, Pietrini P (2001) Distrubuted and Overlapping Representations of Face and Objects in Ventral Temporal Cortex. Science 293:2425–2430.

Haynes JD (2011) Decoding and predicting intentions. Annals of the New York Academy of Sciences 1224:9–21.

Heed T, Beurze SM, Toni I, Roder B, Medendorp WP (2011) Functional Rather than Effector-Specific Organization of Human Posterior Parietal Cortex. Journal of Neuroscience 31:3066–3076.

Himmelbach M, Nau M, Zundorf I, Erb M, Perenin MT, Karnath HO (2009) Brain activation during immediate and delayed reaching in optic ataxia. Neuropsychologia 47:1508–1517.

Hinkley LBN, Nagarajan SS, Dalal SS, Guggisberg AG, Disbrow EA (2011) Cortical Temporal Dynamics of Visually Guided Behavior. Cerebral Cortex 21:519–529.

Hochberg LR, Serruya MD, Friehs GM, Mukand JA, Saleh M, Caplan AH, Branner A, Chen D, Penn RD, Donoghue JP (2006) Neuronal ensemble control of prosthetic devices by a human with tetraplegia. Nature 442:164–171.

Hoshi E, Tanji J (2000) Integration of target and body-part information in the premotor cortex when planning action. Nature 408:466–470.

Hoshi E, Tanji J (2004) Differential roles of neuronal activity in the supplementary and presupplementary motor areas: from information retrieval to motor planning and execution. Journal of neurophysiology 92:3482–3499.

Hoshi E, Tanji J (2006) Differential involvement of neurons in the dorsal and ventral premotor cortex during processing of visual signals for action planning. Journal of neurophysiology 95:3596–3616.

Hoshi E, Tanji J (2007) Distinctions between dorsal and ventral premotor areas: anatomical connectivity and functional properties. Current

Opinion in Neurobiology 17:234–242.

Hwang EJ, Andersen RA (2009) Brain control of movement execution onset using local field potentials in posterior parietal cortex. The Journal of neuroscience : the official journal of the Society for Neuroscience 29:14363–14370.

Jeannerod M, Arbib MA, Rizzolatti G, Sakata H (1995) Grasping objects: the cortical mechanisms of visuomotor transformation. Trends in Neurosciences 18:314–320.

Johnson-Frey SH, Newman-Norlund R, Grafton ST (2005) A Distributed Left Hemisphere Network Active During Planning of Everyday Tool Use Skills. Cerebral Cortex 15:681–695.

Kadmon Harpaz N, Flash T, Dinstein I (2014) Scale-Invariant Movement Encoding in the Human Motor System. Neuron 81:452–462.

Kamitani Y, Tong F (2005) Decoding the visual and subjective contents of the human brain. Nature Neuroscience 8:679–685.

Kilintari M, Raos V, Savaki HE (2014) Involvement of the Superior Temporal Cortex in Action Execution and Action Observation. Journal of Neuroscience 34:8999–9011.

Klaes C, Westendorff S, Chakrabarti S, Gail A (2011) Choosing Goals, Not Rules: Deciding among Rule-Based Action Plans. Neuron 70:536–548.

Kriegeskorte N, Goebel R, Bandettini P (2006) Information-based functional brain mapping. Proceedings of the National Academy of Sciences 103:3863–3868.

Kriegeskorte N, Simmons WK, Bellgowan PSF, Baker CI (2009) Circular analysis in systems neuroscience: the dangers of double dipping. Nature neuroscience 12:535–540.

Kuang S, Morel P, Gail A (2016) Planning Movements in Visual and Physical Space in Monkey Posterior Parietal Cortex. Cerebral Cortex.

Kühn S, Keizer AW, Rombouts SARB, Hommel B (2011) The Functional and Neural Mechanism of Action Preparation: Roles of EBA and FFA in Voluntary Action Control. Journal of Cognitive Neuroscience 23:214–220.

Lau H, Rogers R, Ramnani N, Passingham R (2004) Willed action and attention to the selection of action. NeuroImage 21:1407–1415.

Lehmann SJ, Scherberger HH (2013) Reach and Gaze Representations in Macaque Parietal and Premotor Grasp Areas. Journal of Neuroscience 33:7038–7049.

Leoné FTM, Heed T, Toni I, Medendorp WP (2014) Understanding effector selectivity in human posterior parietal cortex by combining information patterns and activation measures. The Journal of neuroscience 34:7102–7112.

Linden DEJ, Oosterhof NN, Klein C, Downing PE (2012) Mapping brain activation and information during category-specific visual working memory. Journal of Neurophysiology 107:628–639.

Lindner A, Iyer A, Kagan I, Andersen RA (2010) Human posterior parietal cortex plans where to reach and what to avoid. The Journal of neuroscience : the official journal of the Society for Neuroscience 30:11715–11725.

Lingnau A, Downing PE (2015) The lateral occipitotemporal cortex in action. Trends in Cognitive Sciences 19:268–277.

Llanos C, Rodriguez M, Rodriguez-Sabate C, Morales I, Sabate M (2013) Mu-rhythm changes during the planning of motor and motor imagery

actions. Neuropsychologia 51:1019–1026.

Logothetis NK (2003) The underpinnings of the BOLD functional magnetic resonance imaging signal. Journal of Neuroscience 23:3963–3971.

Logothetis NK (2008) What we can do and what we cannot do with fMRI. Nature 453:869–878.

Logothetis NK, Pauls J, Augath M, Trinath T, Oeltermann A (2001) Neurophysiological investigation of the basis of the fMRI signal. Nature 412:150–157.

Logothetis NK, Wandell BA (2004) Interpreting the BOLD signal. Annual review of physiology 66:735–769.

Luppino G, Murata A, Govoni P, Matelli M (1999) Largely segregated parietofrontal connections linking rostral intraparietal cortex (areas AIP and VIP) and the ventral premotor cortex (areas F5 and F4). Experimental Brain Research 128:181–187.

Mars RB, Coles MGH, Hulstijn W, Toni I (2008) Delay-related cerebral activity and motor preparation. Cortex 44:507–520.

Martin A, Haxby JV, Lalonde FM, Wiggs CL, Ungerleider LG (1995) Discrete cortical regions associated with knowledge of color and knowledge of action. Science (New York, NY) 270:102–105.

Mauritz KH, Wise SP (1986) Premotor cortex of the rhesus monkey: neuronal activity in anticipation of predictable environmental events. Experimental Brain Research 61:229–244.

Medendorp WP, Goltz HC, Crawford JD, Vilis T, Pieter W (2005) Integration of Target and Effector Information in Human Posterior Parietal Cortex for the Planning of Action Integration of Target and Effector Information in Human Posterior Parietal Cortex for the

Planning of Action. Journal of neurophysiology 93:954–962.

Mur M, Bandettini PA, Kriegeskorte N (2009) Revealing representational content with pattern-information fMRI - An introductory guide. Social Cognitive and Affective Neuroscience 4:101–109.

Murata A, Gallese V, Luppino G, Kaseda M, Sakata H (2000) Selectivity for the shape, size, and orientation of objects for grasping in neurons of monkey parietal area AIP. Journal of neurophysiology 83:2580–2601.

Nambu I, Hagura N, Hirose S, Wada Y, Kawato M, Naito E (2015) Decoding sequential finger movements from preparatory activity in higher-order motor regions: A functional magnetic resonance imaging multi-voxel pattern analysis. European Journal of Neuroscience 42:2851–2859.

Ogawa S, Lee T-M, Stepnoski R, Chen W, Zhu X-H, Ugurbil K (2000) An approach to probe some neural systems interaction by functional MRI at neural time scale down to milliseconds. Proceedings of the National Academy of Sciences 97:11026–11031.

Oliveira FTP, Diedrichsen J, Verstynen T, Duque J, Ivry RB (2010) Transcranial magnetic stimulation of posterior parietal cortex affects decisions of hand choice. Proceedings of the National Academy of Sciences of the United States of America 107:17751–17756.

Oosterhof NN, Connolly AC, Haxby JV (2016) CoSMoMVPA: Multi-Modal Multivariate Pattern Analysis of Neuroimaging Data in Matlab/GNU Octave. Frontiers in Neuroinformatics 10:273389–27.

Oosterhof NN, Tipper SP, Downing PE (2012a) Viewpoint (In)dependence of Action Representations: An MVPA Study. Journal of Cognitive Neuroscience 24:975–989.

Oosterhof NN, Tipper SP, Downing PE (2012b) Visuo-motor imagery of

specific manual actions: A multi-variate pattern analysis fMRI study. NeuroImage 63:262–271.

Oosterhof NN, Wiestler T, Downing PE, Diedrichsen J (2011) A comparison of volume-based and surface-based multi-voxel pattern analysis. NeuroImage 56:593–600.

Orlov T, Makin TR, Zohary E (2010) Topographic Representation of the Human Body in the Occipitotemporal Cortex. Neuron 68:586–600.

Orsborn AL, Moorman HG, Overduin SA, Shanechi MM, Dimitrov DF, Carmena JM (2014) Closed-loop decoder adaptation shapes neural plasticity for skillful neuroprosthetic control. Neuron 82:1380–1393.

Pastor-Bernier A, Tremblay E, Cisek P (2012) Dorsal premotor cortex is involved in switching motor plans. Frontiers in neuroengineering 5:5.

Pertzov Y, Avidan G, Zohary E (2011) Multiple reference frames for saccadic planning in the human parietal cortex. The Journal of neuroscience : the official journal of the Society for Neuroscience 31:1059–1068.

Pesaran B, Nelson MJ, Andersen RA (2008) Free choice activates a decision circuit between frontal and parietal cortex. Nature 453:406–409.

Pistohl T, Schulze-Bonhage A, Aertsen A, Mehring C, Ball T (2012) Decoding natural grasp types from human ECoG. NeuroImage 59:248–260.

Raos V (2004) Functional Properties of Grasping-Related Neurons in the Dorsal Premotor Area F2 of the Macaque Monkey. Journal of Neurophysiology 92:1990–2002.

Raos V (2005) Functional Properties of Grasping-Related Neurons in the Ventral Premotor Area F5 of the Macaque Monkey. Journal of Neurophysiology 95:709–729.

Rizzolatti G, Camarda R (1988) Functional organization of inferior area 6 in the macaque monkey. Experimental Brain … 6:491–507.

Rizzolatti G, Luppino G (2001) The Cortical Motor System. Neuron 31:889–901.

Schalk G, Leuthardt EC (2011) Brain-Computer Interfaces Using Electrocorticographic Signals - Clinical Application Review. IEEE Reviews in Biomedical Engineering 4:140–154.

Scheperjans F, Eickhoff SB, Hömke L, Mohlberg H, Hermann K, Amunts K, Zilles K (2008) Probabilistic maps, morphometry, and variability of cytoarchitectonic areas in the human superior parietal cortex. Cerebral Cortex 18:2141–2157.

Scherberger H, Andersen RA (2007) Target Selection Signals for Arm Reaching in the Posterior Parietal Cortex. Journal of Neuroscience 27:2001–2012.

Schwarzbach J (2011) A simple framework (ASF) for behavioral and neuroimaging experiments based on the psychophysics toolbox for MATLAB. Behavior research methods 43:1194–1201.

Shanechi MM, Orsborn AL, Carmena JM (2016) Robust Brain-Machine Interface Design Using Optimal Feedback Control Modeling and Adaptive Point Process Filtering. PLoS computational biology 12:e1004730.

Shannon CE (1948) A mathematical theory of communication. The Bell System Technical Journal 27:379–423.

Shenoy KV, Carmena JM (2014) Combining decoder design and neural adaptation in brain-machine interfaces. Neuron 84:665–680.

Simmons WK, Ramjee V, Beauchamp MS, McRae K, Martin A, Barsalou

LW (2007) A common neural substrate for perceiving and knowing about color. Neuropsychologia.

Sladky R, Friston KJ, Tröstl J, Cunnington R, Moser E, Windischberger C (2011) Slice-timing effects and their correction in functional MRI. NeuroImage 58:588–594.

Smith AT, Kosillo P, Williams AL (2011) The confounding effect of response amplitude on MVPA performance measures. NeuroImage 56:525–530.

Soon CS, Brass M, Heinze H-J, Haynes J-D (2008) Unconscious determinants of free decisions in the human brain. Nature neuroscience 11:543–545.

Soon CS, He AH, Bode S, Haynes J-D (2013) Predicting free choices for abstract intentions. Proceedings of the National Academy of Sciences of the United States of America 110:6217–6222.

Thoenissen D, Zilles K, Toni I (2002) Differential involvement of parietal and precentral regions in movement preparation and motor intention. The Journal of neuroscience : the official journal of the Society for Neuroscience 22:9024–9034.

Thura D, Cisek P (2014) Deliberation and commitment in the premotor and primary motor cortex during dynamic decision making. Neuron 81:1401–1416.

Todd MT, Nystrom LE, Cohen JD (2013) Confounds in multivariate pattern analysis: Theory and rule representation case study. NeuroImage 77:157–165.

Toni I, Thoenissen D, Zilles K (2001) Movement preparation and motor intention. NeuroImage 14:S110–S117.

Townsend BR, Subasi E, Scherberger H (2011) Grasp Movement Decoding

from Premotor and Parietal Cortex. Journal of Neuroscience 31:14386–14398.

Tunik E, Frey SH, Grafton ST (2005) Virtual lesions of the anterior intraparietal area disrupt goal-dependent on-line adjustments of grasp. Nature neuroscience 8:505–511.

Tunik E, Rice NJ, Hamilton A, Grafton ST (2007) Beyond grasping: Representation of action in human anterior intraparietal sulcus. NeuroImage 36:T77-86.

Turella L, Lingnau A (2014) Neural correlates of grasping. Frontiers in human neuroscience 8:686.

Turella L, Tucciarelli R, Oosterhof NN, Weisz N, Rumiati R, Lingnau A (2016) Beta band modulations underlie action representations for movement planning. NeuroImage 136:197–207.

Turner R (2016) Uses, misuses, new uses and fundamental limitations of magnetic resonance imaging in cognitive science. Philosophical Transactions of the Royal Society B: Biological Sciences 371:20150349.

Verhagen L, Dijkerman HC, Grol MJ, Toni I (2008) Perceptuo-Motor Interactions during Prehension Movements. Journal of Neuroscience 28:4726–4735.

Verhagen L, Dijkerman HC, Medendorp WP, Toni I (2012) Cortical Dynamics of Sensorimotor Integration during Grasp Planning. Journal of Neuroscience 32:4508–4519.

Verhagen L, Dijkerman HC, Medendorp WP, Toni I (2013) Hierarchical Organization of Parietofrontal Circuits during Goal-Directed Action. Journal of Neuroscience 33:6492–6503.

Watanabe K, Igaki S, Funahashi S (2006) Contributions of prefrontal cue-,

delay-, and response-period activity to the decision process of saccade direction in a free-choice ODR task. Neural Networks 19:1203–1222.

Wong AL, Haith AM, Krakauer JW (2015) Motor Planning. The Neuroscientist 21:385–398.

Wurm MF, Ariani G, Greenlee MW, Lingnau A (2016) Decoding Concrete and Abstract Action Representations During Explicit and Implicit Conceptual Processing. Cerebral Cortex 26:3390–3401.

Wurm MF, Lingnau A (2015) Decoding Actions at Different Levels of Abstraction. Journal of Neuroscience 35:7727–7735.

Zaitsev M, Hennig J, Speck O (2004) Point spread function mapping with parallel imaging techniques and high acceleration factors: Fast, robust, and flexible method for echo-planar imaging distortion correction. Magnetic Resonance in Medicine 52:1156–1166.

Zeng H, Constable RT (2002) Image distortion correction in EPI: Comparison of field mapping with point spread function mapping. Magnetic Resonance in Medicine 48:137–146.

Zhang J, Hughes LE, Rowe JB (2012) Selection and inhibition mechanisms for human voluntary action decisions. NeuroImage 63:392–402.

Zhang J, Kriegeskorte N, Carlin JD, Rowe JB (2013) Choosing the Rules: Distinct and Overlapping Frontoparietal Representations of Task Rules for Perceptual Decisions. Journal of Neuroscience 33:11852–11862.

Zimmermann M, Verhagen L, de Lange FP, Toni I (2016) The extrastriate body area computes desired goal states during action planning. eNeuro 3:1–13.

Acknowledgments

This thesis represents the ultimate product of my PhD work. As such, it contains much of what I have spent most of my time on for the past four years. There is no trace, however, of the daily grind, the struggles, the happy moments, the successes, the travels, the friendships and all the other small, invisible steps and contributions along the way. To the many people who inspired and supported me throughout this journey I owe my most sincere gratitude.

Thank you, Angelika. I want to thank my supervisor, Dr. Angelika Lingnau, for her patience and guidance. Leading by example, and always challenging me to cut out the unnecessary, she has shown me the way to become an independent scientist. I am also grateful for all the opportunities, experiences (including those beyond research), and the excellent laboratory environment that she has provided. Since we first met in Mattarello I had the (correct) impression that you would have been the right advisor for me.

Thank you, Family. I am so incredibly thankful to my family. My parents gave me all the love one can hope for, and support throughout every single stage of my education: never intruding, always ready to help – the PhD was no exception. A former PhD candidate himself, my brother paved the road in front of me, and has always been an impeccable role model. You all know how much I love you back.

Thank you, Lab members and colleagues. I thank all the friends among Lab members and colleagues with whom I have bonded in these years, no matter for how long. It would be impossible to list them all here, so I apologize to the ones that I have left out. I am particularly grateful to Moritz, Nick, Raf, and Seth for helping with several technical aspects related to data analysis, statistics and programming; to Nick, Moritz, Patrik and Luca for comments and constructive criticism both during experiment designing and manuscript writing; finally, to Seth, Raf, Bea, Moritz, Dario, Daniel, Luca, Gilles, Deniz, Patrik, Flavio, Nathan, Nick and Elisa for the many productive, and not, but always enjoyable discussions, the time together during conferences, summer schools, trips abroad, coffee breaks (table-tennis matches included), lab drinks and dinners. All these much needed "distractions" have been source of fun, stress relief, and personal growth. Thank you all!

Thank you, secondary advisors. I certainly owe a debt of gratitude to several secondary advisors like Jens Schwarzbach, James Haxby, Lorella Battelli, Uri Hasson and Jorge Jovicich. Thanks for your scientific support, helpful advice, and excellent ideas that inspired me throughout my PhD.

Thank you, Mattarello people. I would also like to thank the technical and administrative Staff of the LNiF Labs in Mattarello, who assisted me during many data acquisition sessions: Paolo Ferrari, Pietro Chiesa, Valeria Maria Nencini, Claudio Boninsegna, Fabrizio Pallaver, Giulia Fratti, Manuela

Orsini, Lorenzo Giovannelli and Angela Serafin. Thanks for the kindness and for your help with all sorts of practical and bureaucratic issues.

Thank you, Marta and Remo. I take this opportunity to mention also two people that I have never properly thanked enough since my undergrad years: Marta Cazzanelli and Remo Job. I would not be defending my PhD today if it were not for you. Much time has passed since then, and perhaps you do not even remember why I am thanking you, but I will never forget.

Thank you, Dasha. The final and biggest thank you of all goes to the person with whom I have shared most of my time and experiences in the last four years. I am immensely grateful for your constant support and the words of encouragement during stressful times; for the travels together, all the shared food, the mountain hikes, and the Rovereto dogs we came to love; for reminding me that there is more to life than work; for bearing with my woes and forming a bond now stronger than ever. If this PhD has been a journey, you have truly been my co-pilot.

Funding. This PhD work would have not been possible without the financial support by the Univeristy of Trento (UNITN grant) and the Fondazione Cassa di Risparmio di Trento e Rovereto (CARITRO).